



Polymer-based composites by electrospinning: Preparation & functionalization with nanocarbons

Jeremy Kong Yoong Lee^a, Nuan Chen^{a,b}, Shengjie Peng^{a,c,d,*}, Linlin Li^{c,d,**}, Lingling Tian^b, Nitish Thakor^{b,e}, Seeram Ramakrishna^a

^a Center for Nanofibers and Nanotechnology, Department of Mechanical Engineering, National University of Singapore, 117576, Singapore

^b Singapore Institute for Neurotechnology, National University of Singapore, 117456, Singapore

^c Jiangsu Key Laboratory of Electrochemical Energy Storage Technologies, College of Materials Science and Engineering, Nanjing University of Aeronautics and Astronautics, Nanjing, 210016, PR China

^d Key Laboratory of Advanced Energy Materials Chemistry (Ministry of Education), Nankai University, Tianjin 300071, China

^e Department of Biomedical Engineering, Johns Hopkins University, Baltimore, MD21205, USA



ARTICLE INFO

Article history:

Received 22 April 2018

Received in revised form 19 June 2018

Accepted 5 July 2018

Available online 22 July 2018

Keywords:

Electrospinning
Polymer composites
Nanocarbon
Nanofibers
Functionalization
Tissue engineering

ABSTRACT

Electrospinning is a straightforward yet versatile technique for the preparation of polymeric nanofibers with diameters in the range of nanometers to micrometers, and has been rapidly developed in the last two decades. Nanocarbon materials, usually referring to carbon nanotubes, graphene, and fullerenes with their derivatives including quantum dots, nanofibers, and nanoribbons, have received increasing attention due to their unique structural characteristics and outstanding physico-chemical properties. Incorporation of nanocarbons in electrospun polymeric fibers has been used to increase the functionality of fibers, for example, to improve the mechanical, electrical, and thermal properties, as well as confer biofunctionality as scaffolds in tissue engineering and sensors, when the advantageous properties given by the encapsulated materials are transferred to the fibers. In this review, we provide an overview of polymer-based composites reinforced with nanocarbons via the electrospinning technique. After a brief introduction of various types of nanocarbons, we summarize the latest progress of the design and fabrication of electrospun polymeric nanofibers with nanocarbon fillers. With regard to the preparation of composites, we focus on functionalization strategies of nanocarbons and the production of random & aligned polymeric nanocomposites. Then, the physical properties such as mechanical, electrical, and thermal properties are also reviewed for electrospun nanocomposite nanofibers reinforced with nanocarbons, especially carbon nanotubes. Benefiting from the exceptional properties including superior electric conductivity, high porosities, unique mat structure, etc. the polymeric composite nanofibers have demonstrated numerous advantages and promising properties in the fields of tissue engineering and sensors. In the application section, we will give state-of-the-art examples to demonstrate the advantages of electrospun polymer-based nanocomposites. Finally, the conclusion and challenge of the polymer-based nanocomposites are also presented. We believe the efforts made in this review would promote the understanding of the methods of preparation and unique physical and chemical properties of nanocarbon reinforced polymer-based nanocomposites.

© 2018 Elsevier B.V. All rights reserved.

Contents

1. Introduction.....	42
1.1. Overview of the nanocarbon materials	42
1.2. Electrospinning.....	43
2. Preparation of polymer/carbon composites	43

* Corresponding author at: Center for Nanofibers and Nanotechnology, Department of Mechanical Engineering, National University of Singapore, 117576, Singapore.

** Corresponding author at: Jiangsu Key Laboratory of Electrochemical Energy Storage Technologies, College of Materials Science and Engineering, Nanjing University of Aeronautics and Astronautics, Nanjing, 210016, PR China.

E-mail addresses: pengshengjie@nuaa.edu.cn (S. Peng), lilinlin@nuaa.edu.cn (L. Li).

2.1.	Preparation of electrospun carbon nanotube-polymer composites	44
2.1.1.	Co-electrospinning	44
2.1.2.	Surfactant addition to improve dispersability	45
2.1.3.	Chemical modification to improve dispersability	45
2.1.4.	Melt electrospinning	45
2.1.5.	Chemical functionalization	45
2.1.6.	Nanofiber architecture	46
2.1.7.	CNT deposition on electrospun nanofiber and other post processing treatments	47
2.2.	Preparation of electrospun graphene-polymer composites	48
2.2.1.	Co-electrospinning	48
2.2.2.	Graphene oxide functionalization and modification	48
2.2.3.	Deposition of graphene on electrospun nanofiber	49
2.2.4.	Graphene as a nucleating agent	50
2.2.5.	Graphene functionalization and modification	50
2.2.6.	Graphene quantum dots and CNT/graphene hybrids	51
2.3.	Preparation of electrospun fullerene-polymer composites	51
2.4.	Preparation of electrospun carbon nanodiamond-polymer composites	52
2.5.	Preparation of other electrospun nanocarbon-polymer composites	53
3.	Properties of polymer/carbon composites	55
3.1.	Mechanical properties	55
3.2.	Electrical properties	59
3.3.	Thermal properties	62
4.	Applications	62
4.1.	Tissue engineering	65
4.1.1.	Bone, cartilage and dental tissue engineering	69
4.1.2.	Neural tissue engineering	70
4.1.3.	Skeletal muscular tissue engineering	72
4.1.4.	Cardiac and vascular tissue engineering	72
4.2.	Chemical and biosensors	73
4.2.1.	Healthcare sensors	73
4.2.2.	Environmental sensors	74
4.3.	Environmental remediation	75
5.	Challenge	76
6.	Conclusion	77
	Acknowledgements	77
	References	78

Nomenclature

ALP	Alkaline phosphatase
BPM	Beats per min
CNT	Carbon nanotube
CNF	Carbon nanofiber
ECM	Extracellular matrix
FAD	Flavin adenine dinucleotide
GO	Graphene oxide
GOD	Graphene quantum dots
GOX	Glucose oxidase
HA	Hydroxyapatite
HUVEC	Human umbilical vein endothelial cell
LOD	Limit of detection
MSC	Mesenchymal stem cell
mwCNT	Multi-walled carbon nanotube
ND	Nano-diamond
NP	Nanoparticle
PAA	Polyacrylic acid
PAN	Polyacrylonitrile
PANI	Polyaniline
PBAT	Poly (butylene adipate-co-terephthalate)
PCL	Poly(ϵ -caprolactone)

PEDOT	Poly(3,4-ethylenedioxythiophene)
PEG	Polyethylene glycol
PG	Poly(glycerol sebacate)/gelatin
P3HB	Poly-3-hydroxybutyrate
PLA	Poly(lactic acid)
PLLA	Poly(L-lactide)
PLGA	Poly(lactic-co-glycolic acid)
PMMA	Poly(methyl methacrylate)
PNIPA	m-co-MAApoly(N-isopropyl acrylamide-co-methacrylic acid)
PPF	Poly(propylene fumarate)
PU	Polyurethane
PVA	Poly(vinyl alcohol)
PVC	Polyvinyl chloride
PVDF	Polyvinylidene difluoride
rGO	Reduced graphene oxide
rhBMP-2	Recombinant human bone morphogenetic protein-2
SEBS	Styrene-ethylene/butylene-styrene
swCNT	Single-walled carbon nanotube
TNF- α	Tumor necrosis factor alpha
TPU	Thermoplastic polyurethane

1. Introduction

Composite materials are receiving increasing interest for various applications in biology, energy, and environment remediation due to their outstanding properties and versatility. Composites, which are obtained by combining two or more materials possessing different physico-chemical properties, can be divided into polymeric, ceramic, and metallic substances based on the nature of the matrix phase. Among these composites, polymer composites are widely used in various technical applications, because polymers as the matrix phase offers advantages over other materials such as processability, allowing these composites to be fabricated into intricately shaped, lightweight components.

Advances in nanoscience and nanotechnology have been motivated by discoveries of a variety of carbon nanostructures over the last thirty years. Carbon, the sixth element in the periodic table of elements, has received significant attention due to its unique chemical properties, thermal stability, as well as superior mechanical performance for a wide variety of applications. Diamond and graphite represent the only known allotropes of carbon before fullerenes were observed for the first time by Kroto et al. in 1985 [1]. The discovery of fullerenes marked the beginning of the era of synthetic carbon allotropes, progressing to the observation of carbon nanotubes (CNTs) in 1991 and graphene in 2004 – two important milestones in the evolution of carbon allotropes [2–4]. The carbon atom can be sp^3 or sp^2 hybridized and arranged in different structures - sp^2 hybridized carbon have abundant allotropes such as graphite, fullerene, graphene, CNTs and so on [5]. Recently, carbon and its allotropes have been demonstrated in promising applications in key technologies such as ultralight and ultrastrong composites, renewable energy harvesting and storage, as well as active bio-medical materials [6–8].

Apart from carbon materials, nanocomposites are considered one of the most highly researched areas in nanoscience. Nanocarbon reinforced composites are also attracting enormous attention as the next generation of superior functional materials, combining the positive attributes of the host and reinforcement materials in novel ways [9–11]. Current research has been focused on the fabrication of polymer nanocomposites by incorporating carbon nanotubes into various polymer systems. Researchers have been able to show that through dispersion and orientation of nanocarbons, improved physical properties including Young's modulus, toughness, tensile strength, and conductivity can be achieved in polymeric matrices [1–5].

Electrospinning is a powerful one-step technique to prepare polymeric nanofibers and their composites with diameters down to a few nanometers, which can make full use of advantages of constituents [6–8,12–18]. At present, many electrospun functional polymer nanofibers can be reinforced with nanocarbons, including CNTs, graphenes, nanodiamonds, nanodots etc. Introducing nanocarbons, especially carbon nanotubes and graphene, to polymer matrices can significantly enhance the mechanical, electrical, and thermal properties, leading to promising applications in biology and sensors [10]. Despite these achievements, one of the most challenging aspects in preparing such composites is the difficulty in dispersing and aligning the nanofillers in a polymer matrix. This is due to the strong van der Waals attractions between nanocarbons that induce aggregation and prevents dispersion. Thus, there is a critical need for proper dispersion of these nanostructures in a polymer matrix, and several methods have been developed to improve the dispersion of carbon-black, CNTs, graphene, and fullerenes, including chemical modification of nanocarbons.

In this review, we provide an overview of polymer-based composites containing nanocarbons via electrospinning technique. After a brief introduction of the promising nanocarbon materials, the progress of polymer composites containing CNTs, graphenes,

nanodiamonds, and carbon quantum dots using the electrospinning technique are reviewed in detail. In particular, we introduce melt electrospinning to fabricate specific polymer composites in this review. In the following sections, we review the unique mechanical properties of polymer/nanocarbons composites such as the high elastic modulus, tensile strength and strain to fracture, the ability to withstand cross-sectional and twisting distortions and compression without fracture. The electrical and thermal properties are also reviewed for electrospun polymer nanofibers reinforced with nanocarbon. To establish the unique attributes arising from the constituents of polymers and nanocarbons, we subsequently highlight examples of the applications of electrospun polymer/nanocarbon composites in tissue engineering (bone, cartilage, dental, neural, skeletal muscular, cardiac and vascular tissue engineering) and sensors (healthcare sensor and environmental sensor). Finally, the conclusion and outlook of the electrospun polymer/nanocarbon composites are given. This study comprises of a detailed compilation of electrospun polymer nanofibers with various available forms of nanocarbons and their applications.

1.1. Overview of the nanocarbon materials

Nanocarbon materials usually refer to carbon forms with characteristic sizes in the nanoscale region (one dimension being below 100 nm) [5]. The structural state of the carbon allotrope (dimensionality and characteristic size) and hybridization state of the carbon atom are two decisive factors in classifying nanocarbon materials [19].

Among the nanocarbon materials, graphene represents one of the most promising materials for next-generation nanoelectronic devices. Graphene was first discovered by Andre Geim and co-workers in 2004 using a simple Scotch-tape method [4]. Recent years have witnessed many breakthroughs with graphene, especially in developing new production methods and technological applications [20–22]. Graphene, a single layer of carbon atoms in a closely packed 2-dimensional lattice, is considered the basic building block for CNTs, graphite, and fullerenes. It has a large specific surface area, good electrical conductivity, high Young's modulus, and thermal conductivity [23–25]. It also can be composited with polymers or inorganic systems to increase the mechanical strength, thermal and electrical conductivity. Currently, there exist several strategies to synthesize graphene – namely chemical vapor deposition on metal surface (epitaxial graphene), micromechanical exfoliation, exfoliation of graphite in solvents, chemical reduction of graphene oxide, microwave plasma, and arc-discharge [26]. Due to the unique properties of graphene, it has been extensively applied in many areas including sensors, transparent conductive films, and several types of energy devices.

CNTs were observed much earlier by Iijima in 1991 compared to graphene, and was initially considered as cylinders of rolled-up graphene [3]. Distinguished by the layers of the graphene lamella, CNT can be classified into two categories: multi-walled carbon nanotubes (mwCNTs) which are formed by multi layers of graphene lamella, and single-walled carbon nanotubes (swCNTs) which are formed by single layer of graphene. Besides the number of walls, the chirality of the CNTs also play a large deterministic role in its electron conductivity. Due to the unique mechanical, electrical, optical, and thermal properties of CNTs, it is one of the most well investigated and used nanocarbon material, having already shown important applications in ultralight and ultrastrong composites, renewable energy harvesting and storage, as well as active bio-medical materials [27,28]. Furthermore, CNTs can be easily decorated with organic functional groups to provide selective interactions with other polymer or inorganic systems [8]. The synthesis methods for CNT mainly include arc discharge, laser ablation, and

chemical vapor deposition which many other review papers have discussed in detail [27,29].

swCNTFullerenes, which are closed-cage carbon molecules containing pentagonal and hexagonal carbon atoms rings, were first discovered in 1985 by Kroto et al. [1]. The discovery of fullerenes, of which C60 and C70 are the most well studied [30], opened the era of nanocarbon materials and had extremely important significance in the study of carbon allotrope materials. Produced primarily by pulsed arc discharge [31], laser irradiation, resistive heating, pyrolysis, or radio-frequency plasma to vaporize a carbon source, several novel chemistry based techniques are also being studied which could improve yields, reduce the complexity of preparing functionalized fullerenes, give better control over the type of fullerene produced, or synthesize larger fullerenes [32].

Carbon nanodots or carbon quantum dots (CQD) make up an appealing class of recently discovered nanocarbon materials [33] that comprise carbon nanoparticles with sizes below 10 nm. They were first obtained during the purification of swCNT in 2004 by Scrivens et al. and gradually established themselves as a new star in the nanocarbon family [34]. Much progress has been achieved in the study of CQD during the last decade, in both developing processes to synthesize CQDs as well as using CQDs in various applications. The synthesis techniques of CQD can be classified into two main groups: top-down, and bottom-up approaches. Top down approaches include arc-discharge, laser ablation, electrochemical oxidation, chemical oxidation, and ultrasonic synthesis, which utilize macroscopic carbon sources, whereas bottom-up approaches such as microwave synthesis, template-based chemistry, thermal decomposition, and hydrothermal treatment are associated with chemical precursors like simple sugars and citric acid [35]. CQDs have greater sp^2 hybridization character, which is symbolic of nanocrystalline graphite, and contains lower amounts of carbon with higher oxygen content. With the rapid pace of development in this field, CQDs have shown outstanding potential in optical imaging and related biomedical applications [33,36].

Another member in nanocarbon family which is similar in size to CQDs is the nanodiamond. Nanodiamonds are typically prepared by milling microdiamonds, chemical vapor deposition, shockwave, or detonation processes [37]. Generally, they are comprised of about 98% carbon with residual hydrogen, oxygen, and nitrogen, and possess an sp^3 hybridized core, having small amounts of graphitic carbon on the surface. Currently, the nanodiamond is primarily thought to have potential applications in biomedical imaging, drug delivery, and other areas of medicine [7].

1.2. Electrospinning

Electrospinning has been a well-documented nanofabrication technology for the production of ultrafine 1-dimensional nanofibers and 2-dimensional non-woven membranes. It offers many advantages such as simplicity and scalability, which are vitally important in translating the immense potential of nanoscale materials into useful macroscale assemblies. More importantly, compared with analogous nanofiber production methods such as nanolithography, melt fibrillation, self-assembly, etc, electrospinning offers a unique combination of high production rate, low cost, wide material suitability, and consistent nanofiber quality [38].

Additionally, the technique is versatile and easily adaptable, with variants such as needle-less electrospinning, melt electrospinning, co-axial electrospinning, emulsion electrospinning, and co-electrospinning to afford a wide variety of nanoarchitectures like core-shell, tube-in tube, porous, hollow, cross-linked, and particle encapsulated structures [39–42]. Besides designing the nanoarchitecture of the assembled material, there are many other material synthesis controls researchers can exploit, such as modifying the electrospinning parameters, tuning the material chemistry

of the polymers and additives, and leveraging post electrospinning treatments which can alter the nanofiber properties and behaviour to be tailored for specific applications.

There have been several excellent in-depth reviews on the use of electrospinning for various applications which are cited as literature in this review. This process, while initially applied primarily for the preparation of polymeric nanofibers [12,43,44], has been gaining significant traction in the fabrication of other inorganic [45,46], carbon [47], composite materials [39] and metallic [48,49] as well, enabling its adoption for all manner of applications including polymeric nanofiber meshes for filtration, metallic nanofiber webs for solar cells, inorganic nanofiber tissue engineering scaffolds, and composite nanofiber reinforcements for high performance structural materials to name a few [39–42,46–56].

The classic electrospinning setup consists of five components, a high voltage power source capable of applying a DC voltage in the range of kilovolts, a polymer solution to be electrospun, an electrically conductive spinneret (typically a blunted needle), a syringe pump to feed the polymer solution to the spinneret, and a grounded collector. While the set-up is simple, as shown in Fig. 1a, there are complex electro-hydrodynamic and rheological interactions involving the transfer of charges and mass occurring during electrospinning [57,58].

The process consists of three stages, namely jet initiation, elongation, and solidification into a nanofiber. The working principle behind electrospinning is the electrostatic charging of a droplet of polymer solution held at the tip of a fine capillary overcoming the surface tension holding the droplet. During jet initiation, the pendant polymer solution droplet is subject to an electric field applied by the voltage source, inducing charge accumulation on the droplet surface, elongating the droplet into a conical shape known as a Taylor cone. When a critical electric field intensity is achieved, the electrostatic forces on the surface are sufficient to overcome the surface tension holding the droplet together, resulting in a forcible ejection of the polymer solution jet. The critical electric field intensity (V_c) is described by the Eq. (1), where L is the length of the capillary tube, R is the radius of the tube, H is the air gap distance, and γ is the solution surface tension [57].

$$V_c^2 = 4\left(\frac{H^2}{L^2}\right)\left(\ln \frac{2L}{R} - 1.5\right)(0.117\pi R\gamma) \quad (1)$$

As the polymer solution is jettisoned from the Taylor cone tip, several opposing forces act upon the travelling jet, resulting in fluid instabilities. These forces arise from changes in the charge distribution and shape of the jet as it stretches and the solvent evaporates, shifting the balance between surface tension and coulombic forces. To reduce the surface charge concentration, the jet is forced to stretch, increasing the surface area for charge to be distributed. Further high velocity whipping instabilities are initiated as the polymer jet becomes highly stretched and localization of excess charges at different points along the thinning jet causes the jet path to bend and form lateral offshoots that spiral into loops of increasing diameter. This process is responsible for thinning the initial jet into nanometer dimensioned fibers [57,58], and is schematically illustrated in Fig. 1b.

It has been found that electrospinning parameters such as the applied voltage, polymer concentration, molecular weight, interactions, and polydispersity [59], electrospinning solution conductivity and viscosity, feed rate, solvent evaporation characteristics, air gap distance can all play deterministic roles in the spinnability and fiber characteristics from an electrospinning solutions [57,58].

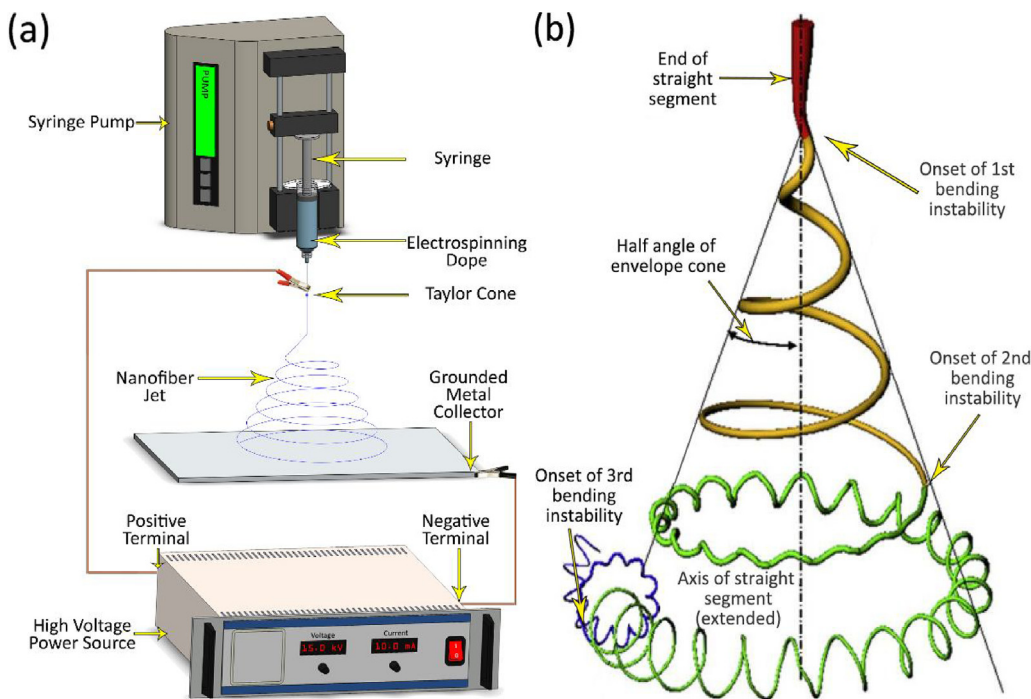


Fig. 1. (a) Schematic showing typical electrospinning setup; (b) Schematic showing bending instabilities causing thinning of the jet issued from the Taylor cone [58]. Copyright 2008, reproduced with permission from Elsevier Ltd.

2. Preparation of polymer/carbon composites

2.1. Preparation of electrospun carbon nanotube-polymer composites

Carbon nanotubes with their outstanding mechanical, electrical, and thermal properties have long been considered prime candidates as reinforcing nanofillers for polymers in a wide variety of applications including composite structural materials [60–62], energy devices like solar cells [63], phase change materials for thermal energy storage [64], supercapacitors [65–67], tissue engineering scaffolds [68,69], drug delivery systems [64], biological catalyst supports [70], sensors [71,72], functional ferroelectric materials [73], and filtration membranes [74–78]. However, in transitioning the superlative properties of the nanoscale CNT toward the useful macroscale applications, the dispersion and alignment of the CNT during the fabrication process, along with adhesion to the matrix, have proven to be significant challenges to overcome [79].

2.1.1. Co-electrospinning

Co-electrospinning of CNTs in a well-dispersed polymer solution could be a simple and scaleable way to produce high performance, confinement enhanced composites, where the electrohydro-dynamic spinning process leads to the CNTs being highly oriented along the axis of the nanofiber to maximize their extraordinary anisotropic characteristics [58,80].

Fabrication of these composite nanofibers typically proceeds via a technique called co-electrospinning in which a solution consisting of the CNT dispersed in a polymer solution is electrospun to yield nanofibers. While the approach is straightforward, there are complex interactions between the solvent, polymer, CNT, and any additives used, which governs the eventual characteristics of the nanofibers [81,82]. Interactions such as polymer-chain solvation could be affected by the amphiphilic nature of any surfactants used, functionalized CNTs could form dipole interactions with polar polymer chains to alter their solvation behaviour, dispersability,

and solution viscosity. Furthermore, the aspect ratio, type, functionalization of CNTs added could alter the electrical conductivity and viscosity of the electrospinning dope, and also the nanofiber crystallization behaviour [83–87]. This necessitates the careful optimization of the electrospinning solution apart from the typical electrospinning parameters.

The archetypical co-electrospinning process was adopted by Ayutsede et al. in the preparation of swCNT reinforced silk fibroin nanofibers. swCNT, prepared by high-pressure disproportionation of CO (HipCO), was first dispersed in formic acid and ultrasonicated to yield a series of dispersed swCNT solution with CNT content ranging between 0.5–5%. Regenerated silk fibroin protein was then added to the mixtures (12 wt%) and further agitated by sonication and mechanical stirring to give the electrospinning dope. The dope was electrospun using a single needle setup with the nanofibers formed collected as nonwoven mats or as aligned, bundled yarns. The researchers observed that when silk was added to the swCNT dispersion, a silk coating was formed around the bundles of swCNT, which acted as a dispersing agent preventing CNT aggregation, a problem particularly difficult to overcome for unmodified swCNTs owing to their notoriously extensive van der waals' interactions. It was postulated that the incorporation of small amounts of CNTs led to a nucleating effect on the silk fibroin, thereby increasing the crystallinity, and eventual mechanical performance, of the spun nanofiber [88]. Similar methodology was adopted by several other groups, incorporating CNTs in solutions of Nylon 6,6 in formic acid [89], PVA in water [90], poly(butylene terephthalate) (PBT) [91] and PLGA [92] in hexafluoroisopropanol, polyurethane in a mixed solvent of DMF/THF [93,94], polyindole blended with PEO in chloroform [66], PMMA in DMF [72], PVDF in DMF and acetone [95], and polyaniline blended with PEO in chloroform [65], achieving dispersion of the CNT by mechanical means alone. Wan et al. modified this process slightly, introducing ultrasonic vibrations during the electrospinning process rather than at the solution preparation stage via the application of a SFSA-1 ultrasonic generator. The mWCNT filled PAN nanofibers fabricated this way showed a smoother surface morphology compared to those spun without the

ultrasonic vibrations [96]. There have also been other modifications to augment the basic needle electrospinning method such as Lee's research group who applied near IR laser irradiation to the fluid jet below the spinneret to assist the alignment and orientation of the PET polymer chains and embedded mwCNTs as the nanofiber solidifies [97].

2.1.2. Surfactant addition to improve dispersability

The limited dispersability of the CNT in the chosen polymer/solvent system may limit the choice of polymers for electrospinning available. Furthermore, it should be noted that nanotube fragmentation could occur when exposed to a prolonged duration of ultrasonication undermining the effectiveness of the nanotube filler [98]. To that end, researchers have incorporated surfactants in order to overcome the strong van der waal's interactions between the carbon nanotubes and achieve CNT dispersion in aqueous solutions. Dror and colleagues applied the idea of surfactant stabilized CNT solutions for the electrospinning of multi-walled CNT (mwCNT) reinforced Polyethylene oxide (PEO) nanofibers collected on a rotating disk with a tapered edge, using either sodium dodecyl sulfate (SDS) or Gum Arabic (GA) as the amphiphiles to adsorb to, and disperse the bundles of the hydrophobic mwCNTs. The surfactant, mwCNT, and water were mixed and sonicated to yield a homogenous dispersion before a solution of PEO in a mixture of ethanol and water was introduced to give the solution sufficient viscosity to be electrospun. Results from TEM analysis of the resulting PEO nanofiber showed well dispersed, individually embedded CNTs, a majority of which were aligned with the fiber axis [99]. Wrapping the CNTs with DNA has also proved an effective way to separate bundles of CNTs in an aqueous solution, wherein DNA molecules enfold around the sidewalls of the CNT *via* van der waal's interactions. Hee and coworkers prepared DNA wrapped CNT suspensions by sonicating oxidized double walled CNTs together with double stranded salmon DNA in water. Ultracentrifugation yielded separated isolated CNTs which were then added to PEO/DNA solutions to obtain an electrospinning solution [100]. Non-covalent supramolecular functionalization of swCNTs using conjugated polyelectrolytes such as a-PPE to achieve dispersion has also been achieved by Naeem and colleagues [101]. Other surfactants that have been used to disperse CNTs include lignosulfonic acid sodium salt [85], SDS [102–105], and PVP [102] for the electrospinning of CNT filled PVA nanofibers; GA [106], SDS [104], and amphiphilic styrene-sodium maleate co-polymer for CNT reinforced PEO nanofibers [107].

2.1.3. Chemical modification to improve dispersability

One drawback from the surfactant stabilized CNT dispersion solution for electrospinning is the relatively high surfactant content incorporated into the eventual nanofibers which could affect the eventual properties of the nanofiber adversely - typically a solution containing 0.35 wt% CNT will require up to 1 wt% of surfactant [99]. A common alternative way to improve the dispersion of the CNT in solution would be to modify the CNT by chemical methods such as acid treatment of the CNT which oxidizes the CNT and confers carboxylic acid ($-COOH$) or hydroxyl ($-OH$) functionalization on the CNT surface. Fang et al. prepared the mwCNTs by immersing them in 6 M nitric acid for 12 h under reflux, then filtered, washed with DI water, and dried. The obtained $-COOH$ functionalised mwCNTs were then dispersed in DMF *via* sonication before being added to a 12.5 wt% PAN DMF solution to give a 10 wt% PAN DMF solution containing mwCNT concentrations of various concentrations up to 1 wt%. The $-COOH$ functionalisation was identified in FTIR analysis, and titration results showed the functional group concentration increased 8-fold over their unoxidized counterparts, accounting for much improved dispersability of mwCNTs in the DMF solvent, and allowing the mwCNTs to be

well-dispersed and aligned within the electrospun PAN nanofibers [108]. Xu et al. also achieved well aligned, well-dispersed mwCNTs in their Polyimide nanofiber through the use of $-COOH$ functionalized nanotubes, as imaged by TEM shown in Fig. 2c [67]. Similar approaches have also been used for preparing nanofibers of CNT reinforced Poly(Acrylonitrile-co-Acrylic Acid) [70], PAN-co-PMMA [109], PET [84], PAN [108,110,111], cellulose [112], PVA [113], PVP [114,115], Polyurethane [116,117], Polyimide [118,119], chitosan [69], silk [120], PVDF [73,86], PLLA or PLDA [121], PVA blended with chitosan [122], PLA blended with PCL [123,124], PVDF blended with PAN [125], PANI blended with PEO [126], PANI blended with Pan using a needless electrospinning setup [127], nylon 6 [64,128], and PLGA [81] among others.

2.1.4. Melt electrospinning

Besides solution electrospinning, melt electrospinning has also been used to prepare the electrospinning dope for polymers in which dissolution is difficult. Electrospun polypropylene nanofibers reinforced with mwCNTs have been reported by Su et al. by a melt electrospinning process in which a screw extruder was used to compound the polymer and CNT filler (up to 0.25 wt%) under elevated temperatures of 185 °C with paraffin liquid to help improve spinability. Electrospinning of the compounded particles proceeds at even high temperatures of 265 °C, yielding the composite nanofibers presenting good morphological characteristics [129]. Melt compounding in a rheometer has also been used in the preparation of composites of Poly(trimethylene terephthalate) (PTT) and functionalized CNTs to be dissolved in a mixed solvent of trifluoroacetic acid and methylene chloride to be electrospun [130]. It was observed by Wu that carboxylic functionalised CNTs, which have better affinity toward the PTT were more uniformly dispersed in the PTT nanofiber than their hydroxyl functionalized counterparts which showed a lower degree of alignment [130].

2.1.5. Chemical functionalization

Chemical modification of the CNT could also serve to improve the interaction between the CNT and the polymer matrix, or even impart added functionality, affording the spun composite nanofibers a wider range of chemical, electrical, and optical properties [131]. Thiophene conjugation has been used by Wickham and co-workers to modify CNTs achieving better mwCNT dispersability without affecting the morphology of the co-electrospun PCL composite nanofibers [132]. Likewise, ester functionalised CNTs allow for better adhesion to polystyrene and polyurethane matrices to enhance the load transfer for strengthening in works presented by Sen and colleagues [133]. Mangeon et al. also grafted Poly(3-hydroxyalkanoate) onto mwCNTs using a catalyst free, transesterification approach to boost the compatibility and interactions between the reinforcing filler and the host PHA matrix [134].

Qi et al. utilized mwCNTs to encapsulate the drug compound doxorubicine hydrochloride prior to being added into the PLGA solution to be electrospun. The drug loaded CNT incorporation in the nanofiber provided a dual layer drug "container" which afforded effective loading and sustained drug release kinetics [64]. Amine functionalized CNTs were dispersed in formic acid with ultrasonication by Zainab et al. in the preparation of an electrospinning solution consisting of polyamide 6 dissolved in formic acid for CO₂ capturing membranes. Besides providing mechanical reinforcement, the presence of the $-NH_2$ sites on the CNT surface and the resulting high surface area of the electrospun nanofiber web serve to capture carbon dioxide efficiently [74].

CNTs can also be modified by Fried-Crafts acylation and in-situ polymerization leading to polyamide grafted CNTs [135,136]. When incorporated into solutions of PI or a PI/PANI blend and electrospun, the resulting composite nanofibers proved effective as reinforcing agents for an epoxy matrix, where the existing amine

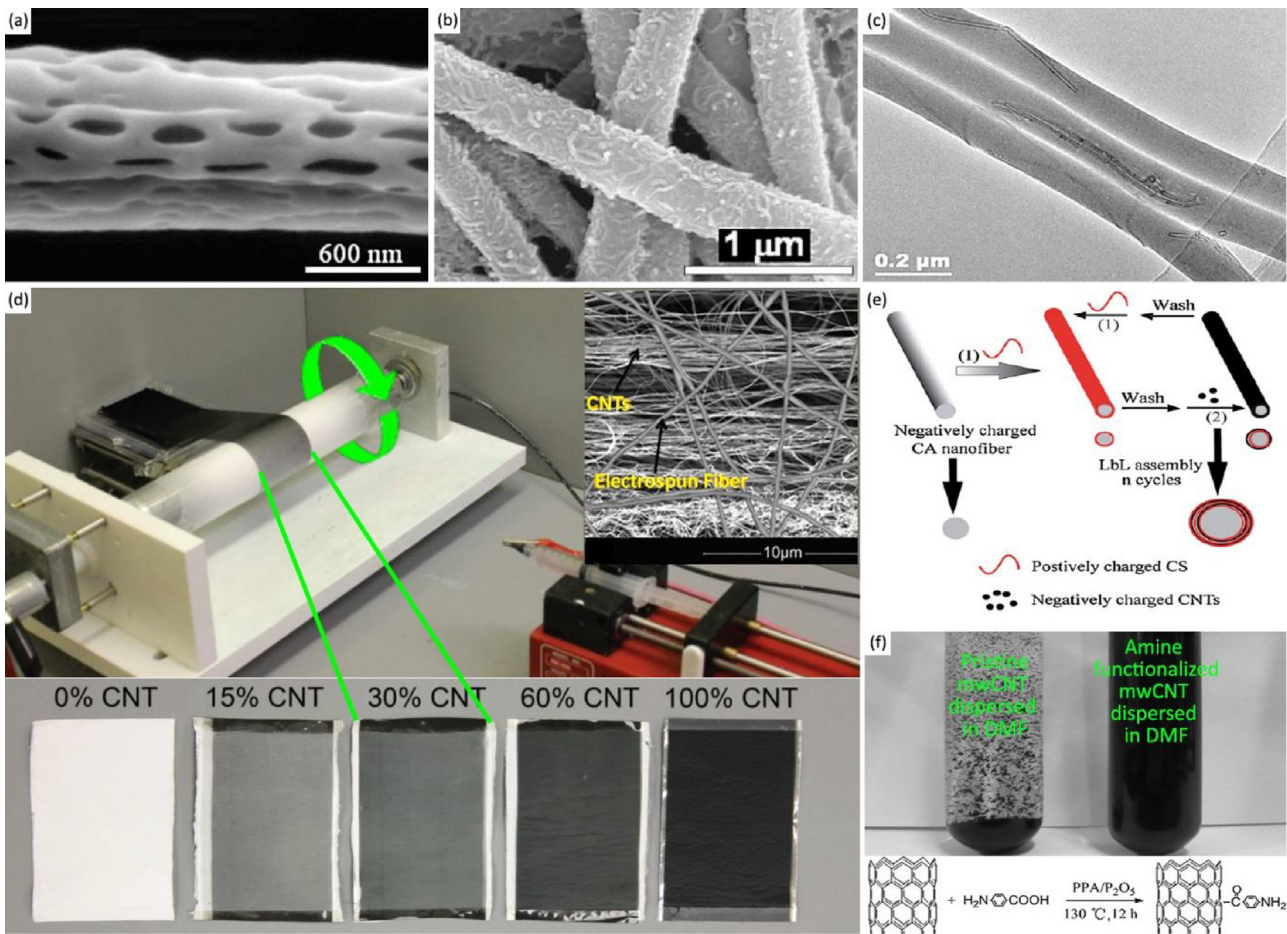


Fig. 2. (a) SEM detailing the nanoporous structure of a polycarbonate nanofiber co-electrospun with mwCNTs [154]. Copyright 2005, reproduced with permission from Elsevier Ltd; (b) SEM showing uniform CNT adsorption onto the surface of nylon 6 nanofibers [157]. Copyright 2006, reproduced with permission from John Wiley & Sons Inc; (c) TEM showing the dispersion and alignment of mwCNTs along the polyimide nanofiber axis [67]. Copyright 2014, reproduced with permission from Elsevier Ltd; (d) Experimental set-up for preparing hybrid fabrics by electrospinning PEO directly onto a horizontally-aligned mwCNT sheet being drawn by a rotating mandrel, as well as the hybrid fabric with different mwCNT layer thicknesses controlled by varying the mandrel rotation speed. The inset shows the microstructure of the hybrid fabric having thicker nanofibers laid over thinner bundles of mwCNTs [164]. Copyright 2015, reproduced with permission from the Royal Society of Chemistry; (e) Schematic illustrating the alternate deposition of negatively charged mwCNT and positively charged chitosan onto cellulose acetate nanofibers to fabricate a multi-layered nanofiber composite [165]. Copyright 2013, reproduced with permission from Elsevier Ltd; (f) Photograph showing effect of amine functionalization via Friedel-Crafts acylation on the dispersability of carbon nanotubes in a polar solvent along with reaction scheme detailing the amine functionalization [141]. Copyright 2010, reproduced with permission from John Wiley & Sons Inc.

functionality on the CNT surface allowed greater interactions with epoxide groups present in the polymer matrix to assist in stress transfer [9,136] Friedel-Crafts acylation was also used by Saeed et al. to prepare amine functionalized mwCNTs which were then grafted with PCL and sonicated with a PCL solution in a mixed solvent of chloroform and methanol. Electrospinning the resulting solution produced composite nanofibers which had the mwCNT fillers well dispersed throughout, and covalently bonded to the polymer matrix as evidenced by FTIR, conferring better mechanical and thermal properties resulting from the improved compatibility of the functionalized mwCNT filler [137]. Kong's group adopted the same methodology, utilizing the PCL grafted mwCNTs in co-electrospinning with PLA employing a parallel plate collector to obtain aligned composite fibers [138]. PAN grafted mwCNTs have also been prepared by reacting acid functionalized mwCNTs in DMF solvent with a PAN terpolymer in the presence of DCC and DMAP [139], via plasma induced grafting polymerization [140], or by Friedel-Crafts acylation followed by in-situ or ex-situ polymerization, as shown in Fig. 2f, [141] for better compatibility with the host polymer.

Other modifications to the properties of an electrospun mat that have been achieved include tuning the hydropho-

bility through the surface fluorosilanization of CNTs with 1H,1H,2H,2H-perfluoroctyltriethoxysilane (FTES). This eliminates the hydrophilic hydroxyl groups while improving the CNTs dispersability in solvent prior to co-electrospinning in a PVDF-HFP polymer solution [142], increasing the hydrophobic nature of CNTs [78] even further benefitting certain membrane distillation applications.

2.1.6. Nanofiber architecture

Composite nanofibers prepared by the co-electrospinning method can be further assembled into many macroscopic structures depending on the nanofiber collector used. Ko et al. took this approach to obtain yarn assemblies of aligned swCNT reinforced PAN/PVA nanofiber through a continuous drawing and twisting process [143], Imazumi collected mwCNT filled PVB nanofiber bundles on a rotating disk collector and twisted them into nanofiber yarns [80], Bazbouz employed a rotating disk in tandem with a take-up spool to impart twist and enable the continuous spinning of mwCNT filled nylon 6 nanofiber yarns [144]. Rakesh utilized rectangular slotted collectors plates with rounded ends to collect aligned mats of mwCNT reinforced PVA nanofibers [145]. Choi et al. utilized an interdigitated electrode for the collection of nanofibers

spun from a solution of PEDOT:PSS blended with PVP and acid functionalised mwCNT for use as a chemireistor.

Complex architectures of the individual electrospun CNT reinforced polymer composite nanofiber have also been achieved in the form of coaxial and porous nanostructures which have properties such as ion transport characteristics and larger surface areas that imbue additional performance advantages in certain applications [42]. Core-shell nanofibers with mwCNT core and cellulose shell were fabricated by Miyauchi et al. as insulated conductive cable fibers using a coaxial spinneret and an ionic liquid (1-Ethyl-3-methylimidazolium acetate) which acts as a non-volatile solvent for the electrospinning process. The core solution was prepared by grinding the ionic liquid together with the mwCNTs to form a gel, while the shell solution was prepared by diluting the commercially available cellulose ionic liquid solution. The nanofibers fabricated from the coaxial electrospinning were collected in a coagulation bath of water and ethanol to eliminate the ionic liquid, resulting in the precipitation of the core-shell nanofiber [146]. Longson et al. investigated the use of different solvent systems in the preparation of core-shell fibers containing a polymer free mwCNT core encapsulated in a PMMA shell via coaxial electrospinning. It was observed that the hollow core-sheath structures can be formed when the core solvent is immiscible with the shell solvent and is a non-solvent of the shell polymer, while the most clearly defined mwCNT bundle cores were formed when the core solvent was partially miscible with the shell solvent and is a solvent for the shell polymer [147]. The use of the core-shell nanostructure can also be extended to actuation as explored by McKeon-Fischer and colleagues. A core solution of PCL and acid-functionalized mwCNTs in a mixed solvent of DMF and DCM was coaxially electrospun with a hydrogel shell solution of an electroactive polyacrylic acid blended with PVA dissolved in ethanol and water. The fabricated nanofibers were collected on a rotating mandrel and cross linked to give the final scaffold in which the CNT functioned as an inner electrode [148].

On the other hand, Ojha et al. electrospun core shell nanofibers with CNT reinforced PEO sheaths covering PEO instead of having the CNTs in the core. This allows for a reduced percolation threshold for improved mechanical and electrical properties to be observed at lower CNT loadings. In their work, Gum Arabic was used to disperse the mwCNTs in water with the assistance of ultrasonication before a PEO solution was added. Characterization of the prepared core-sheath fibers showed no significant surface morphological difference to the single-layered PEO nanofibers, but a clearly discernible core-shell structure revealed from TEM analysis. It was also observed that the degree of mwCNT aggregation was more significant at equivalent CNT loadings when the CNTs are confined to the shell in the coaxially spun fiber [149]. mwCNTs were also incorporated locally in the shell material to decrease the percolation threshold by Sarvi's research group which prepared core-shell nanofibers having a PVDF core, and PVDF/PANI/CNT shells. Confining the CNT to the shell as well as incorporating conductive PANI to form bridges between the nanofibers served to improve the conductivity of the nanocomposite mat at similar filler loading levels thereby allowing the sheath layer to act as a transfer medium to interface with the piezoelectric PVDF core [150].

Porous architectures of CNT loaded polymer composite nanofibers can also be developed via electrospinning. Yang's research group investigated the use of different solvents in the electrospinning of CNT loaded PLA nanofibers from a PLA/chloroform solution and found the nature of the solvent played a big part in the nanofiber morphology, where volatile assistant solvents led to the formation of columnar, porous surfaces, and non-volatile assistant solvents favoured the development of flat nanofibers with grooves [151]. Dai et al. employed the use of a tri-block co-polymer F108 ((PEO)₁₃₃(PPO)₅₀(PEO)₁₃₃) as an emulsifier to disperse the

enzyme laccase as well as acid treated mwCNTs in a gel solution of PLLA dissolved in methylene dichloride. Electrospinning the prepared solution yielded composite nanofibers of PLLA encapsulating laccase and mwCNTs. SEM characterization showed a porous morphology resulting from the phase separation mechanism between air and the polymer in addition to the immobilization of the CNTs. The porous structure exposes more surface area for the enzymatic action and facilitates mass transport to improve the catalyst kinetics while CNTs improved charge transfer and mechanical stability [77]. Based on the technique pioneered by Amini et al. [152], Ebadi's group used co-electrospinning to prepare the poly(acrylic acid) nanofiber mesh reinforced by mwCNTs, then subsequently immobilized the enzyme acetylcholinesterase in by introducing the enzyme solution in the presence of cross linking agents [153].

Kim and coworkers fabricated porous mwCNT filled polycarbonate nanofibers by electrospinning a solution of commercially available polycarbonate-mwCNT nanocomposite and diluted in chloroform. TEM studies showed the mwCNTs embedded in the porous nanofibers are uniformly dispersed and well aligned. They posit that the nanoscale pores, as shown in Fig. 2a, were formed as a result of rapid solvent evaporation during electrospinning causing temperature changes along the jet as it is ejected from the pendant drop, causing thermodynamic instabilities. This in turn leads to phase separation via spinodal decomposition as solvent-rich and polymer-rich regions are formed, that form the pore and polymer matrix respectively [154]. Bayley and colleagues exploited the amphiphilic nature of the copolymer PAN grafted with PDMS to produce electrospun porous microfibers, where the porosity originates from phase segregation and self-assembly of the different domains of the copolymer. The addition of mwCNTs appeared to result in fibers of smaller diameters while preserving porosity, with the CNTs appearing to be exfoliated by the polymer and dispersed homogenously throughout the fiber [155]. Variations on producing nanofibers with porous morphology have been performed by Bounioux et al. via a single-step co-electrospinning of mwCNT filled Poly(3-octylthiophene) from a chloroform solution. Electrospinning of such conjugated polymers with controllable nanofiber morphologies is enabled by adjusting the polymer concentrations and solvent compositions [156].

2.1.7. CNT deposition on electrospun nanofiber and other post processing treatments

Apart from co-electrospinning to embed CNTs into electrospun nanofibers, another method of fabricating electrospun CNT polymer composites involves the deposition of CNTs onto the nanofiber substrates. Kim et al. pioneered a simple method of decorating Electrospun nylon 6 nanofibers with mwCNTs by firstly preparing a dispersion of acid functionalised CNTs in either an organic solution or with the aid of surfactants and ultrasonication, then immersing the spun nylon nanofiber mat in the dispersant, followed by simple washing and drying of the coated nanofibers. CNT adsorption, as shown in Fig. 2b, was found to occur densely and uniformly throughout the nanofiber mat with strong interactions between the amide group in the nylon and the acid groups on the mwCNTs [157]. The same technique was also applied to polyamide 11 nanofibers used as templates for the deposition of a mwCNT coating on the nanofiber surface by Havel et al. for transparent, conductive, thin films [158], as well as by Mercante et al. using electrospun polyamide 6/poly(allylamine hydrochloride) nanofibers for dopamine sensors [159]. Li and colleagues using nylon 6 nanofiber membranes for sulfhydryl sensors [160], Kang et al. using silk fibroin nanofibers for conductive electromagnetic interference shields [161], and Gao et al. using polyurethane nanofibers and ultrasonication to achieve hard, uniform CNT coatings [162]. Besides these methods, reducing agents has also been employed to achieve electrophoretic deposition to fabricate similarly CNT

coated nanofibers. Jose et al. co-electrospun PAN together with a gold precursor salt HAuCl₄, and reduced the hybrid nanofibers by soaking in a NaBH₄ solution and then in a HAuCl₄ solution to allow crystalline gold nanoparticle growth on the nanofiber surface forming a coating. Electrophoretic deposition then proceeds by immersing the coated nanofibers in a dispersion of mwCNTs with the aid of a Triton X-100 surfactant. Under an applied direct current bias, the negatively charged –COOH functionalised mwCNTs migrate to the positively charged nanofiber and sheath the gold primed nanofiber [163].

A different approach adopted by Yildiz and coworkers for the preparation of electrospun nanofibers composited with CNTs involves the direct deposition of nanofibers onto a separate carbon nanotube sheet layer, with their set-up presented in Fig. 2d. Vertically aligned, vapour grown CNTs were first sheared flat on the substrate using a razor blade and drawn from the horizontal orientation onto a rotating mandrel and taken up as a buckypaper sheet. A PEO in water solution was then electrospun onto the rotating mandrel electrode to deposit PEO nanofibers onto the rotating sheet of horizontally aligned CNT to encapsulate them. The hybrid fabric was then pressed, heated, and subject to pulsed plasma functionalization. The hybrid fabrics produced this way showed outstanding barrier properties and high specific surface area, mechanical flexibility, lightweight, and porosity [164]. Luo et al. employed a layer-by-layer, electrostatically driven self-assembly technique, alternately depositing the negatively charged, –COOH functionalised mwCNTs, and positively charged chitosan on the electrospun cellulose acetate nanofibers simply by immersing the nanofibers in a NaOH solution to give it an initial negative charge, then cyclically immersing the charged nanofibers in the chitosan solution, rinsing, then immersing in the mwCNT dispersion until the multi-layered nanofiber structure comprising mwCNT/chitosan bilayers has formed. Their methodology is schematically presented in Fig. 2e [165].

Several fabrication routes adopted by research groups include post processing steps that can alter the physical and chemical properties of the electrospun nanofibers such as cross-linking the co-electrospun mats [113,122], mechanical hot stretching [139], annealing [106], and chemical reactions like imidization [118,119] or deacetylation [112], offering researchers many more opportunities to prepare functional, high performance composite materials for many applications.

2.2. Preparation of electrospun graphene-polymer composites

The possibility of incorporating graphene and its derivatives in nanofibers is an exciting one especially since the 2D nanocarbons offer better thermal and electrical conductivities compared to their 1D CNT counterparts [131]. In the preparation of the electrospinning dope, the interactions, such as hydrogen bonding, between the polymeric component and the graphene based nanofiller affect the dope viscosity, conductivity, and rheology, and therefore electrospinning characteristics [166]. Careful control over parameters such as nanofiller concentration and chemistry, polymer and solvent interactions, as well as electrospinning conditions therefore determine the eventual nanofiber morphology and performance.

2.2.1. Co-electrospinning

Most electrospun graphene oxide based polymer composite nanofibers are fabricated via co-electrospinning a polymer solution incorporating graphene oxide (GO), typically prepared via Hummers method, with the aid of sonication to achieve dispersion of the synthesized graphene oxide in the solution, this could be followed by a reduction of the graphene oxide to graphene [167]. A wide variety of graphene reinforced polymer composite nanofibers with different morphologies can be prepared via this technique, such

as hollow PVA nanofibers as shown in Fig. 3b, which are formed as a result of solution rheology characteristics [168]. Other polymers such as PI [169], PLGA/collagen [170], PLA [171], PVDF, PVA [172], GO/PANI/PVDF [173], PCU [174], PCL [175,176] have also been electrospun using this method, with PEO occasionally being used to modulate the solution characteristics increasing solution spinnability [177], and stabilizers like Docusate sodium salt [176], Triton X100 [178], SDBS [179] or SDS [180] occasionally incorporated to reduce the surface tension of the solution or assist in the dispersion of the nanofiller.

Graphene oxide filled chitosan/cellulose nanofibers prepared using this method were much thinner compared to pristine chitosan/cellulose nanofiber, with FTIR analysis showing intermolecular hydrogen bonding between the oxygen functional moieties on the GO sheets, carbonyl and hydroxyl groups of bacterial cellulose, and amino groups on chitosan in work reported by Azarniya [177]. Shao et al. blended tussah silk fibroin and GO in with a PLGA polymer solution to electrospin a thin nanocomposite fiber scaffold for a bone tissue engineering scaffold, the hierarchical structure shown in Fig. 3c [181]. Nirmala et al. used a similar method to obtain conductive nylon nanofibers enriched with graphene oxide, and found that the presence of GO reduced the mean nanofiber diameter and improved the nanofiber electrical conductivity [182]. Albañil-Sánchez et al. prepared graphene oxide dispersed in formic acid via sonication, then added nylon 6,6 and hydrazine monohydrate to perform the reduction in-situ. The partially reduced graphene oxide, nylon polymer mixture was then electrospun to obtain reduced graphene oxide reinforced composite nanofibers, where residual oxygen functionalities increased filler-host interactions [183]. Wu prepared PVA nanofiber mats loaded with glucose oxidase and graphene by simple co-electrospinning, then cross-linking the PLA mats with glutaraldehyde and sulfuric acid. Graphene facilitated the electrocatalytic activity of the immobilized glucose oxidase enzyme by stabilizing the biological catalyst's conformation and improving charge transfer [184].

2.2.2. Graphene oxide functionalization and modification

Modification of graphene oxide with functional groups could improve their dispersability in organic solvents and provide novel chemistry for the incorporation of other materials that offer functional characteristics. Leyva-Porras et al. used the oxoammonium salt (Br-TEMPO) with triethylamine in DMF and introduce nitroxide functional groups on graphene oxide. The incorporation of the nitroxide groups helps play an important role in exfoliating the graphene sheets, and lead to embedded, well dispersed, thin platelets of graphene oxide in polymer nanofibers when co-electrospun with nylon 6 [185]. Glycine modified graphene oxide deposited with nanogold was also used as nanofillers in the preparation of PVA nanofibers. Yu et al. used a modified Hummers method to prepare graphene oxide, then grafted glycine amino acids on the surface of the graphene oxide by mixing with a glycine solution. The added glycine molecules enabled the reduction of HAuCl₄, to form gold nanoparticle decorations homogenously distributed on the graphene. The glycine functionalization further served to exfoliate the graphene oxide and also allowed hydrogen bonding with the PVA polymer matrix in which the nanofiller was co-electrospun with, thereby improving the nanofiber morphology and dispersing the filler more homogenously [365]. Li et al. used sodium citrate as a reducing agent in the presence of silver nitrate and nanoscale graphene oxide to prepare self-assembled silver nanoparticle/graphene hybrids that were mixed with a PVA solution and electrospun. A TEM micrograph showing the well incorporated hybrid particles within the nanofibers is shown in Fig. 3e [186]. A hydrothermal approach was employed by Almeida et al. to decorate GP with TiO₂ nanoparticles to be used as func-

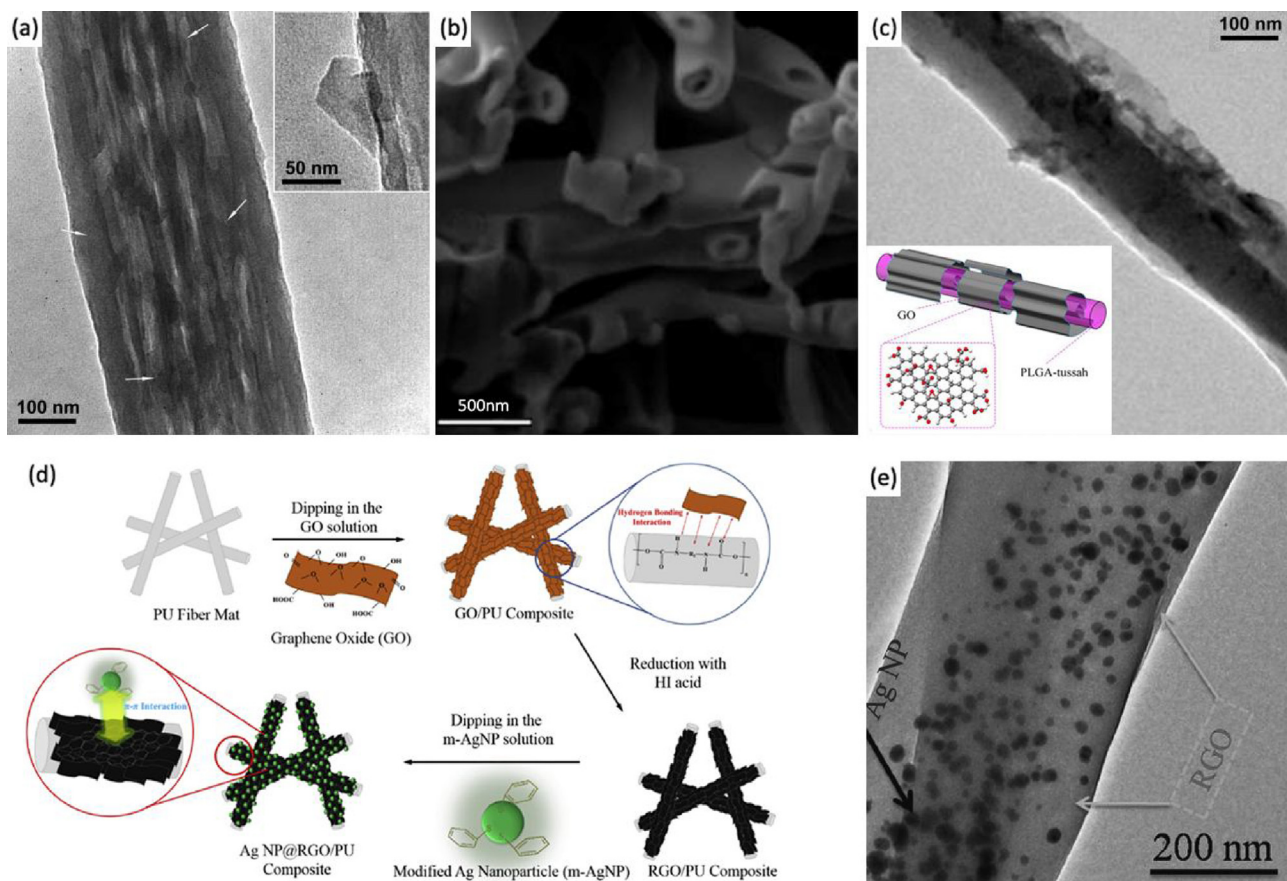


Fig. 3. (a) High-magnification TEM of graphene reinforced-PBASE/PVAc nanofiber with arrows indicating the presence of graphene flakes. Inset shows an expanded image with PBASE grafted graphene embedded in the sidewall of a PVAc nanofiber [190]. Copyright 2010, reproduced with permission from John Wiley & Sons Inc; (b) SEM of hollow PVA based composite nanofiber structures formed from co-electrospinning a 2 wt% thermally reduced graphene oxide [168]. Copyright 2015, reproduced with permission from the Royal Society of Chemistry; (c) TEM of graphene oxide reinforced PLGA-silk tussah nanofibers with inset showing a schematic of the hierarchical core-sheath structure achieved through dip-coating [181]. Copyright 2016, reproduced with permission from Elsevier Ltd; (d) Schematic showing the methodology for preparing graphene dip-coated composite nanofibers decorated with silver nanoparticles through non-covalent interactions [197]. Copyright 2015, reproduced with permission from Elsevier Ltd; (e) TEM of silver nanoparticle decorated graphene oxide incorporated within co-electrospun in PVA nanofibers [186]. Copyright 2016, reproduced with permission from John Wiley & Sons Inc.

tional composite nanofillers in electrospun P(VDF-TrFE) copolymer nanofibers for photocatalyst applications [187].

Besides modification with small molecules like amino acids, graphene oxide has also been functionalized with organic moieties and stabilized by polymerization. Savari et al. functionalized GO with TAA via an esterification reaction and co-polymerized the modified GO with conductive polymers like 3DDT or 3TEt via oxidation polymerization, thereby preparing conducting nanocomposites with much improved solubility in organic solvents. Co-electrospinning these nanofillers in PCL yielded electroactive, biocompatible nanofibers with potential applications in tissue engineering [188]. Zhang and colleagues grafted PEG on the surface of graphene oxide by first introducing carboxylic acid functionalization on GO in the presence of sodium hydroxide, then undergoing an esterification reaction between the carboxylic groups on GO and hydroxyl groups on PEG. The PEG grafted GO then can be coelectrospun with PLA, with PEG improving the matrix compatibility and surface adhesion, leading to composite nanofibers of superior mechanical and thermal properties [189].

Other non-covalent modification approaches include $\pi-\pi$ interactions with 1-pyrenebutanoic acid, succinimidyl ester (PBASE), which acts to separate graphene sheets by electrostatic repulsion, facilitating dispersion within the nanofiber, as shown in Fig. 3a [190]. Moayeri and colleagues adopted this modification to prepare conductive PANI/PEO nanofibers filled with the modified graphene

that demonstrated much improved electrical conductivity. Their approach eschewed covalent functionalization which introduces sp^3 sites on the graphene sheets, which would adversely affect its electrical properties [191]. Core-shell nanofibers consisting of P3HT-graphene cores and PEO shells were electrospun using a coaxial needle by Lin et al. for high performance field effect transistors. P3HT, as a conjugated polymer, assists in the dispersion of graphene to form a blend solution, and the eventual dispersion and confinement of graphene in the nanofiber upon electrospinning. The charge carrier mobility improvements were attributed both to the presence of graphene which provides preferential transport pathways, and also to the nanofiber alignment brought about by the specially designed rotating collector [192].

2.2.3. Deposition of graphene on electrospun nanofiber

Dip coating electrospun nanofibers has proven a popular and simple technique in fabricating graphene based nanofiber polymer composites. Aznar-Cervantes and colleagues fabricated silk fibroin nanofiber mats by electrospinning followed by annealing in methanol to induce β -sheet conformation. The mats were then immersed in aqueous graphene oxide solutions of varying concentrations and dried, with the process repeated several cycles to adsorb GO as a coating. Immersion in ascorbic acid then followed to partially reduce the graphene oxide *in situ*, leading to the formation of a conductive nanocomposite mat for biological

applications [193]. Adapting this approach, Lin et al. fabricated core-shell nanofiber mats comprising PVC and PLGA blended cores sheathed in a reduced GO shell by directly electrospinning the PVC/PLGA blend into an aqueous solution of dispersed GO. The formed hydrosol was then subject to heat treatment in a water bath prior to drying, which yielded a condensed coating of GO on the nanofiber, which was then reduced in hydroiodic acid and washed with ethanol for densification and to improve conductivity [194]. Polyurethane nanofibers with hydrogen bonded graphene oxide coatings were prepared in a similar dip coating manner by Hu et al. prior to reduction by hydrazine to leave a conformal graphene coat on the nanofiber surface for the fabrication of strain sensors [77]. Huang's group similarly coated nylon6,6 membranes with graphene oxide and performed the reduction through a combination of thermal reduction and hydrazine vapor exposure [195]. Yuan's approach was also similar, immersing the positively charged cross-linked electrospun PVA/PEI blended polymer nanofibers in the negatively charged GO solution, allowing electrostatic interactions drive the self-assembly of GO on the nanofiber before drying and subject the composite to a reducing vapor of hydrazine [196].

An analogous technique used by Hsiao et al. involves the electrospinning of PU nanofibers, dip coating with graphene oxide to allow hydrogen bonding to adsorb GO sheets onto the nanofiber surface, before reduction by hydriodic acid. Thiophenol modified silver nanoparticles were then introduced, forming $\pi-\pi$ interactions to adsorb to the nanofiber surface and enhance electrical conductivity. Their process is illustrated schematically in Fig. 3d [197]. His group also adopted a layer-by-layer approach for the preparation of water-borne PU nanofibers loaded with reduced GO. Oppositely charged suspensions of a positively charged DDAB-adsorbed GO and the negatively charged GO were used in an alternating fashion to deposit on the negatively charged PU nanofibers before reduction by hydroiodic acid, eventually forming bilayered reduced GO structures wrapped around interconnected PU nanofibers [198]. Zhou et al. fabricated graphene-polyelectrolyte multilayer scaffolds also using layer-by-layer assembly by alternately incubating polyethyleneimine primed electrospun PCL scaffolds in hydrazine reduced graphene oxide solutions mixed with either heparin or poly-l-lysine, with the assembled scaffolds capable of electroactivity and bio-functionality. Electrostatic interactions between the positively charged PEI primer and negatively charged graphene/heparin mixture serves as the driving force, allowing the formation of the smooth, multi-layer structure with interconnected porosity [199].

An alternative to dip coating, electrodeposition of a graphene on the surface of electrospun materials is an interesting approach for facile nanocomposite preparation. Gan et al. utilized a solution containing 1 mg mL^{-1} of graphene oxide, pyrrole monomer, and Sodium p-toluenesulfonate for the in-situ electro-polymerization of PPY. Electrospun PAN was first carbonized into conductive carbon nanofibers, which was then immersed in the solution as the working electrode substrate and a positive 0.8 V bias applied to "grow" the graphene/PPy composite on the surface without a binder, leading to a composite demonstrating improved capacitive performance attributed to an interwoven, porous structure with graphene in the shell facilitating charge transfer [200]. Another approach relied on hot pressing to densify a PAN nanofiber membrane later covered with a graphene oxide sheet layer for the preparation of a bilayer nanofiltration membrane. Vacuum assisted filtration was used to deposit graphene oxide from an aqueous GO suspension onto the pressed PAN nanofiber membrane, then dried and thermally reduced to form the reduced graphene layer of the bilayer membrane [201]. This vacuum assisted deposition method was also adopted by Cheng and coworkers for the preparation of a PVA-graphene oxide bilayer membrane [201].

2.2.4. Graphene as a nucleating agent

Graphene can also be dispersed in solution via ultrasonication in a suitable solvent, then blended with polymer solutions containing PCL/gelatin blends [202], PLLA [203], Nylon 6,6 [204] to be co-electrospun into nanofibers. Multi-layered graphene dispersions obtained from disaggregation, filtration, re-dispersion of graphite flakes in chloroform have been co-electrospun with PLA, and have demonstrated by Dias et al. to result in thinner nanofibers, and act as effective as nucleating agents in promoting PLA crystallization, reducing the half crystallization time from 10.98 min to 3.41 min as the graphene content increases from 0 to 1 wt% [205]. Making use of graphene oxide nanofillers to temper the crystallinity of an electrospun polymer composite has interesting implications in terms of modulating the physical and electromechanical properties. Issa et al. prepared PVDF/GO composites by adding the GO/DMF solution in a solution of PVDF in a mixed DMF and acetone solvent and ultrasonicating the mixture prior to electrospinning. They noted that the addition of a small amount of GO (0.1 wt%) resulted in an increase in the electroactive β phase of PVDF, positing that the strong interactions between the electron pairs on the GO and strongly electronegative fluorine on the PVDF chains induced the arrangement of PVDF polymer chains into the β configuration during crystallization [206]. Huang et al. likewise prepared a book-shaped triboelectric nanogenerator also using graphene oxidized reinforced PVDF nanofibers, with the incorporated GO dispersed in the fibers, modifying the electrification surface and acting as charge trapping sites, increasing the available interface for storing charge [207]. Liu's group utilized the same technique to incorporate hydroxyapatite in addition to GO in the electrospun PLA nanofibers membrane [208] whereas a further photopolymerization step was included in Diez-Pascual's method to crosslink the PGA and PPF copolymer by incorporating the photoinitiator BAPO and exposing the electrospun nanofibers to UV light [209]. Barzegar et al. on the other hand prepared graphene foam utilizing chemical vapor deposition on a nickel foam substrate, which is then removed by etching using HCl, having drop-coated PMMA to preserve the graphene. PMMA was then removed via immersion in acetone then isopropanol before annealing in an oven. The prepared graphene foam was then ultrasonicated and added to 10 wt% PVA solutions before centrifugation and electrospinning to give graphene reinforced PVA hollow nanofibers, with the hollow nanostructure attributed to the polarization of the solvent used, causing solvent molecules to align and form the core [210].

2.2.5. Graphene functionalization and modification

While graphene has drawn keen interest as nanofillers for electrospun nanofibers, achieving good dispersion of graphene sheets, as compared to graphene oxide, is extremely challenging due to van der waal's forces induced aggregation. Covalently modified graphene nanoflakes with carboxylic acid functionalization was used by Khan et al. in the fabrication of co-electrospun graphene reinforced PAN and PMMA nanofibers. The electrospinning dope was prepared utilizing a simple ultrasonication dispersion process enabled by the dispersability of the functionalized graphene. It was found that many of the properties like ionic conductivity and wettability were improved as a function of incorporated graphene content [211].

Dispersing graphene through harsh chemical oxidation and thermal reduction [167,168] could result in defects and other undesirable oxidative damage. Non-covalent functionalization of graphene offers a simple way of dispersing pristine graphene through the use of a polymer stabilizer. Das and colleagues prepared graphene dispersions using expanded graphite in water with the assistance of PVP and ultrasonication to disperse the graphite and centrifugation to remove agglomerates. Subsequent addition of PVA to the supernatant forms the viscous electrospin-

ning dope which is then electrospun to give graphene reinforced PVA nanofibers with 0.5 wt% graphene loading relatively well distributed throughout the fiber. They observed for the graphene incorporated dope, a relatively high flow rate of 15 mL h^{-1} , and voltage of 15 kV was required to form bead-free nanofibers, with the higher elasticity and conductivity of the jet attributed to the addition of graphene [167].

2.2.6. Graphene quantum dots and CNT/graphene hybrids

Apart from electrospinning graphene or GO, electrospun polymer nanofibers containing graphene quantum dots (GQD) also present an exciting research direction, where the smaller sizes of the graphene platelets used present altogether new unique properties resulting from their edge effect and quantum confinement. Zhang and coworkers prepared graphene quantum dots by a hydrothermal method, starting with an aqueous graphene oxide solution mixed with ammonia, and subjecting the mixture to sonication and autoclaving to obtain the filtrate. Boiling the filtrate and dialyzing the suspension yielded the graphene quantum dot solution. PVA was added to the GQD solution with ultrasonication and the polymer solution electrospun to give GQD filled PVA nanofibers which demonstrated good nanofiller distribution and photophysical properties [212].

Besides GQDs, there are other examples of graphene based nanocarbon structures that have been electrospun, such as hybrids of CNT and graphene [213,214]. Holmes used an arc-discharge method to prepare carbon nanomaterial mixture of swCNT and graphene before incorporation in an coelectrospun PCL nanofiber [213]. Yao et al. used graphene oxide as a dispersant for mwCNTs through $\pi-\pi$ interactions, and co-electrospinning PVA nanocomposite fibers filled with GO and mwCNT, and finally reducing the material with hydrazine [215]. In another work, Liu et al. prepared hybrid CNT-graphene nanofillers by partial longitudinal unravelling of mwCNTs, carried out by dispersing mwCNTs in concentrated sulfuric acid and adding the oxidizing agent powdered potassium permanganate and phosphoric acid to the dispersant. The dispersant was then added to ice water containing hydrogen peroxide and allowed to coagulate, with the precipitate washed with HCl, dialized, then reduced by exposure to hydroiodic acid to form the hybrid fillers. CNT-graphene nanoribbon hybrids which have a unique structure consisting of CNTs acting as linking bridges between graphene sheets and having appreciable interfacial interactions. When co-electrospun with PAA and subject to a thermal imidization process, the resulting polyimide nanofibers containing 0.5 wt% - 9 wt hybrid fillers showed homogenous nanofiller dispersion in the fibers and enhanced mechanical, electrical, and thermal properties [214].

Matsumoto et al. adapted the same methodology and prepared graphene loaded nanofibers assembled into macroscopic yarns. Their method employed the same mwCNT unzipping process to prepare GO nanoribbons which are then added to PAN/DMF solutions to be electrospun, where the nanofibers are collected on a rapidly rotating disk collector as aligned bundles which are then twisted into yarns and subject to thermal treatment to densify the yarn. GO nanoribbons were observed to be well aligned in the fiber direction as a result of the electrospinning, and further contributed as a promoter of the ordered graphitic structure during the carbonization of PAN into carbon nanofiber in subsequent steps [216].

2.3. Preparation of electrospun fullerene-polymer composites

Fullerenes are a class of nanocarbon compounds described as “cage-like” arrangements of carbon atoms presenting pentagonal and hexagonal faces [217,218]. The distinctive combination of their molecular level 3-dimensional structure, in tandem with functionalizable chemistry imbue fullerenes with a novel set of physical

and electrochemical properties [219] that hold much promise in the preparation of advanced materials for numerous applications in fields such as photovoltaics [220,221], hydrogen storage [222], and nanobiology [223,224]. Fullerenes are thus a compelling candidate for incorporation into polymeric nanofibers where their potential properties can be exploited.

Li et al. adopted a simple approach to prepare the electrospinning solution for the fabrication of a cellulose/polyhydroxy fullerenol ($C_{60}-(OH)_n$) biocompatible electroactive actuator. The cellulose acetate polymer was first dissolved in a mixed solvent consisting of DMAc and acetone by vigorous stirring, followed by the addition of commercially available $C_{60}-(OH)_n$ added and sonicated to yield a homogenous solution. Using the typical needle electrospinning approach yielded a mat of nanofibers having localised fullerenols dispersed in the core, with porous morphology mimicking the fibrous structure of muscle tissue. The minute concentrations of dispersed fullerenols provided the cellulose nanofibers with the necessary electrochemical and mechanical properties to achieve the actuation effects, however, higher concentrations tended to give rise to beading instabilities. This is the result of strong elongational forces attributed to repulsion between charges accumulated at agglomerates of the electrostrictive fullerenols within the polymer jet. As such, careful tuning of the fullerenol content of the spinning solution is needed [225].

Qiao et al. similarly prepared an electrospinning solution by first preparing fullerene-like carbon nanoparticles (FLCNP) by combusting castor oil, followed by mixing the collected soot with a solution of 6 wt% Polyvinylpyrrolidone (PVP) in ethanol. Electrospinning the prepared solution onto a nickel foam collector gave rise to PVP nanofibers containing the nanoparticles decorated on the surface, as well as within the nanofiber, with relatively homogeneous particle distribution. Nano-crystalline silicon (Nc-Si) shells were then deposited on the nanofibers using a plasma enhanced-chemical vapor deposition technique to prepare FLC core/Nc-Si shell nanofibers composite electrodes without the addition of conductive binders. Their technique is schematically represented in Fig. 5a [226]. Bounioux et al. prepared electrospun Poly(3-Hexylthiophene) (P3HT) nanofibers loaded with single-walled carbon nanotubes (swCNT) along with a fullerene derived electron acceptor phenyl-C₆₁-butyric acid methyl ester (PCBM) for organic photovoltaic applications as well. The electrospinning solution was prepared by dispersing the swCNT and PCBM in chloroform with tri-block copolymer PEO as a surfactant followed by sonication, centrifugation, and decanting to collect the homogenous, “ink-like” supernatant containing the nanocarbon. Various amounts to these dispersions were then added to a solution of P3HT dissolved in chloroform and trichloroethylene, with PEO added to increase the viscosity of the solution to facilitate electrospinning. Electrospun P3HT-PCBM-swCNT nanofibers showed long, thin, uniform morphology, with flow induced stretching of the P3HT chains and swCNTs [227].

PolyLactide-co-Glycolide (PLGA) nanofibers loaded with fullerenes have also been co-electrospun on quartz crystals for the preparation of gluconic acid monitoring sensors. The fullerenes were first dissolved in DCM till saturation, and then added to THF and DMF in a 3:1:1 proportion – The DCM contributed to the mechanical aspects of the spun nanofiber and THF and DMF served to tune the solution conductivity to enable electrospinning. PLGA was then added to a 20 wt%, and the prepared solution electrospun as a nonwoven mat onto the surface of cleaned gold quartz crystals, dried in a vacuum, and exposed to UV light for sterilization prior to use [228].

Fullerenes have also been incorporated in poly(L-lactide) (PLLA) nanofibers to obtain a core-sheath architecture for bioimaging and drug delivery applications, leveraging the fullerene's fluorescent properties and outstanding cell permeability characteristics.

In both cases, Liu et al. adopted a blend electrospinning methodology, to incorporate the water soluble fullerenes with different functionalities in PLLA nanofibers where the fullerenes were encapsulated in the nanofiber core. Their simple approach begins with the treatment of the fullerene to obtain fullerene-tetraethylene glycol nanoparticles (C_{70} -TEGs), followed by dialysis and lyophilization to obtain nanoparticle powders. A solution of PLLA in chloroform was then added to a solution of the C_{70} -TEGs in DMF and blended together with therapeutic drugs like paclitaxel and homogenized to form the electrospinning solution. Composite nanofiber mats electrospun from these solutions can then be dried before implantation into the host, whereupon the biodegradable PLLA breaks down, releasing the fullerene nanoparticles for therapeutic/imaging purposes. The water soluble fullerenes were also noted to produce a hydrophilic effect on the nanofibers which could modulate drug release rates [229,230].

Rather than incorporating the fullerene additive into the electrospinning solution *via* mechanical means like ultrasonication, a different approach was adopted by Pierini et al. which involves the grafting of a C_{60} fullerene onto a copolymer poly[3-dodecylthiophene-co-3-(6-fullerenylhexyl)thiophene] (CoP(3DDT)) to give CoP(3DDT)-(C₆₀HT). The grafted copolymer was then dissolved in chloroform and added to a separate solution of PEO in chloroform to give an electrospinning solution consisting of 3.3 wt% CoP(3DDT)-(C₆₀HT) and 0.7 wt% PEO. The nanofibers produced from electrospinning the mixed solution under careful climate controlled conditions were collected as an aligned mat on a rotating metal drum collector, and washed in isopropanol at elevated temperatures to selectively remove the PEO to leave CoP(3DDT)-(C₆₀HT) nanofibers, which were then dispersed in chlorobenzene and deposited by doctor blading onto a photovoltaic device [231]. A similar approach was adopted by Stoilova et al., where poly(ϵ -caprolactone) (PCL) was grafted on a C₆₀ fullerene core by azide-facilitated chemical reaction to form a nanohybrid. The fullerene core, star-shaped nanohybrid can then be dissolved in chloroform, or be added to known amounts of a PCL solution to tube the solution concentration. The star-shaped fullerene polymers are expected to be less efficient at forming chain networks as opposed to linear polymers, hence needing higher concentrations for electrospinning to be effective, however, observations showed that grafting with lower molecular weight arms led to thinner fibers with less beading. It was posited that the hydrophobic interactions between the C₆₀ cores may have contributed to stabilizing the electrospun fibers, thus accounting for the relatively low polymer concentrations required for fiber spinning [232].

Complexes of syndiotactic-PMMA with unfunctionalized fullerenes (C₆₀ and C₇₀) prepared by high temperature electrospinning have been reported by Matthew et al. C₆₀ or C₇₀ was first added into a 1:1 (v/v) mixture of toluene : 1,2-dichlorobenzene (DCB) with stirring and heating to allow for dissolution. On cooling, the obtained gel was subject to centrifugation, with the solvent mixture decanted with fresh toluene introduced to rinse the gel and the process repeated to remove uncomplexed fullerenes before drying the washed gel in a vacuum oven. DMF was then introduced, together with equal amounts of toluene and DCB, to dissolve the dried gel, exploiting the higher dielectric constant of DMF to facilitate the electrospinning. The prepared 20%wt complex suspension was then heated to give a solution and charged to a syringe fitted to a condenser filled by a heated oil reservoir to maintain the solution viscosity. Nanofibers resulting from the heated electrospinning were collected between split-electrode plates to achieve uniaxial alignment, with the fullerenes shown to be fully encapsulated within the helical cavity of the PMMA. This resulted in the stiffening of the fibers, leading to greater

orientational effects in the shear field that the fibers are subject to as they are spun [233].

2.4. Preparation of electrospun carbon nanodiamond-polymer composites

Nanodiamonds (ND) have received much attention in the biomedical field for their outstanding mechanical and chemical properties along with their bioamenable attributes [234,235] in applications ranging from tissue engineering scaffolds [236] to vehicles for drug delivery [237] and bio imaging/sensing [238]. The relatively economical and scaleable synthesis of NDs, coupled with the straightforward modification routes to achieve different chemical properties [239,240], make NDs a good candidate for functional fillers in polymeric nanofibers to achieve improved mechanical and biological performance.

Works by Parizek et al. and Brady et al. based on incorporating NDs in electrospun polymer nanofibers represent the typical blueprint to obtaining the electrospinning solution. PolyLactide-co-Glycolide (PLGA) of 85% L-lactide and 15% glycolide was first dissolved in a solvent mixture of methylene chloride (MCL) and N, N-dimethyl formamide (DMF), before NDs were added, mixed, and sonicated to obtain the well-dispersed electrospinning solution. In their methodology, a needle-less electrospinning approach was employed to fabricate the composite nanofibers. The electrospinning solution was repeatedly deposited by micropipette onto a spike-like electrode, from which nanofibers were expelled toward the counter electrode and collected on a polypropylene fabric to build up the thickness of the nanofiber layer [241,242]. It was found that NDs tended to be organized as beads in the core of the nanofibers or else as clusters that bulge from the fibers [242].

Cai and coworkers added NDs to a PLA electrospinning solution to fabricate ND reinforced PLA nanofibers by typical needle electrospinning. They found the ND content affected the nanofiber morphology in terms of diameter and uniformity. Higher ND loadings resulting in increased solution conductivity which favors the formation of thinner nanofibers, whereas ND aggregation at high loading levels are responsible for the beaded morphology observed in SEM micrographs of the nanofibers, as shown in Fig. 4 [236].

Cao et al. prepared fluorescent nanodiamond filled electrospun polycaprolactone by firstly passivating commercially obtained detonation nanodiamonds with octadecylamine (ODA) to obtain ODA-functionalized NDs. To incorporate these ODA-functionalized NDs into the electrospinning solution of polycaprolactone (PCL), the powdered ODA-functionalized NDs were simply added to a heated solution of PCL dissolved in acetone with vigorous stirring for 2 h. The solution was then electrospun onto aluminum plate collectors to yield randomly aligned non-woven PCL nanofiber mats that have improved mechanical strength, but also added optical functionality [243].

Ullah et al. prepared polymethylmethacrylate (PMMA) nanofibers filled with nanosized mono-crystalline diamonds functionalized with hydrazine hydrate for composite reinforcement applications. Varying amounts of the functionalized diamond particles were dispersed in DMF, then added to the polymer solution and mixed to form a PMMA/diamond particle solution which was subsequently optimized for electrospinning to obtain nanofibers with smooth morphology. It was found that the reaction with hydrazine led to amine functionalized diamond particles which were better able to have interactions with the solvent while forming the polymer jet during electrospinning, increasing the solvent evaporation time, thereby leading to thinner nanofibers compared with their non-functionalized diamond particle counterpart [244].

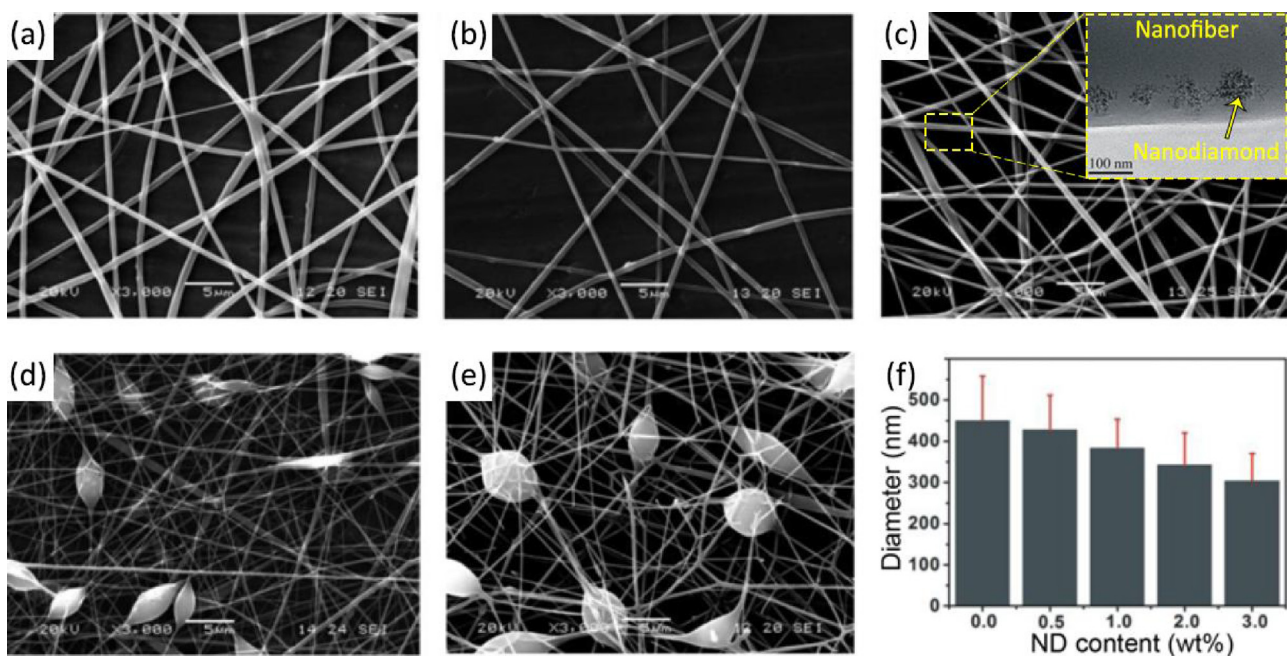


Fig. 4. (a) SEM showing uniform morphology of neat PLA nanofibers; (b) SEM showing uniform morphology of PLA nanofibers loaded with 0.5 wt% ND; (c) SEM showing uniform morphology of PLA nanofibers loaded with 1 wt% ND. Inset shows the TEM highlighting the presence of nanodiamond clusters within the nanofiber; (d) SEM showing beaded morphology of PLA nanofibers loaded with 2 wt% ND; (e) SEM showing heavily beaded morphology of PLA nanofibers loaded with 3 wt% ND; (f) Bar chart illustrating the decreasing trend of nanofiber diameter with increasing ND loadings [236]. Copyright 2014, reproduced with permission from Springer.

Electrospun composite polyvinylalcohol (PVA) nanofibers with nanodiamond fillers were also fabricated by Wang and coworkers to improve mechanical strength of the prepared nanofibrous scaffold. Their technique uses relatively benign synthesis conditions eschewing the use of organic solvents, using a water-soluble polymer instead. A solution-intercalation approach was adopted to prepare the electrospinning solution, where NDs were first dispersed in water by stirring, followed by sonication. The dispersion was subsequently heated, and PVA powder added gradually to form the eventual electrospinning solution. The ND addition was also shown to have played an important role in modulating the conductivity of the electrospinning solution, acting as a “lubricant” and facilitating the stretching of the expelled jet in the electrostatic field during electrospinning, thus increasing the homogenization of the composite nanofibers [245].

Behler and colleagues adopted the electrospinning methodology to suppress the re-agglomeration of nanoparticles in nanocomposites. Their methodology involved acid treatment of the ND according to the polymer/solvent system they would be introduced to, followed by the addition of the appropriate solvent with stirring and sonication to achieve dispersion. The polymers are then introduced to suspensions of different ND loadings to form the electrospinning solution, which is then electrospun into nanofiber mats. They reported a selective increase in surface carboxylation upon acid treatment after air oxidation of the NDs, leading to increased solubility in polar solvents, and a reduced tendency for agglomeration. The morphology of the nanofibers produced from their approach is shown in Fig. 5c. Through their methodology, large volume fractions of ND powder incorporated in electrospun polyacrylonitrile and polyamide nanofibers was achieved, up to 80 wt% and 40 wt% respectively, paving the way to develop ND coatings for protective applications [246].

Multi-walled carbon nanotube (mwCNTs) have also been combined with NDs in fabricating composite polyazopyridine nanofibers by Kausar et al. for the development of reinforced epoxy composites. Their synthesis pathway begins by grafting polyamide (PA) on the mwCNT surface through in-situ polymerization and

Friedel-Crafts acylation, and is then followed by dissolving the PA grafted mwCNT together with the AP in N, N-dimethylacetamide (DMAc). The nanodiamond component is separately prepared by dissolution in DMAc and sonicated to achieve dispersion. The two prepared solutions are then mixed to obtain the electrospinning solution, which is then used to obtain composite nanofibers of a polyazopyridine matrix, loaded with both ND and PA grafted mwCNT fillers, and collected on a spinning disk shaped collector before being dried and dipped into Diglycidylether of bisphenol A (DGEBA) and cured to form a reinforced epoxy composite [247].

Another interesting approach to fabricating these polymer/ND composite nanofibers was proposed by Mahdavi et al. The employed the biopolymers chitosan and bacterial cellulose, and incorporated NDs to facilitate the electrospinning process, decrease the fabricated chitosan fiber diameter, improve the mechanical performance, and allow the incorporation of bioactive compounds. The electrospinning solution was prepared by dissolving the chitosan in water and acetic acid and blended together with a gel of bacterial cellulose. A PEO solution was then prepared and incorporated in the previous solution order to reduce the gel viscosity. Similarly, the ND solution was prepared by dispersing ND in water, followed by sonication then added to the polymer solution and sonicated again. Nanofibers spun from this electrospinning solution were then collected on a rotating drum collector [248].

2.5. Preparation of other electrospun nanocarbon-polymer composites

While much research attention has been focused on nanocarbons such as fullerenes, carbon nanotubes, and graphene, other polymorphs of carbon such as superfine activated carbon, carbon black, nanographite, and carbon quantum dots have also been utilized as nanofillers in electrospun polymer nanofibers, enriching the nanofibers with unique properties, while also presenting possible cost, environmental, and processing advantages over their more well-studied nanocarbon counterparts [249].

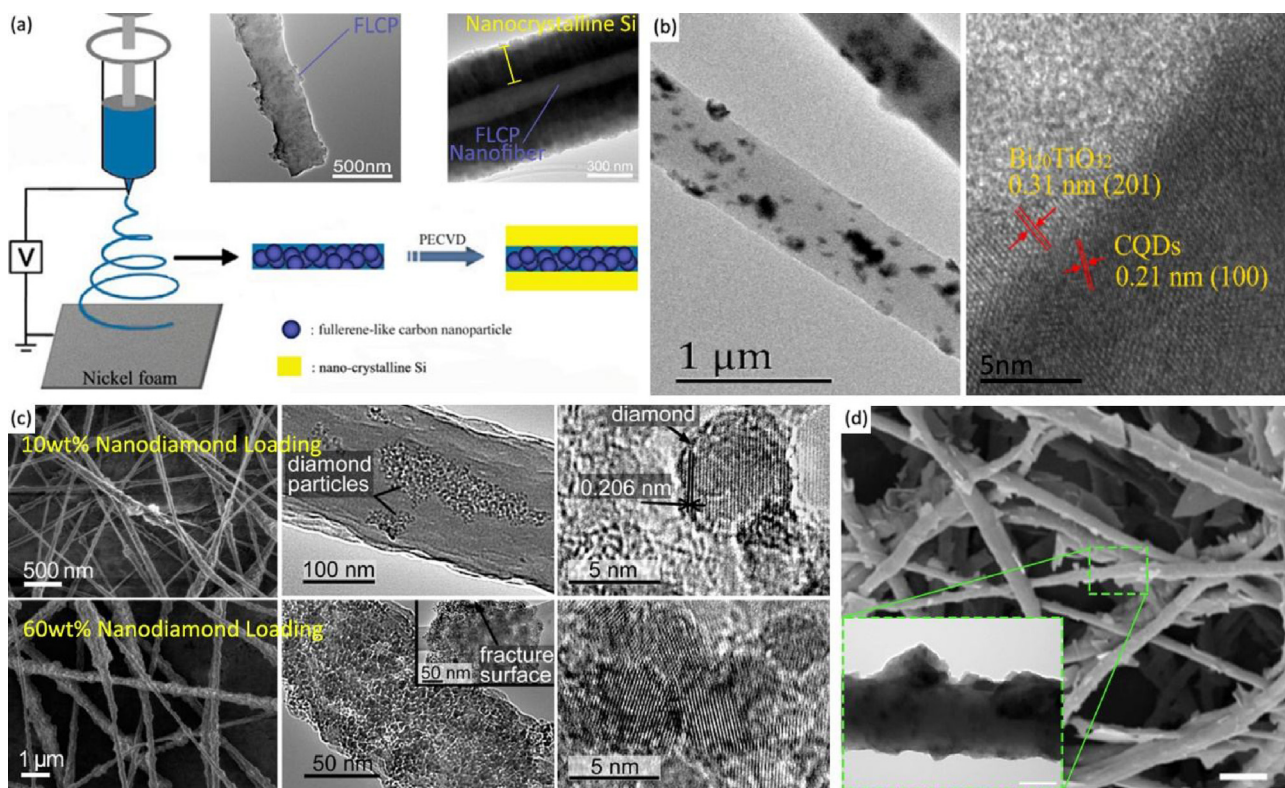


Fig. 5. (a) Schematic showing the encapsulation of fullerene like carbon nanoparticles (FLCP) in PVP nanofibers with post processing plasma enhanced CVD to grow crystalline nanosilicon on the nanofiber surface forming a core-sheath structured organic/inorganic hybrid material [226]. Copyright 2013, reproduced with permission from Elsevier Ltd; (b) (Left) TEM of PAN nanofibers incorporating evenly distributed hybrid CQDs- $\text{Bi}_{20}\text{TiO}_{32}$ nanofillers by co-electrospinning. (Right) High resolution TEM scan showing distinct fringe patterns corresponding to the different crystal lattices of the CQD and $\text{Bi}_{20}\text{TiO}_{32}$ in the hybrid photocatalyst [255]. Copyright 2017, reproduced with permission from Elsevier Ltd; (c) (Top row) SEM and TEM micrographs showing the morphology and structure of 10 wt% nanodiamond incorporated PAN nanofibers. (Bottom row) SEM and TEM micrographs showing the morphology and structure of 60 wt% nanodiamond incorporated PAN nanofibers, with inset showing fracture surface of the composite nanofiber [246]. Copyright 2009, reproduced with permission from the American Chemical Society; (d) Microstructure of graphite nanoplatelet anchored polyurethane nanofibers obtained through ultrasonic agitation induced collisions with the nanofiber, with inset showing the TEM detailing the rough surface texture [261]. Copyright 2013, reproduced with permission from the American Chemical Society.

Apul et al. achieved superfine powdered activated carbon (sPAC) incorporated polymer nanofibers *via* a one-step co-electrospinning method for the preparation of an organic pollutant filtration membrane. They applied wet bead milling to pulverize powdered activated carbon (PAC) into sPAC, having particle diameters between 100–400 nm, a hundred times smaller than the original PAC particles. Then, 5 wt% of the sPAC was dispersed in DMF *via* sonication prior to the addition of polystyrene to prepare the co-electrospinning solution. The collected nanofibers contained sPAC incorporated well in the PS matrix while conserving the availability of adsorption sites and greatly increasing the available surface area of the membrane [250].

An allotrope of carbon with great industrial significance is carbon black, which when incorporated in polymer matrix, allows the polymer to undergo an insulator-conductor transition if a critical percolation of the incorporated conductive carbon black filler is achieved [251]. Besides the use of intrinsically conducting polymers such as PANI, which are difficult to spin [252], electrospun polymer nanofibers utilizing carbon black as a conductive filler have been shown to possess high porosity and large surface areas with controllable morphologies and architectures, enabling their use in a wide variety of fields such as electronics, biomedicine, energy devices, and filtration [249]. Schiffman and co-workers managed to incorporate a high loading of carbon black (62.5 wt%) in chitosan nanofibers through co-electrospinning of a dope prepared by simply mixing CB with a chitosan/TFA solution. Crosslinking the

electrospun nanofibers using glutaraldehyde vapor resulted in the fabrication of a chemically stable membrane in acidic and basic aqueous solutions without leaching, demonstrating the effective encapsulation and immobilization of carbon black in the nanofiber [251]. Hwang et al. incorporated CB in a PU nanofiber also by co-electrospinning, using a sonicator to achieve dispersion of the CB in the DMF/chloroform solvent system prior to adding the PU. They observed the filler content playing a deterministic role in the fiber morphology and bonding structure of the nanofiber mesh, thereby affecting the macroscopic properties of the nanofiber web [252]. Similar approaches have also been used in the preparation of PVA [253] and PAN [249] nanofibers loaded with CB.

Carbon quantum dots (CQD) are another class of nanocarbon materials that have piqued research interest due to their unique tunable optical, electrical, and photochemical properties. Encapsulating these CQDs in an electrospun nanofiber allows the preservation of single CQD fluorescent behaviors by dispersing them in a polymer matrix to avoid Förster resonance energy transfer between adjacent CQDs [254]. Xie and colleagues made use of a facile hydrothermal process to obtain CDQs, then prepared CQD modified $\text{Bi}_{20}\text{TiO}_{32}$ photocatalysts *via* a solvothermal process in which the CQDs were uniformly decorated on the $\text{Bi}_{20}\text{TiO}_{32}$ [255]. These composite photocatalysts were then incorporated in a PAN solution and co-electrospun using a core-shell needle to obtain core-sheath nanofibers having a PAN core and a PAN/photocatalyst shell, effectively decorating the nanofiber surface with the com-

posite photocatalyst, as revealed in TEM and SEM micrographs in Fig. 5b. CQDs functioned as up-converting photosensitizers for absorbing near infrared light, and also prevented electron-hole recombination in the composite photocatalyst thereby improving catalytic performance [255].

Co electrospinning was also adopted by Alam et al. in the preparation of CQD reinforced blended PAN/PAA polymer nanofibers. Nitrogen containing CQDs prepared via microwave assisted pyrolysis were dispersed in DMSO and used to dilute a PAN/PAA solution in DMSO to form the electrospinning solution. Electrospinning yielded transparent composite nanofibers exhibiting rough textures with CQDs uniformly present throughout the fibers as determined from TEM analysis. They observed that the OH- and COOH- groups present on the CQD surface facilitated dispersion in the polar DMSO solvent, and enabled ester-bond stabilization by PAA, contributing to the dispersion and confinement of the CQD in the blended polymer matrix [254].

Hybrid electrospun nanofibers decorated with CQDs and mesoporous silica have also been prepared by the Stöber approach facilitated by CTAB. Li et al. prepared an electrospun PAN nanofiber mat and immersed it in a solution of CQDs, TEOS, and CTAB in ethanol and water with ammonium hydroxide to form a cladded nanofiber structure having a PAN core cladded with a mesoporous silica shell with CQDs distributed uniformly in the cladding. The hierarchical structure led to a passivation of the CQD active surface by hydrogen bonding during the immobilization, resulting in greater photostability [256].

CQDs also have tunable chemistries which can be exploited for fabricating a wide variety of functional nanofibers. Mosconi et al. prepared N-doped, amino terminated CQDs using a microwave facilitated hydrothermal method using arginine and 1,2-ethylenediamine as precursors. Crosslinked nylon-like polymers, prepared by interfacial polymerization of 1,6-hexamethylene-diamine, sebacoyl chloride, and the amino groups of the CQDs in a two-step process, were then dissolved in formic acid and electrospun to give covalently linked, N doped CQD reinforced nylon nanofibers. They found that larger fibers were obtained when the CQD content increases, likely due to heavier crosslinking [257].

Nanographite platelets and expanded graphite reinforced electrospun nanofibers have also been fabricated by several research groups through co-electrospinning with polymer solutions of PET [258], PAN [259], PVDF [260], and PU [261]. In a typical approach, Mack et al. prepared platelets of nanographite by an intercalation and exfoliation approach, first heating graphite powder in the presence of a potassium intercalating agent under vacuum to form crystalline KC₈. The addition of an aqueous solution then results in the solvation of the potassium and subsequent separation of the graphite layers into exfoliated graphite nanoplatelets (GNPs) which are then incorporated into an electrospinning solution of PAN and spun into GNP embedded nanofibers. Gao's eschewed the typical co-electrospinning approach and managed to fabricate GNP reinforced PU nanofibers where GNPs were decorated on the surface rather than in the bulk in order to better exploit the GNP's mechanical, electrical, and thermal properties. They prepared an exfoliated GNP solution with the aid of ultrasonication to disperse the heat treated expanded graphite material in water. Subsequently, PU nanofibers fabricated from electrospinning were immersed in the prepared solution under ultrasonication. The sonication process further exfoliates the GNP sheets, but also results in shock waves and microjets near the GNP from cavitation bubbles, energetically driving the GNPs toward the nanofiber and causes collisions that sinter the GNPs into the nanofiber. The morphology of the nanofibers produced by this technique is shown in Fig. 5d. They found that when GNPs were of similar size to the nanofibers, good attachment was achieved, with FTIR analysis also showing the existence of chemical interactions between the matrix and nanofiller [261].

tence of chemical interactions between the matrix and nanofiller [261].

3. Properties of polymer/carbon composites

The mechanical, electrical and thermal properties of electro-spun polymer/nanocarbon composites prepared through the many methods described in section 2 will be summarized and tabulated in section 3, and compared with the control values of the electro-spun polymer to quantify the performance improvements resulting from the incorporation of the nanocarbon filler.

3.1. Mechanical properties

Fig. 6 visually represents the data presented in Table 1 arranged according to the nanofiller type and ascending improvements to the mechanical properties. From Fig. 6, it can be seen that the addition of nanocarbon materials overwhelmingly result in improvements to the mechanical properties such as tensile strength and young's modulus. Comparing the efficacy of the different forms of nanofillers, it is clear that graphene and CNT based nanofillers resulted in the most pronounced improvements to tensile strength, with several papers reporting an increase of over 300% [11,148,152,188,270,271,273,275], owing to their intrinsically high strength derived from the very strong C–C bonds. On the contrary, carbon black nanofillers tended to result in the decrease in mechanical properties of the nanofiber, causing on average a decrease in strength and elongation of approximately 32% and 77% respectively, while only increasing the stiffness by 11.7% as measured by the Young's modulus [251–253]. The incorporation of nanodiamonds and graphite tended to have more significant effects on the hardness and stiffness of the nanofiber, with ND incorporation leading to an average of a 2-fold increase in hardness, while the incorporation of graphite led to an increase in hardness of over 7-fold [241,246,259]. The differences in the effect of the various nanofillers can be ascribed to the intrinsic properties of the nanofiller themselves, along with the extent of interactions they have with the polymeric host and their degree of dispersion. Ostensibly, strong, well dispersed nanofillers having strong interactions with the host polymer will give rise to composite with the best mechanical properties (Table 2).

In general, amorphous carbon black particles act as rigid particle nanofillers which causes the stiffness to increase in the viscoelastic polymer matrix, however, these same nanofillers represent defects which compromise the mechanical integrity of the composite, especially without good interfacial adhesion between the matrix and the particle, accounting for the decrease in the strength and stiffness [253]. On the other hand, graphene and CNT based materials have been intensively studied for their outstanding mechanical properties to be used as reinforcing fillers in composite applications, wherein stress-transfer from the weaker polymer host to the stronger nanofiller allows a higher loading to be achieved by the composite material, thus the improvement in strength. In many of the studies surveyed in this review, it is observed that there has been a decrease in the elongation to failure resulting from incorporating the carbon based nanofiller, consistent with the trade-off between stiffness and ductility that is commonly observed in stiffened materials. At the microscopic level, the nanofillers prevent the reorienting of the polymer chains during plastic deformation [248] hence resulting a decrease in ductility.

Modification to the nanofiller prior to electrospinning has been shown to be an effective method to increase the mechanical properties of the composite, aiding in the dispersion of the nanofiller in the fiber, as well as for improving the interfacial interactions with the host, thereby enhancing the load transferring to the

Table 1

Compilation of mechanical properties of tensile strength, Young's modulus, and elongation at break for nanocarbon reinforced polymer composite nanofibers from literature.

Nanofiller	Polymer	Nanofiller Treatment	Fabrication Technique	Loading (wt%)	Tensile Strength (MPa)		Young's Modulus (GPa)		Elongation at Break (%)		Reference
					Composite	Control	Composite	Control	Composite	Control	
Carbon black	Chitosan	–	Co-electrospun + crosslinking	2.5	~250	~1250	~0.000150	~0.15	~0.25	~10	[251]
Carbon black	PVA	–	Co-electrospun	10	4.44	7.37	0.1556	0.0806	22.9	162.2	[253]
Carbon Black	Polyurethane	–	Co-electrospun	3.65	7.48	6.06	0.00105	0.00074	322.22	613.51	[252]
Fullerene NP	PLLA	TEG modified	Co-electrospun	5	3.5	4.1	.1328	.1486	103.5	112.3	[229]
Fullerene NP	PLLA	TEG modified + PTX loaded	Co-electrospun	5	4.2	4.5	0.1424	0.1486	104.4	114.3	[230]
ND	PLA	–	Co-electrospun	1	1.12	0.33	0.00995	0.0041	56.82	23.02	[236]
ND	PLGA	–	Co-electrospun	23	–	–	0.13	0.06	–	–	[241]
ND	Cellulose / Chitosan	–	Co-electrospun	1	25.3	21.7	0.458	0.353	9.9	15.4	[248]
ND	Polyamide 11	–	Co-electrospun	20	–	–	~8	~2	–	–	[246]
ND	PVA	–	Co-electrospun	0.1	8.6	7	0.0512	0.0846	–	–	[237]
ND	PVA	–	Co-electrospun	2	115.3	45.2	0.0068	0.0036	99.8	46.7	[245]
ND + mwCNT	poly(azo-pyridine) in DGEBA	Polyamide functionalized	Co-electrospun + cured	3	359.4	323.6	32.3	26.1	24.2	19.9	[247]
swCNT	Silk	–	Co-electrospun	1	7.4	19.1	0.705	0.312	1.4	5.8	[88]
swCNT	PAN	–	Co-electrospun + hot drawing	0.1	~500	~425	10.86	9.59	–	–	[262]
mwCNT	Collagen / PCL	-COOH functionalized	Co-electrospun	1	3.38	3.32	0.0233	0.0326	70.93	34.54	[263]
mwCNT	Polyacrylamide	-COOH functionalized	Co-electrospun + crosslinking	3	5.7	0.52	0.1219	0.0271	–	–	[152]
mwCNT	PAN	-COOH functionalized	Co-electrospun	10	370	265	10.9	4.5	8.2	17.8	[111]
mwCNT	Cellulose Acetate	-COOH functionalized	Dip coated LBL assembly	5.5 bilayers	4.81	3.71	0.0459	0.0608	13.44	7.83	[165]
mwCNT	Polyurethane	–	Co-electrospun	0.75	12.5	7.8	–	–	308.4	255.1	[93]
mwCNT	Polyurethane	-COOH functionalized	Co-electrospun	0.1	8.6	5.1	0.0036	0.0015	453	540	[116]
mwCNT	PLA	–	Co-electrospun	0.25	–	–	0.0554	0.0149	–	–	[264]
mwCNT	Shell - PAA/PVA hydrogel Core - PCL	-COOH functionalized	Coaxial electro-spun + crosslinking	0.05	644.8	60.8	0.0125	0.00444	–	–	[148]
mwCNT	PLA	–	Co-electrospun	0.25	1.54	2.07	55.35	14.87	–	–	[83]
mwCNT	PLA	–	Co-electrospun	1	1.99	2.07	0.0112	0.0149	–	–	[83]
mwCNT	PEO	–	Co-electrospun + annealing	0.25	~125	~135	~0.325	~0.25	–	–	[106]
mwCNT	PLGA	-COOH functionalized	Co-electrospun	1	5.23	3.5	0.188	0.100	128.77	58.64	[81]
mwCNT	PLGA	–	Co-electrospun	1	~17.5	~16.5	~0.155	~0.255	~110	~120	[265]
mwCNT	PLGA	–	Co-electrospun	3.33	~20	~16.5	~0.175	~0.255	~8	~120	[265]
mwCNT	PAN/PANI	–	Co-electrospun	3	0.55	2.21	0.04	0.137	–	–	[127]
mwCNT	Polyimide	-COOH functionalized	In-situ polymerization + Co-electrospun	3.5	239.7	186.8	2.56	2.47	90.5	64.1	[119]
mwCNT	PLLA	-COOH functionalized	Co-electrospun	3.75	3.43	1.85	.1253	.0621	28.8	21.5	[123]
mwCNT	PAN	-COOH functionalized	Co-electrospun	5	80	45.7	3.1	1.8	2.5	10.7	[110]
mwCNT	Silk	–	Co-electrospun	1	9.94	6.26	0.1075	0.0325	9.25	19.26	[266]
mwCNT	C540 Styrene-butadiene-styrene	–	Co-electrospun	1.5	2.23	1.73	0.00017	0.00017	437	333	[267]

Table 1 (Continued)

Nanofiller	Polymer	Nanofiller Treatment	Fabrication Technique	Loading (wt%)	Tensile Strength (MPa)		Young's Modulus (GPa)		Elongation at Break (%)		Reference
					Composite	Control	Composite	Control	Composite	Control	
mwCNT	PAN	Amine functionalized	In-situ polymerization + Co-electrospun	1	30.4	18.46	0.05432	0.00868	-	-	[141]
mwCNT	PET	-	Co-electrospun	3	4	5.9	~0.110	~0.125	~350	~375	[84]
mwCNT	PVA/Chitosan	-COOH functionalized	Co-electrospun + crosslinked	1	9.6	8.35	158.60	156.65	6.24	3.68	[122]
mwCNT	Nylon 6	Amine functionalized	In-situ polymerization + Co-electrospun	1	38.16	20.36	0.02896	24.49	24.7	22.7	[135]
mwCNT	Nylon 6	-	In-situ polymerization + Co-electrospun	1	35.22	20.36	0.02429	24.49	16.9	22.7	[135]
mwCNT	PLA/PCL	-COOH functionalized	Co-electrospun	1	3.81	2.45	0.1143	0.0817	77.5	96	[268]
mwCNT	Polypropylene	-	Blended + melt electrospun	0.05	~2.25	~1.25	-	-	~45	~80	[129]
mwCNT	Silk	-COOH functionalized	Co-electrospun	2	3.65	8.07	0.0746	0.0312	4.89	30.19	[120]
mwCNT	PCL/PEDOT	-COOH functionalized	Co-electrospun	0.025	0.904	0.7024	0.0007411	0.0005984	-	-	[269]
mwCNT	PHBV	PHBV grafted	Co-electrospun	3	5.1	4.6	0.131	0.126	38	27	[134]
mwCNT	PHBV	-OH functionalized	Co-electrospun	3	4.5	4.6	0.085	0.126	36	27	[134]
mwCNT	PCL	Thiophene conjugated	Co-electrospun	20	1.3	0.9	0.011	0.0084	131	48	[132]
mwCNT	Silk	-	Co-electrospun + mechanical stretching	1	58.04	7.75	6.549	0.17498	0.93	5.05	[270]
mwCNT	PEO	-	Electrospun onto CNT sheet + Calendering	30	239	3.98	-	-	-	-	[164]
mwCNT	PLA	-COOH functionalized	Co-electrospun	1	8.8	1.8	0.461	0.178	-	-	[271]
mwCNT	PAN	PAN-Terpolymer-Grafted	Co-electrospun	2	215.9	71.9	3.6	2.2	-	-	[139]
mwCNT	Polyvinylidene fluoride-co-hexafluoropropylene	-	Co-electrospun	5	19.9	9	0.0837	0.0182	79.6	99.8	[78]
mwCNT	Gelatin	-COOH functionalized	Co-electrospun with HA + crosslinked		7.9	6.3	0.82	0.368	-	-	[272]
mwCNT	Polyimide	-COOH functionalized + PEO stabilized	Co-electrospun	3	~108	~72			~13.8	~7	[118]
mwCNT	Poly(butylene terephthalate)	-	Co-electrospun	2	0.2202	0.163	0.0003347	0.000304	60.8	52.13	[87]
mwCNT	poly(-glycerol sebacate):gelatin	-COOH functionalized + gelatin coated	Co-electrospun	1.5	~1.35	~0.1	~300	~100	~160	~240	[273]
mwCNT	Poluyurethane	-COOH functionalized	Co-electrospun (2 nozzle)	1	8.8	7.4	0.0022	0.0021	748	606	[274]
mwCNT	Poluyurethane	-COOH functionalized	Co-electrospun	1	7.9	7.4	0.0029	0.0021	376	606	[274]
mwCNT	PI in DGEBA	Polyamide grafted	Co-electrospun + cured	3	249.9	212.2	19.8	15.2	29.3	27.8	[136]
mwCNT	PI/PANI in DGEBA	Polyamide grafted	Co-electrospun + cured	3	332.6	212.2	25.3	15.2	33.5	27.8	[136]
mwCNT	Shell – Cellulose/[EMIM][Ac] Core – [EMIM][Ac] /mwCNT	-	Co-electrospun + enzymatic removal of cellulose	20	5.14	6.22	-	-	5.5	7.5	[146]

Table 1 (Continued)

Nanofiller	Polymer	Nanofiller Treatment	Fabrication Technique	Loading (wt%)	Tensile Strength (MPa)		Young's Modulus (GPa)		Elongation at Break (%)		Reference
					Composite	Control	Composite	Control	Composite	Control	
Graphene	PLLA in PBS	–	Co-electrospun + cured	1.3	24.7	22.5	–	–	3.5	4.4	[203]
	Polyvinylidene Fluoride	–	Co-electrospun	1	2.5	0.7	0.72	0.41	–	–	[275]
GO	PVA	Glycine grafted + Gold NP deposition	Co-electrospun	0.5	–	–	–	–	–	–	[365]
					–	–	–	–	–	–	
GO	PLA	PEG grafted	Co-electrospun	5	5.2	2.1	–	–	84	97	[189]
GO	Polyimide	–	Co-electrospun	2	–	–	–	–	–	–	[169]
GO	Chitosan/ Cellulose	–	Co-electrospun	1.5	35	21	.73	.34	9.5	16	[177]
GO	PVA	–	Co-electrospun	0.02	9.37	0.22	–	–	180	145	[172]
GO	PLGA-co-PPF	PGA functionalized + PPF copolymerized	Co-electrospun with HA	5	79.1	40.9	3.78	1.75	3.78	5.31	[209]
GO	PLA	–	Co-electrospun with HA	2	0.57	0.27	0.01673	0.00858	–	–	[208]
GO	Poly(carbonate urethane)	–	Co-electrospun	1.5	35.6	11.67	–	–	–	–	[174]
GO	Silk	–	Dip coated + in-situ reduction	5 immersion cycles (1 mg/ml)	1.8	1.6	0.023	0.020	9	13.9	[193]
GO	PAN	–	Co-electrospun	0.5	171	68	–	–	10.15	12.67	[216]
GO	PVDF	–	Co-electrospun	0.7	~9.3	~5.5	–	–	–	–	[206]
GO	PLGA/silk tussah	–	Co-electrospun	1	~9	~3	~0.055	~0.010	~150	~275	[181]
GO	PVAc	Non covalent PPV bonded	Co-electrospun	0.07	9.52	6.13	0.456	0.513	96.8	12.4	[190]
GO	PVAc	PBASE modified	Co-electrospun	0.07	12.39	6.13	0.642	0.513	52	12.4	[190]
GO	PVAc	4-(2-(pyridin-4-yl)vinyl)Phenyl-modified	Co-electrospun	0.07	11.78	6.13	0.598	0.513	82.5	12.4	[190]
rGO	Silk	–	Dip coated + in-situ reduction	5 immersion cycles	1.6	1.6	0.0261	0.02	7.1	13.9	[193]
rGO	Silk	–	Dip coated + in-situ reduction	5 immersion cycles (3 mg/ml)	1.9	1.6	0.0318	0.020	8.9	13.9	[193]
rGO	PVA	–	Co-electrospun	2	5.51	2.97	0.08567	0.06473	–	–	[168]
rGO	PCL	Copolymerized with PDDT	Co-electrospun	2	86	1.52	0.394	0.005438	32	54.34	[188]
rGO	PCL	Copolymerized with PTet	Co-electrospun	2	56	1.52	0.407	0.005438	45	54.34	[188]
Graphite	PAN	–	Co-electrospun	4	–	–	~2	~1	–	–	[259]
Graphite	PAN	–	Ultrasonic Embedding	5.1	–	–	–	–	–	–	[261]

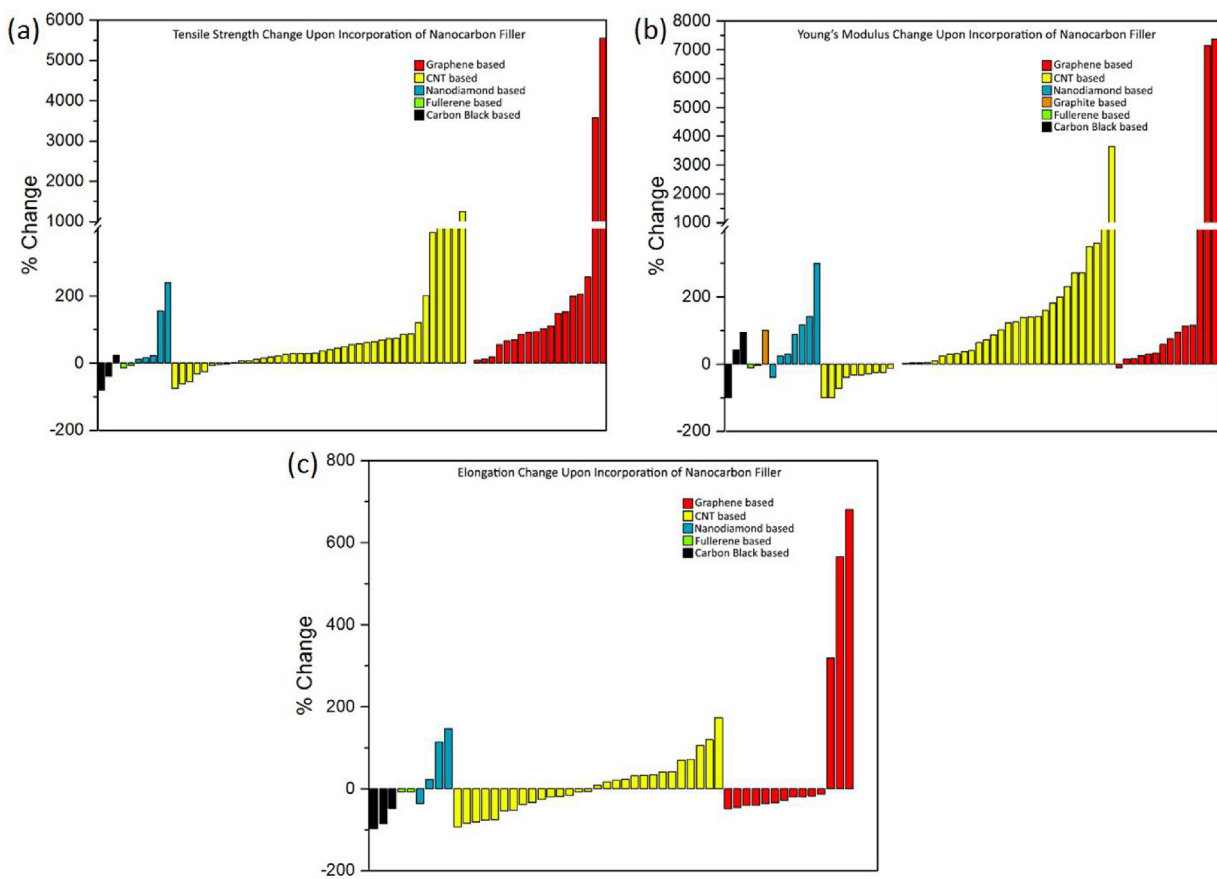


Fig. 6. (a) Bar chart comparing the tensile strength changes upon addition of various carbon nanofillers; (b) Bar chart comparing the Young's modulus changes upon addition of various carbon nanofillers; (c) Bar chart comparing elongation changes upon addition of various carbon nanofillers.

strong filler. In a paper published by Mangeon et al., a comparison was made between –OH functionalized mwCNTs and mwCNTs grafted with PHBVH when co-electrospun in a PHBVH nanofiber. Mechanical analysis showed the grafting resulted in an improved crystallization behaviour of the PHBVH in addition to the interfacial interaction effects, allowing the grafted mwCNT to outperform the unmodified mwCNT in tensile strength (5.1 vs 4.5 MPa), elastic modulus (131 vs 85 MPa), and elongation at break (38 vs 36%) [134].

It is also observed that in many cases, there exists an optimum nanofiller loading which maximizes the mechanical properties, typically at low levels. Zha et al. compared the use of different mwCNT loadings between 3 vol% to 14 vol% in polyimide nanofibers and found that the mechanical properties were optimal at 3 vol%, as shown by the stress-strain curve in Fig. 7b [118]. Similarly Chen et al. found an optimal loading of 3.5% mwCNT fillers in polyimide nanofibers for the optimal mechanical strength as shown by the stress-strain curve in Fig. 7a [119]. In both these studies, high strength, low ductility polyimide nanofibers experienced enhancements in strength, modulus, and elongation, exhibiting the toughening effect of mwCNT addition at carefully optimized loading concentrations. Functionalized mwCNTs were found to improve interface interactions and CNT dispersion in solution at low loadings, as shown in Fig. 7(c–e), however, with higher loading, difficulty in dispersing the fillers increases, leading to aggregation of the mwCNT which not only reduces their effectiveness, but also results in stress concentrations developing in the matrix, causing a deterioration in the mechanical properties [119].

While the general trends observed in the above meta-analysis are consistent with expectations, it should also be noted that the wide range of results has its roots in the variability among the works surveyed including the type, molecular weight, and crystallinity of

the polymer, the purity, length, aspect ratio, particle sizes, and functionalization of the nanofiller, along with electrospun nanofiber diameters, porosity, architecture and post processing modifications being among the many sources of variability.

3.2. Electrical properties

From the data tabulated in Table 3, it can clearly be seen that the incorporation of nanocarbons into polymeric nanofibers increases the electrical conductivity, with several hybrid materials reaching electrical conductivities in the order of hundreds of siemens/cm [100,164]. In the instances where the pristine polymeric nanofiber's electrical conductivity was measured as a reference, the incorporation of nanocarbons has led to increases in electrical conductivity from 35% [65], up to over 14 orders of magnitude [271].

A critical parameter often discussed in the literature relates to the percolation threshold, *i.e.* the critical concentration of conductive fillers necessary to form an interconnecting network, below which the composite remains essentially non-conducting, and above which the electrical conductivity plateaus and would not significantly be increased with increasing filler content. Mazinani et al. explored the effect of different loadings of CNTs with the objective of determining the percolation threshold for various types of CNTs. Their results interestingly showed that at a 1 wt% loading, the electrical conductivity was approximately 10^{-15} S/cm, while increasing the loading to 2% resulted in a sharp increase in conductivity to the order of 10^{-3} S/cm, beyond which at 5%, the conductivity was approximately constant at 10^{-3} S/cm, as shown in Fig. 8a. They concluded that the high aspect ratio mwCNT fillers formed a percolated conductive network at 2 wt% necessary for electron transport to turn the system conductive. Furthermore, they also explored

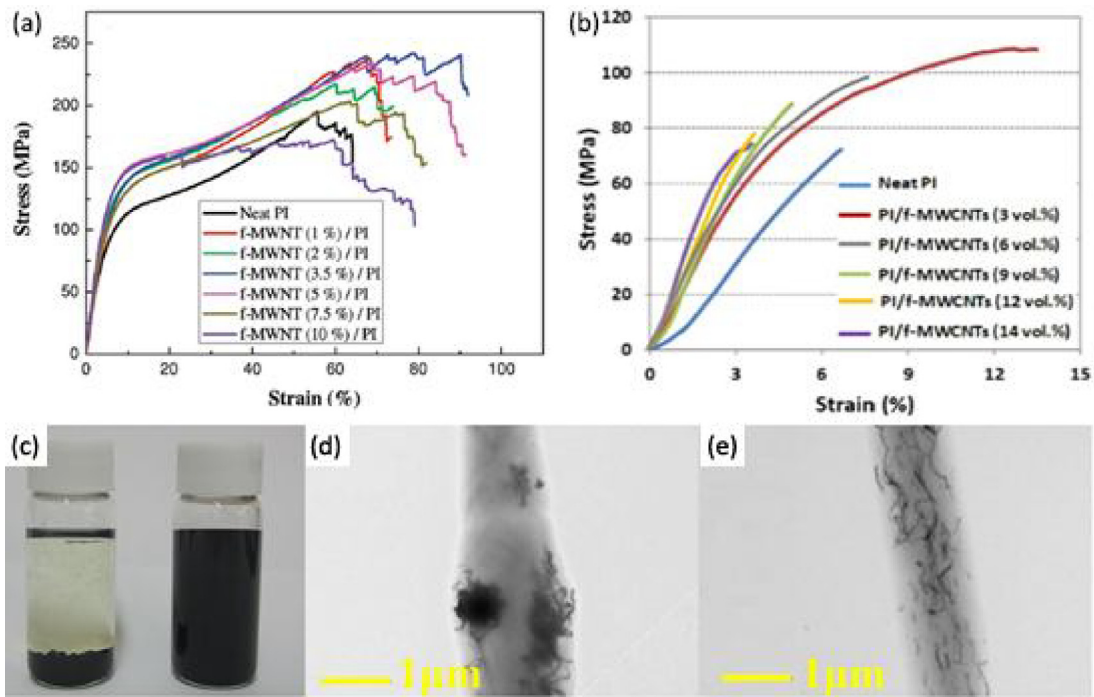


Fig. 7. (a) Stress-strain curve showing effect of different functionalized mwCNT loadings on aligned electrospun PI nanofibers [119]. Copyright 2009, reproduced with permission from the American Chemical Society; (b) Stress-strain curve showing effect of different functionalized mwCNT loadings on non-aligned electrospun PI nanofibers [118]. Copyright 2014, reproduced with permission from AIP Publishing LLC; (c) Solutions containing pristine mwCNT (left) and functionalized mwCNT (right) [118]. Copyright 2014, reproduced with permission from AIP Publishing LLC; (d) TEM of PI nanofiber containing aggregations of pristine mwCNTs [118]. Copyright 2014, reproduced with permission from AIP Publishing LLC; (e) TEM of PI Nanofiber containing well dispersed functionalized mwCNT [118]. Copyright 2014, reproduced with permission from AIP Publishing LLC.

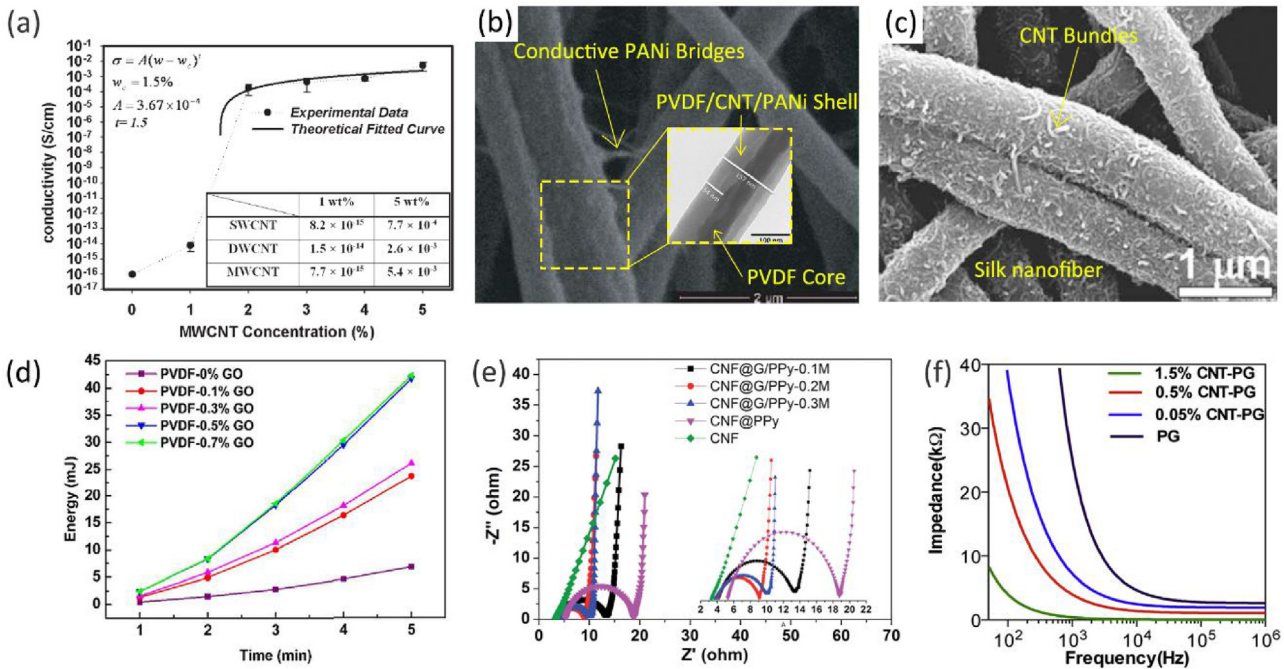


Fig. 8. (a) Electrical conductivity vs mwCNT loading curve showing percolation threshold at 2% loading [84]. Copyright 2010, reproduced with permission from John Wiley & Sons Inc; (b) SEM showing morphology of hybrid electrospun nanofibers bridged by electrically conducting PANi with inset showing distinct core-sheath layering having CNTs in the thin shell layer [150]. Copyright 2014, reproduced with permission from John Wiley & Sons Inc; (c) SEM showing dip coated CNT bundles over silk nanofibers forming an interconnected network [161]. Copyright 2007, reproduced with permission from Springer; (d) Stored energy in a 2.2- μ F capacitor over 5 min (540 cycles) connected to a book-shaped triboelectric nanogenerator consisting of graphene oxide doped filled PVDF/PHBV nanofibers [86]. Copyright 2013, reproduced with permission from the American Chemical Society; (e) Nyquist plots for a carbon nanofiber electrodes electrodeposited with graphene and PPY from various concentrations of the electrodeposition solution, with inset showing the magnified view in the high frequency region [200]. Copyright 2015, reproduced with permission from the Royal Society of Chemistry; (f) Impedance vs frequency curves showing effect of CNT concentration on the impedance of electrospun poly(-glycerol sebacate):gelatin nanofibers [273]. Copyright 2014, reproduced with permission from Elsevier Ltd.

Table 2 Compilation of mechanical properties of hardness, storage modulus, and toughness for nanocarbon reinforced polymer composite nanofibers from literature.

Nanofiller	Polymer	Nanofiller Treatment	Fabrication Technique	Loading (wt%)	Hardness (GPa)		Storage Modulus (MPa)		Toughness (GPa)		Reference
					Composite	Control	Composite	Control	Composite	Control	
ND	PLGA	–	Co-electrospun	23	0.015	0.004	–	–	–	–	[241]
ND	Polyamide 11 poly(azo-pyridine) in DGBA	–	Co-electrospun	20	~0.14	~0.05	–	–	–	–	[246]
ND + mwCNT	Polyimide	Polyamide functionalized -COOH functionalized	Co-electrospun + cured	3	–	–	–	–	7.7	4.2	[247]
mwCNT	poly(ε-glycerol sebacate);gelatin	-COOH functionalized+gelatin coated	In-situ polymerization+Co-electrospun	3.5	–	–	~3500	~3100	–	–	[119]
mwCNT	PI in DGEBA	Polyamide grafted	Co-electrospun + cured	1.5	–	–	–	–	~0.2	~0.025	[273]
mwCNT	PI/PANI in DGEBA	Polyamide grafted	Co-electrospun + cured	–	–	–	–	–	–	–	[136]
mwCNT	PVA	Glycine grafted + Gold	Co-electrospun	0.5	–	–	~310	~205	–	–	[136]
GO	PIA	NP deposition	Co-electrospun	3	–	–	–	–	5.332	4.22	[365]
GO	Polyimide	PEO grafted	Co-electrospun	3	–	–	–	–	6.916	4.22	[189]
GO	PLGA-co-PPF	PEO functionalized + PPF copolymerized	Co-electrospun	0.5	–	–	–	–	–	–	[169]
GO	HA	–	Co-electrospun	5	–	–	140	380	–	0.0177	0.0121
GO	GO	GO	Ultrasonic Embedding	5	–	–	–	–	–	–	[209]
GO	GO	GO	–	1.5	–	–	600	350	0.01389	0.0061	[174]
GO	Graphite	Poly(carbonate urethane)	Co-electrospun	0.7	–	–	~50,000	~20,000	–	–	[206]
GO	Graphite	PVDF	Ultrasonic Embedding	5.1	0.06	0.007	–	–	–	–	[261]

the differences in the number of CNT walls and found that swCNTs achieved a lower conductivity at the same loadings due to the increased van der waal's interactions for swCNTs leading to difficulties in dispersing the filler in the electrospinning solution [84].

Post-processing steps incorporated in the fabrication process to restore the conductivity of the nanofillers, remove unwanted impurities, and to anneal the spun nanofibers have also been shown to increase the electrical conductivity. For instance, thermal annealing of GO coated polyamide nanofibers in the presence of hydrazine reduced the GO to rGO, deoxygenating the graphene oxide, restoring the conductivity of graphene and improving the surface resistivity [195].

Introducing hierarchical architectures to the nanofibers allows the percolation threshold to be reached at lower nanocarbon loadings. Sarvi et al. observed that due to the highly oriented nature of CNT fillers within aligned electrospun polymer nanofibers, electrical percolation may be harder to achieve as the CNT fillers form short order connections but may have discontinuities where there are gaps between adjacent tubes. Their work leveraged conductive PANi to act as a conductive component and to bridge the electrospun PVDF nanofibers to reduce the air spaces between them, as well as to selectively sequester the CNTs to the surface of the nanofibers *via* coaxial electrospinning, as shown in SEM and TEM micrographs given in Fig. 8b. This increases the probability of forming an interconnected conducting network at sufficiently low CNT concentrations in the thinner shell, without adversely affecting the spinnability of the electrospinning solution [150]. The idea of essentially forming a conductive network on the surface of the nanofiber rather than the bulk in order to imbue the material with electrical conductivity is also exploited by various groups adopting the dip-coating [161], resulting in the adhesion of a conductive carbon nanotube coating on the nanofiber as shown in Fig. 8c, or layer-by-layer assembly techniques [198].

Apart from electrical conductivity, the incorporation of nanocarbons has also been shown to have beneficial effects on the capacitative performance of the hybrid material. Huang et al. fabricated triboelectric nanogenerators from graphene oxide loaded PVDF and PHBV nanofibers, with the layered graphene oxide modulating the surface electrification, providing charge-trapping sites and supplied the interface for storing charge. Electrons generated from the tribological material can be stored in the quantized energy levels of the graphene sheets or the graphene oxide dielectric, both of which serve to increase surface charge on the nanofiber and hold them in position effectively retarding the surface potential decay [86]. Graphene incorporation of 0.7% resulted in an increase in charging current (from 0.581 to 1.438 μA) and power (from 0.023 mW to 0.141 mW) considerably [86], while also increasing the specific capacitance from 265 to 386 F/g, and consequently the stored energy in the capacitor with time as shown in Fig. 8d. Furthermore, there was also enhanced cycling stability as a result of the improved charge transfer with the incorporation of electrically conducting graphene [86]. In terms of the dielectric performance of the composite material, the incorporation of mwCNTs up to the point of percolation (~12 vol%) has been shown by Xu's group to improve the AC conductivity, dielectric permittivity, and energy storage density of polyimide, achieving a maximal energy storage density of 1.957 Jcm⁻³ compared to 0.404 Jcm⁻³ for the neat polymer. This was attributed to the formation of micro-capacitor structures with the well-dispersed fillers in an insulating matrix, thereby forming good interfacial polarization [67].

The inclusion of certain nanocarbons have also improved the electrochemical impedance performance of the hybrid composite nanofibers. Sapountzi et al. showed that incorporating CNTs in a copolymer of PVA and styrylpuridinium led to a significant enhancement of charge transfer efficiencies, with the 10% mwCNT

loaded nanofibers reaching anodic peak intensity efficiencies of up to $398 \mu\text{A}/\text{cm}^2$ versus $25 \mu\text{A}/\text{cm}^2$ for electrodes modified with nanofibers absent CNT, this is consistent with the decrease in resistivity following incorporation of conductive CNTs, and the decrease in the tunneling requirements for electron transfer through the insulating polymer regions between the CNTs [113]. This is similarly observed in work by Kharaziha et al., in which was observed that incorporation of CNTs effectively lowered the impedance values of electrospun poly(-glycerol sebacate):gelatin nanofibers due to improved electrical conductivity. This was reflected in the leftward shifts in the impedance vs frequency curves with increasing CNT content, as shown in Fig. 8f [273].

Gan and colleagues reported an electrochemical deposition approach to deposit reduced graphene oxide and in-situ polymerize PPY on the surface of electrospun carbon nanofiber electrodes, resulting in graphene supported PPY chains nucleated on the nanofiber. Their porous electrodes exhibited excellent electrolyte penetration kinetics and conductivity to facilitate charge transport, with the optimum PPY electrodeposition concentration determined to be 0.2 M, beyond which agglomeration can occur to reduce the capacitative performance. This electrochemical performance is reflected in the decreasing arc diameter (equivalent series resistance) of the Nyquist plots shown in Fig. 8e. The incorporation of graphene was shown to decrease charge transfer resistance, improve conductivity, and boost cycling stability, allowing the electrode to operate under high current densities of 10 Ag^{-1} , as well as enhancing the power density up to 2820 W kg^{-1} coupled with a 10.5 Wh kg^{-1} energy density [200]. Yu et al. likewise found that glycine modified, nanogold decorated graphene oxide imbued electrospun PVA nanofibers showed improved electrical conductivity, with increased loadings leading to further reductions in the diameters of the semi-circle arcs of the Nyquist plots. In their work, increasing the conductive nanofiller loadings from 0.1 wt% to 1 wt% caused a reduction in the Z_{real} from $1.35 \text{ G}\Omega$ to $0.58 \text{ G}\Omega$ at low frequencies [365].

3.3. Thermal properties

Nanocarbons like CNTs, having intrinsically good thermal conductivity and thermal stabilities, are likely to improve the host's thermal properties when incorporated in a composite material [116]. Electrospun hybrid nanofibers imbued with these nanocarbons have shown enhanced thermal behaviour compared to their pristine counterparts, with particular improvements in thermal stability i.e. thermal degradation onset temperature, glass transition temperature, and thermal conductivity, as evidenced in Table 4. The positive correlation between the loading level and the thermal behaviour of the composite can be clearly observed in work by Cai et al. The glass transition temperature of the PLA composite nanofibers shifts rightwards with increasing addition of the more thermally stable ND as a result of the interactions between the PLA polymer chains and the ND [236].

Ge et al. found that incorporating surface oxidized mwCNTs into the electrospinning solution led to CNT filled PAN nanofibers not only having improved thermal stabilities, with decomposition onset temperature shifting from 268 to 292°C (with 5 wt% loading), but also demonstrated an increased softening temperature (from 83 to 94°C for 10 wt% CNT loaded). Furthermore, the mechanical deformation above the softening temperature was also greatly reduced, indicating the dimensional stability of the composite surpasses that of the pristine nanofibers as evidenced by the dimensional changes from thermal mechanical analysis and the coefficient of thermal expansion (180×10^{-6} to 13×10^{-6}), shown in Fig. 9a. These improvements are thought to be derived from the nanofillers suppressing the polymer's molecular segmental motions as a result of various mechanical and chemical interactions and

charge transfer complexes formed at the interface between the matrix and filler [111] (Table 5). Similar results are also shown in research by Chen et al. who showed a positive relationship between the storage modulus and functionalized mwCNT nanofiller loading in PI nanofibers shown in Fig. 9d [119].

Yu and co-workers' work on glycine modified GO as a nanofiller for PVA nanofibers similarly found that incorporating nanocarbon fillers had an ameliorative effect on the thermal stability. They observed that increasing the loading beyond an optimal level actually led to a decrease in the decomposition onset temperature, with their 0.5 wt% loaded nanofibers having a T_d of 288°C compared to 284.9°C for the 1 wt% loaded counterparts, as demonstrated in the TGA thermogram shown in Fig. 9b. This was attributed to the poor dispersion of the nanofiller resulting in the formation of spheres in the nanofiber, as well as phase separation of the nanofillers as the loading is increased beyond the optimum level [184]. Work by Hwang et al. on carbon black filled electrospun polyurethane composite nanofibers also showed the same pattern, with T_d increasing at low loading to an optimal level before decreasing [252]. Chen et al. observed that the use of surface oxidation functionalization of mwCNTs prior to spinning may have competing effects on the thermal performance in where improvements in the dispersion of the nanofiller and removal of impurities could benefit the thermal properties, but the chemical functionalities ($-\text{COOH}$ or $-\text{OH}$) introduced may be easily thermally degraded and compromise the thermal stability of the composite [119].

Dias et al. attributed graphene's effect in the improvement of the composite's thermal stability to an alternative mechanism, the shielding effect, in which well dispersed, thermally inert graphene increases the decomposition by-product's diffusion path or act as a gas barrier to stave off the onset of decomposition [172,205]. Furthermore, the presence of nanocarbons may also induce certain physical changes in the host material which could indirectly impact the composite's thermal performance. Sarvi et al. observed that the addition of mwCNTs, acting as nucleating site, led to an increase in the formation of the β phase crystal of PVDF, which in turn led to an increase in the glass transition temperature of the material from ~ 160 to $\sim 170^\circ\text{C}$, as can be seen from the DSC thermogram in Fig. 9c [150]. While the addition of nanocarbons tended to have a positive impact on thermal stabilities in the literature surveyed, there are some exceptions. Wang and co-workers prepared GO reinforced PVA nanofibers and found the addition of GO reduced the thermal stability (T_d decreases from 259 to 245°C), and linked this decrease to two possible causes. The reduction of GO leading to the evolution of by-products (H_2O , CO_2 , etc) which accelerate the decomposition of PVA, and secondly to the formation of air pockets within the nanofiber matrix due to curled up GO causing outgassing to break down the polymer more quickly [172,180].

The nanocarbon filler graphene has also been shown to proportionally improve the thermal conductivity of electrospun PMMA and PAN nanofibers in work by Khan et al., from 1 to 5 W/m.K and 1 to 2.7 W/m.K respectively with loadings of 8% as reflected in Fig. 9e. However, since the thermal conductivity of graphene can approach 5300 W/m.K , the improvements seem underwhelming, which can be attributed to air spaces between the nanofibers of the mat, interface resistance between graphene layers and between graphene and the polymer, phonon scattering, and also the poor polymer crystallinity [211].

4. Applications

The enhanced mechanical, electrical, and thermal performance as described above in section 3 provides a glimpse into the potential of such nanocarbon enhanced nanofibers in practical applications. Section 4 of this review article discusses the functional perfor-

Table 3
Compilation of various electrical properties of nanocarbon reinforced polymer composite nanofibers from literature.

Nanofiller	Polymer	Nanofiller Treatment	Fabrication Technique	Loading (wt%)	Electrical Conductivity (S/cm)		Sheet Resistance (Ω/sq)		Ionic Conductivity (S/cm)		Dielectric Constant		Specific Capacitance (F/g)		Reference
					Composite	Control	Composite	Control	Composite	Control	Composite	Control	Composite	Control	
Carbon Black	Chitosan	–	Co-electrospun	62.5	0.109	1.14×10^{-8}	–	–	–	–	–	–	–	–	[251]
Carbon Black	Polyurethane	–	Co-electrospun	7.87	6.8×10^{-5}	1.14×10^{-7}	–	–	–	–	–	–	–	–	[252]
Carbon Black	PAN	–	Co-electrospun	60	5×10^{-5}	–	–	–	–	–	–	–	–	–	[249]
Fullerenol	Cellulose Acetate	–	Co-electrospun	0.5	–	–	–	–	18.1×10^{-4}	8.2×10^{-4}	–	–	–	–	[225]
swCNT	Silk	–	Co-electrospun + annealing	1	0.114	0.028	–	–	–	–	–	–	–	–	[270]
swCNT	PEO	a-PPE functionalized	Co-electrospun	1.2	0.02	–	–	–	–	–	–	–	–	–	[101]
swCNT	PANI/PEO	–	Co-electrospun	11.9	1.2	3.55×10^{-4}	–	–	–	–	–	–	–	–	[126]
dwCNT	PEO	DNA wrapped	Co-electrospun	5	372	2.54×10^{-4}	–	–	–	–	–	–	–	–	[100]
swCNT	PET	–	Co-electrospun	5	7.7×10^{-4}	–	–	–	–	–	–	–	–	–	[84]
dwCNT	PET	–	Co-electrospun	5	2.6×10^{-3}	–	–	–	–	–	–	–	–	–	[84]
mwCNT	PET	–	Co-electrospun	5	5.4×10^{-3}	–	–	–	–	–	–	–	–	–	[84]
swCNT	PET	–	Co-electrospun	1	8.2×10^{-15}	–	–	–	–	–	–	–	–	–	[84]
dwCNT	PET	–	Co-electrospun	1	1.5×10^{-14}	–	–	–	–	–	–	–	–	–	[84]
mwCNT	PET	–	Co-electrospun	1	7.7×10^{-15}	–	–	–	–	–	–	–	–	–	[84]
mwCNT	PVA	-COOH functionalized	Co-electrospun	10	0.025	–	–	–	–	–	–	–	–	–	[145]
mwCNT	PAN	-COOH functionalized	Co-electrospun	20	1	–	–	–	–	–	–	–	–	–	[111]
mwCNT	PLA	–	Co-electrospun	1	0.001	–	–	–	–	–	–	–	–	–	[264]
mwCNT	PVDF/PANI	–	Co-electrospun	10	4.08×10^{-16}	–	–	–	–	–	–	–	–	–	[150]
mwCNT	Shell - PVDF/PANI/mwCNT	–	Coaxial electropun	10	2.75×10^{-9}	–	–	–	–	–	–	–	–	–	[150]
mwCNT	Core - PVDF	–	–	–	–	–	–	–	–	–	–	–	–	–	[148]
mwCNT	Shell - PAA/PVA hydrogel Core - PCL/mwCNT	-COOH functionalized	Coaxial electro-spun + crosslinking	0.05	0.039	–	–	–	–	–	–	–	–	–	[146]
mwCNT	Shell - Cellulose/[EMIM][Ac]	–	Co-electrospun + enzymatic removal of cellulose	45	0.107	–	–	–	–	–	–	–	–	–	[146]
mwCNT	Core - [EMIM][Ac]/mwCNT	–	–	–	–	–	–	–	–	–	–	–	–	–	[276]
mwCNT	Chitosan	–	Co-electrospun	0.6	9×10^{-5}	–	–	–	–	–	–	–	–	–	[147]
mwCNT	Shell - PMMA	–	Coaxial electropun + thermal removal of PMMA	0.5	0.90	–	–	–	–	–	–	–	–	–	[277]
swCNT	PLLA	–	Co-electrospun	3	0.006	10^{-9}	–	–	–	–	–	–	–	–	[277]
mwCNT	PLLA	–	Co-electrospun	3	0.005	10^{-9}	–	–	–	–	–	–	–	–	[277]
mwCNT	PLA	–	Co-electrospun	0.3	0.001	–	–	–	–	–	–	–	–	–	[83]
mwCNT	Silk/PEO	-COOH functionalized	Dip coated	1 immersion cycle (3 mg/ml)	2.4×10^{-4}	4.4×10^{-15}	–	–	–	–	–	–	–	–	[161]
mwCNT	PAN/PANI	–	Co-electrospun	7	0.0797	5.69×10^{-4}	–	–	–	–	–	–	–	–	[127]
mwCNT	PLA	–	Co-electrospun	3	10^{-5}	10^{-18}	–	–	–	–	–	–	–	–	[151]
mwCNT	C540 Styrene-butadiene-styrene	–	Co-electrospun	0.5	10^{-8}	3×10^{-12}	–	–	–	–	–	–	–	–	[267]
mwCNT	Silk	–	Co-electrospun	1	1.2×10^{-4}	5.04×10^{-14}	–	–	–	–	–	–	–	–	[266]
mwCNT	Polypropylene	–	Blended + melt electrospun	0.05	10^{-6}	10^{-8}	–	–	–	–	2.5	0.25	–	–	[129]
mwCNT	PLGA	–	Co-electrospun	0.5	1.34×10^{-4}	8×10^{-5}	–	–	–	–	–	–	–	–	[278]
mwCNT	PEO	–	Electrospun onto CNT sheet + Calendering	60	205	–	–	–	–	–	–	–	–	–	[164]

Table 3 (Continued)

Table 4

Compilation of thermal properties of nanocarbon reinforced polymer composite nanofibers from literature.

Nanofiller	Polymer	Loading (%)	T _{decomposition} (°C)		T _{glass} (°C)		Coefficient of Thermal Expansion (10 ⁻⁶)		Thermal Conductivity W/(m K)		Reference
			Composite	Control	Composite	Control	Composite	Control	Composite	Control	
mwCNT	PAA	3	~260	~225	~260	~260	–	–	–	–	[152]
mwCNT	PAN	5	292	268	–	–	–	–	–	–	[111]
mwCNT	PAN	10	–	–	94	83	–	–	–	–	[111]
mwCNT	PAN	20	–	–	–	–	13 × 10 ⁻⁶	180 × 10 ⁻⁶	–	–	[111]
GO	PVA	0.5	288	268.5	69.19	66.38	–	–	–	–	[365]
GO	PVA	1	284.9	268.5	69.5	66.38	–	–	–	–	[365]
mwCNT	PVDF/PANI	10	–	–	~170	160	–	–	–	–	[150]
CB	PU	4.58	284.35	276	–	–	–	–	–	–	[252]
CB	PU	12.6	269.70	276	–	–	–	–	–	–	[252]
mwCNT	PI	10	610	582	–	–	–	–	–	–	[119]
Graphene	PVA/PVP	0.5	–	–	73	74	–	–	–	–	[167]
Graphene	PLA	0.5	337.9	319.3	–	–	–	–	–	–	[205]
GO	PVDF	0.7	466	465	–	–	–	–	–	–	[206]
mwCNT	PVDF/HFP	3	–	–	–	–	–	–	0.065	0.052	[75]
Graphene	PAN	8	–	–	–	–	–	–	2.7	1	[211]
Graphene	PMMA	8	–	–	–	–	–	–	5	1	[211]
mwCNT	PCL	5	–	–	56.26	66.5	–	–	–	–	[281]
Graphene	PANI/PEO	5	321	285	–	–	–	–	–	–	[191]
GO	PVA	8mg	245	259	78	69	–	–	–	–	[180]
Graphene	PVAc	0.07	335	330	–	–	–	–	–	–	[190]
Graphene	PVA	2	281	197	–	–	–	–	–	–	[168]
Graphite	PU	5.1	403.4	360.7	–	–	–	–	–	–	[259]
GO	PVA	5	283.7	257.7	–	–	–	–	–	–	[166]
rGO	PVA	5	273.4	257.7	–	–	–	–	–	–	[166]
Graphene	PA	1.5	–	–	58.25	48.73	–	–	–	–	[204]
mwCNT	Nylon	7.5	–	–	92	85	–	–	–	–	[128]
mwCNT	PI	10	560	501	–	–	–	–	–	–	[67]
Graphene	PBS/PLLA	1.3	379	376	–	–	–	–	–	–	[203]
GO	PGA-co-PFF	5	356	326	–	–	–	–	–	–	[209]
mwCNT	Nylon	0.056	360	320	–	–	–	–	–	–	[279]
GO	PLA	3	–	–	62.5	56.2	–	–	–	–	[208]
mwCNT	PLLA	4	–	–	60.5	60.3	–	–	–	–	[121]
mwCNT	PDLA	4	–	–	60	59.5	–	–	–	–	[121]
mwCNT	PCL	0.5	360	316	–	–	–	–	–	–	[138]
GO	PVA	0.2	245	295	–	–	–	–	–	–	[172]
Graphene	PVA	0.08g	393	383	–	–	–	–	–	–	[210]
mwCNT	PBT	5	425	416	–	–	–	–	–	–	[91]
rGO	PU	9.8	~400	~375	–	–	–	–	–	–	[197]
Nanodiamond	PLA	3	57	52	–	–	–	–	–	–	[236]
GO+HA	PLA	8.6 + 4.3	338.8	228.9	–	–	–	–	–	–	[171]
mwCNT	PCL	5	340	310	–	–	–	–	–	–	[137]
nwCNT	PCL	1	–	–	62.17	61.68	–	–	–	–	[138]
GO	PI	2	603	503	323	317	–	–	–	–	[169]
GO	PLA	5	341.9	328.4	–	–	–	–	–	–	[189]
mwCNT	PVB	10	290	295	–	–	–	–	16.8	–	[80]

mance of these nanofibers when applied in fields as diverse as tissue engineering scaffolds to water filtration membranes, highlighting research work done to address many of the world's greatest challenges.

4.1. Tissue engineering

The damage and loss of portions of or whole tissues caused by diseases and accident are among the thorniest problem in medicine. Although the body exhibits functional self-recovery after injury, the kind of self-healing is quite limited for those with severe tissue loss or low regenerative potential [282]. Traditional transplant methods realize the replacement of damaged or lost organs, but the scarcity of donor organs and immune rejection remain a serious problem [283,284]. The idea of tissue engineering was raised in the early 1970, when study was conducted on cartilage regeneration *in vivo* [285]. Tissue engineering is targeted to inspire the body's own potential to functionally heal previously irreparable tissues with the help of scaffolds, cells and bioreacting condition [286]. To improve the compatibility of implanted scaffold, the design of regenerative scaffold focused on mimicking of extracellular matrix (ECM), the native cell's environment consisting of nanosized colla-

gen fibers and biomolecules [287]. A nanofibrous scaffold would be realized by different techniques such as template synthesis, electrospinning and self-assembly and electrospinning is one of the most popular techniques among them owing to its wide applicability for different materials and high flexibility in functionalities [43,288,289].

Due to the good biocompatibility and biodegradability, polymers like poly(ϵ -caprolactone) (PCL), poly(lactic acid) (PLA), and silk fibroin were employed to prepare electrospun regenerative scaffold. However, these polymeric scaffolds showed limited mechanical strengths and electrical conductivity [193,265,281,290], which may not be able to support chronic tissue regeneration and efficient signal transmission. These issues could be addressed by incorporation of mechanically strong and electrically conductive materials such as carbon materials. The primary hindrance to employing nanocarbon materials for tissue engineering applications is their potential toxicity issues. Animal studies showed that inhalation and intratracheal instillation of CNTs induced sustained inflammation, fibrosis, gene damage and even lung cancer [291]. However, the CNT toxicity showed dependence on the dose, size and functionalization of CNT [287]. The toxicological properties of CNTs can be mitigated through

Table 5

Summary of recent progresses on electrospun polymer-carbon composite for tissue engineering.

Polymer	Nanofiller	Nanofiller loading(w/w%)	Fabrication technique	Diameter (nm)	Biological assay	Application	Reference
PLA	mwCNT	0.25-1	co-electrospinning	~700	—	General	[83]
silk	swCNT	1	co-electrospinning	~150	—	General	[270]
PCL	mwCNT	0.1-5	co-electrospinning	~117-252	3 days <i>in vitro</i> (L-929, NIH 3T3)	General	[281]
PLA	swCNT	6.67	co-electrospinning	—	1 day <i>in vitro</i> (human MSC)	General	[302]
silk	mwCNT	0.25-1.5	co-electrospinning	—	7 days <i>in vitro</i> (3T3, beagle's lingua mucosa cell)	General	[290]
PNIPAm-co-MAA	PANI-mwCNT	100	co-electrospinning	~500-600	7 days <i>in vitro</i> (L929)	General	[303]
PLLA/PCL	mwCNT	1.25-3.75	co-electrospinning	~530-610	7 days <i>in vitro</i> (rabbit adipose-derived stem cell)	General	[123]
chitosan poly(N-isopropylacrylamide)	mwCNT PANI-mwCNT	0.6 —	co-electrospinning co-electrospinning	~275 —	— 7 days <i>in vitro</i> (L929, A549, NHDF, NHLF, RLE6TN, HEK293)	General General	[276] [304]
PU	mwCNT	0.1-1	co-electrospinning	~322-584	—	General	[274]
cellulose acetate	chitosan-mwCNT	—	LBL	—	7 days <i>in vitro</i> (L929)	General	[165]
PU	mwCNT	0.1-1	co-electrospinning	~600-1000	7 days <i>in vitro</i> (3T3)	General	[94]
TPU	mwCNT	1	co-electrospinning	~738	—	General	[301]
PLA/PCL	mwCNT	0.25-2	co-electrospinning	~736-870	7 days <i>in vitro</i> (3T3)	General	[268]
PLA	mwCNT	1-4	co-electrospinning	~500-600	2 days <i>in vitro</i> (HUVEC)	General	[121]
P3HB	mwCNT	0.5-1.25	co-electrospinning	~310-690	—	General	[265]
PLA	PEG-g-GO, GO	1-5	co-electrospinning	~593-863	10 days <i>in vitro</i> (3T3)	General	[189]
PVA	graphene	1-7.5	co-electrospinning	~371-521	3 days <i>in vitro</i> (3T3)	General	[179]
silk fibroin	GO, rGO	—	dip coating	~4200-5200	7 days <i>in vitro</i> (L929)	General	[193]
PVA/chitosan	mwCNT	1	co-electrospinning	~170	7 days <i>in vitro</i> (L929)	General	[122]
PLA	mwCNT	0.25-1	—	~700	14 days <i>in vitro</i> (human MSC)	Bone	[264]
PLGA/HA	mwCNT	6	co-electrospinning	~2150	—	Bone	[311]
PLGA/HA	mwCNT	2	co-electrospinning	~503-1090	5 days <i>in vitro</i> (rat MSC)	Bone	[310]
PLA	mwCNT	1-5	co-electrospinning	~232-281	7 days <i>in vitro</i> (rat osteoblast)	Bone	[280]
PLGA	mwCNT	1.6-8.3	co-electrospinning	~1257-2193	5 days <i>in vitro</i> (rat MSC)	Bone	[313]
PLGA	mwCNT	1	co-electrospinning	~1257	7 days <i>in vitro</i> (rat MSC)	Bone	[317]
PCL	CNF	0.1-0.5	co-electrospinning	~400-500	7 days <i>in vitro</i> (human MSC)	Bone	[314]
PLGA	ND	23	co-electrospinning	~270	7 days <i>in vitro</i> (MG-63)	Bone	[242]
PVA	ND	0.1-0.5	co-electrospinning	~253-338	1 day <i>in vitro</i> (human MSC)	Bone	[237]
PVA	GO	0.5-5	co-electrospinning	—	4 days <i>in vitro</i> (MC3T3-E1)	Bone	[178]
PCL	GO	0.1-1	co-electrospinning	—	7 days <i>in vitro</i> (mouse MSC)	Bone	[176]
gelatin/HA	mwCNT	—	co-electrospinning	~180	7 days <i>in vitro</i> (human fetal osteoblastic cell)	Bone	[272]
PLGA	ND	23	co-electrospinning	~270	9 days <i>in vitro</i> (human MSC)	Bone	[241]
PBAT	mwCNT	0.1-0.5	co-electrospinning	~250-272	14 days <i>in vitro</i> (MG-63)	Bone	[308]
PLGA/silk	GO	1	co-electrospinning	~130	14 days <i>in vitro</i> (MSC)	Bone	[181]
PLGA/PVC	rGO	—	heat-driven self-assembly	~580	7 days <i>in vitro</i> (human MSC)	Bone	[194]
PLLA	mwCNT	0.5-1	co-electrospinning	~1332-3390	14 days <i>in vitro</i> (human MSC)	Cartilage	[318]

Table 5 (Continued)

Polymer	Nanofiller	Nanofiller loading(w/w%)	Fabrication technique	Diameter (nm)	Biological assay	Application	Reference
PLA	mwCNT	1	co-electrospinning	~2080	3 days <i>in vitro</i> (human chondrocyte)	Cartilage	[271]
PCL	graphene/mwCNT	0.5-1	co-electrospinning	–	14 days <i>in vitro</i> (human MSC)	Cartilage	[213]
PLLA/HA	mwCNT	0.30	co-electrospinning	–	3 days <i>in vitro</i> (human dental pulp stem cell)	Dental	[322]
PLLA/HA	mwCNT	0.30	co-electrospinning	~1000	7 days <i>in vitro</i> (Human periodontal ligament cell, human gingival epithelial cell) 4 weeks <i>in vivo</i> (mouse)	Dental	[321]
PVA/HA	mwCNT	0.5-5	co-electrospinning	–	14 days <i>in vivo</i> (Chicken embryo)	Dental	[323]
PLGA	mwCNT	–	PLGA fiber on mwCNT yarn	–	22 days <i>in vitro</i> (mouse NR6 fibroblast)	Neural	[341]
fibronectin	silk/mwCNT	–	fibronectin fibers collected on freeze-dried silk/MNWT	–	14 days <i>in vitro</i> (U373) 5 weeks <i>in vivo</i> (rat)	Neural	[335]
collagen/PCL	mwCNT	1	co-electrospinning	~564	3 days <i>in vitro</i> (rat schwann cell) 4 months <i>in vivo</i> (rat)	Neural	[263]
PLLA	mwCNT	0.25	co-electrospinning	~400	2 days <i>in vitro</i> (SH-SY5Y)	Neural	[334]
PLGA/Silk	mwCNT	1.30	co-electrospinning	~745	5 days <i>in vitro</i> (human adipose-derived stem cell)	Neural	[329]
PLLA	swCNT	3	co-electrospinning	–	21 days <i>in vitro</i> (rat olfactory ensheathing glial cell)	Neural	[327]
PCL	GO	0.1-1	co-electrospinning	–	7 days <i>in vitro</i> (PC12)	Neural	[176]
PCL	graphene	–	LBL	~1100	7 weeks <i>in vivo</i> (rat)	Neural	[199]
PLGA	mwCNT	0.05-0.5	co-electrospinning	~841-3209	8 days <i>in vitro</i> (rat primary cortical neuron)	Neural	[92]
silk	rGO	–	dip coating	~5157	10 days <i>in vitro</i> (PC12)	Neural	[328]
silk	mwCNT	0.5-2	co-electrospinning	~80-105	–	Neural	[266]
PCL/PAA/PVA	mwCNT	0.10	co-electrospinning	~1704-1861	28 days <i>in vitro</i> (rat primary muscle cell)	Skeletal muscle	[148]
gelatin	mwCNT	–	co-electrospinning	~250-500	6 days <i>in vitro</i> (C2C12)	Skeletal muscle	[336]
SEBS	mwCNT	0.05-1.5	co-electrospinning	~11000	3 days <i>in vitro</i> (C2C12)	Skeletal muscle	[267]
PLGA	mwCNT	0.5-8	co-electrospinning	<1000	7 days <i>in vitro</i> (C2C12)	Skeletal muscle	[278]
PCL/PEDOT	mwCNT	0.10	co-electrospinning	~2190	–	Skeletal muscle	[269]
PCL	GO	–	co-electrospinning	–	11 days <i>in vitro</i> (C2C12)	Skeletal muscle	[175]
PLA	swCNT	6	co-electrospinning	–	14 days <i>in vitro</i> (human MSC)	cardiac	[337]
poly(glycerol sebacate)/gelatin	mwCNT	0.05-1.5	co-electrospinning	~210-270	7 days <i>in vitro</i> (rat cardiomyocyte)	cardiac	[273]
cellulose acetate	swCNT	0.25-0.5	co-electrospinning	~500	5 days <i>in vitro</i> (HUVEC)	vascular	[338]
PU	mwCNT	3	co-electrospinning	–	7 days <i>in vitro</i> (HUVEC)	vascular	[339]
PU	mwCNT	–	co-electrospinning	~300-500	7 days <i>in vitro</i> (HUVEC)	vascular	[340]

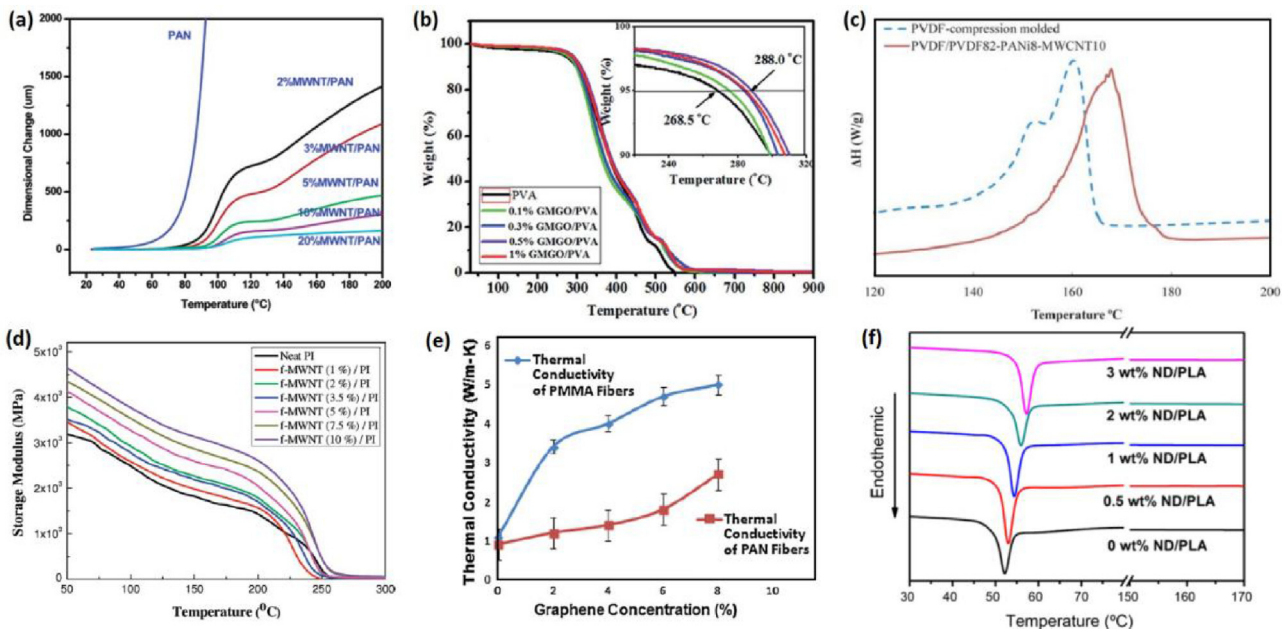


Fig. 9. (a) TMA curves for composite PVA nanofibers containing mwCNT showing reduced mechanical deformations above softening temperatures with increasing filler loadings [111]. Copyright 2004, reproduced with permission from American Chemical Society; (b) TGA thermogram showing optimal graphene based nanofiller loadings at 0.5 wt% beyond which onset decomposition temperature decreases with inset showing magnified region of 5% weight loss [184]. Copyright 2014, reproduced with permission from The Royal Society of Chemistry; (c) DSC thermogram showing increased glass transition temperature resulting from increased crystallinity with the addition of mwCNTs and the application of electrospinning [150]. Copyright 2014, reproduced with permission from John Wiley and Sons; (d) DMA curves showing increasing storage modulus at each temperature for different mwCNT filler loadings in PI nanofibers [119]. Copyright 2009, reproduced with permission from American Chemical Society; (e) Graph charting the thermal conductivity of PMMA and PAN nanofiber with increasing graphene loading [211]. Copyright 2014, reproduced with permission from John Wiley and Sons. (f) DSC thermogram showing increasing trend of glass transition temperature with increasing nanodiamond loading in PLA nanofibers [236]. Copyright 2014, reproduced with permission from Springer.

well control of these parameters [287]. A recent study evaluated the *in vivo* biocompatibility of a PLGA/swCNT composite for bone regeneration through signs of morbidity, overt toxicity, weight gain, food consumption, haematology, urinalysis and histopathology [292]. Similar results were exhibited between the PLGA/swCNT composites and the PLGA over a period of 12 weeks, which may indicate that a low amount of swCNT may not elicit a localised or general overt toxicity in tissue engineering application [292]. Another concern about the application of the nanocarbon materials on tissue engineering is the biopersistence. The physical and chemical nature of nanocarbon materials make them inert, stable, recalcitrant, and difficult to degrade [293,294]. Nanocarbons like CNT and GO were found to trigger inflammasome activation and retain in the organs *in vivo* [295]. Fortunately, recent researches have demonstrated the susceptibility for enzymatic degradation of these nanomaterials *in vivo* through mediation of neutrophil and macrophage and renal excretion route [295,296]. The biodegradation and biodistribution of the nanocarbons were enhanced by surface functionalization of the materials [295,297]. In addition to nanocarbon materials, the combined degradation product of polymer and carbon may be toxic. The combination of mwCNT and lactic acid, the degradation product of PLA, showed inhibition to the activity of human bone marrow stromal cells although free-dispersed mwCNT did not show cytotoxicity in the same study [298].

Considering the superior electrical and mechanical properties of nanocarbons and great potential on mitigated toxicity and biodegradation of the composite [299,300], polymer-carbon electrospun composite would be a promising scaffold for tissue engineering. Further research and clarification is needed in terms of the cytotoxicity and biodegradation of the nanocarbon materials. Improvement on design of the polymer-carbon composite targeted to high biocompatibility and comprehensive understanding and

evaluation of the biological interaction of the polymer-carbon composite should be conducted for safe application.

Carbons were incorporated into electrospun polymeric scaffold by direct co-electrospinning or post-treatment of polymeric scaffold though methods such as dip coating and layer-by-layer assembly [165,193,270]. The weight percentage of carbon in polymer matrix ranged from 0.1% to 7.5% [179,274,281]. Polymer-carbon fibers with a diameter of hundreds of nanometers [83,270,276,281,301] or several micrometers [193,290] were obtained by selecting the host polymer and tuning percentage of carbon. The fibrous scaffolds displayed more than 80% porosity, which would be highly favourable for cell attachment and nutrition transport [83,123,265,281]. The tensile strength of the scaffold was changed after the incorporation of carbon materials. The strength could be increased up to around 3 folds with low amount of carbon [290] while high amount of carbon seemed to reduce the strength due to aggregation [193,290]. Carbon nanotube significantly improved the mechanical strength of silk fibroin scaffold by more than 2 folds [270,290]. As for incorporating method, dip coating seems not as efficient as co-electrospinning on reinforcement by carbon [189,193,270,290]. The effect of carbon percentage on scaffold's mechanical strength varied from different polymers. The optimized carbon percentage was 0.5–1% for silk fibroin, PCL, PU and P3HB [94,265,270,274,281,290] while 1–2% carbon showed better improvement for PLA [189,302]. In addition to the improvement on mechanical strength, the carbon materials showed promotion on the electrical conductivity of the scaffold. Silk/swCNT nanofibrous scaffold showed around 7 times electrical conductivity compared to neat silk one [270]. The degradation of the scaffold plays an important role in regeneration process as it should provide enough structural support at the beginning of regeneration and degrade gradually without cytotoxicity. Carbon materials were shown to tune the degradability of the polymer

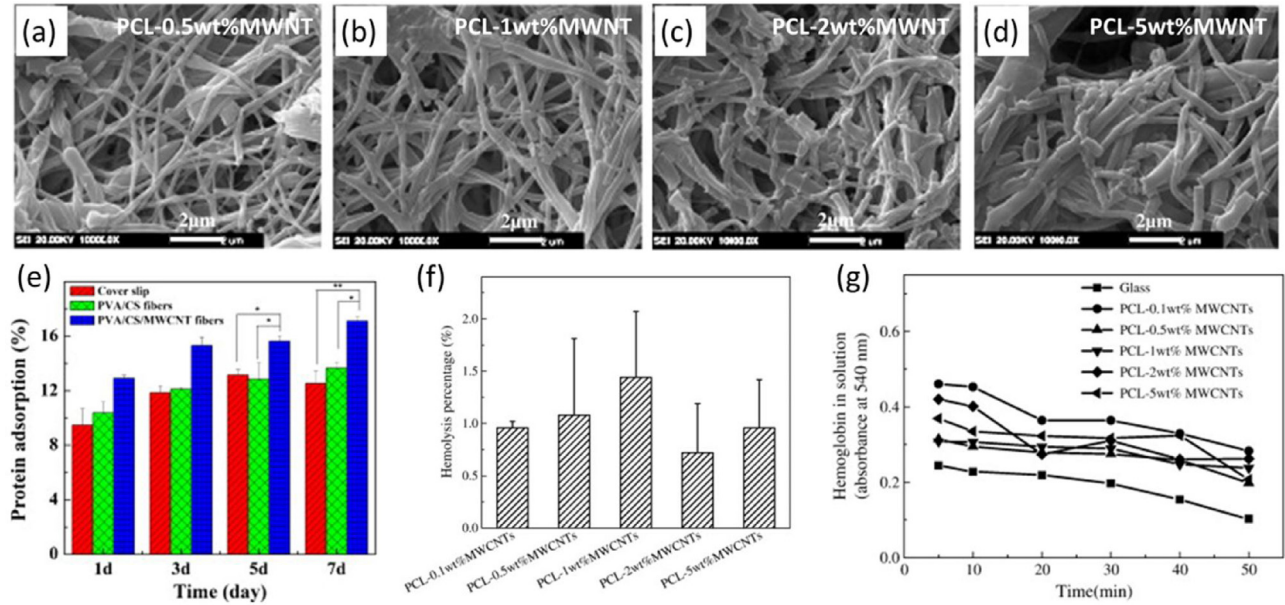


Fig. 10. (a-d) Morphology of electrospun PCL-mwCNTs nanofiber membrane after degradation for 4 and 8 weeks [281]. Copyright 2010, reproduced with permission from Elsevier Ltd; (e) The adsorption of protein onto coverslip, PVA/chitosan nanofibrous mats without mwCNTs, and PVA/chitosan/mwCNTs nanofibrous mats (the data are expressed as mean \pm S.D., $n = 3$, * $p < 0.05$, ** $p < 0.001$, *** $p < 0.0001$) [122]. Copyright 2011, reproduced with permission from Elsevier Ltd; (f) Hemolysis percentage of electrospun PCL-mwCNTs electrospun nanofiber membranes; (g) Dynamic clotting time of electrospun PCL-mwCNTs nanofiber membranes [281]. Copyright 2010, reproduced with permission from Elsevier Ltd.

scaffold. CNT accelerated the degradation of the PCL scaffold which has a slow degradation originally (Fig. 10a-d) while the presence of CNT appeared to enhance the physical stability of PLA scaffold and slow down degradation [281,302]. The protein absorption of the polymer-carbon scaffold was also characterized. More protein absorbed on the nanofibrous scaffold with carbon than those without carbon (Fig. 10e) [122,165].

The biocompatibility of the polymer-carbon composite scaffold for general tissue engineering application was first tested through *in vitro* culture of fibroblasts and stem cells. The majority of study showed higher or similar fibroblasts cell number on polymer-carbon fibers compared those on neat polymer fibers and control (well plates or coverslips) after one-week culture [94,122,165,179,189,193,268,290,303,304] while others showed lower cell number on polymer-carbon fibers after 2–3-day culture [121,281]. Cell attached less but grew slightly faster on polymer-carbon fibers compared to neat polymer fiber and control [122,123,281]. The amount of carbon in the composite fibers influenced the biocompatibility of the scaffold. High carbon percentage may impair the biocompatibility of the scaffold due to protruding of the carbon on the fiber surface and reduced mechanical property [94,121,165,193,281]. The incorporation of carbon into the scaffold showed no negative effect on stem cell viability/density [123,302]. In addition to cytotoxicity, the hemocompatibility of the polymer-carbon fibers was tested. The fibers showed less than 3% hemolysis percentage and good anticoagulant property (Fig. 10f and g), which indicated good hemocompatibility [165,281]. Structural guidance was effective on the polymer-carbon nanofibers, where the attached cell spread in a pattern of reorientation parallel to the aligned fibers [123]. Recent progresses on electrospun polymer-carbon nanofibers for different kinds of tissue engineering application were summarized in Table 4.

4.1.1. Bone, cartilage and dental tissue engineering

Owning to the intrinsic capacity for regeneration, bone tissue exhibits self-healing process in response to injury and continuous remodeling throughout adult life. However, the regeneration ability may be impaired when diseases or trauma induce large defect

and loss of supporting environment such as avascular necrosis and atrophic non-unions [305]. During the past ten years, bone tissue engineering has emerged for therapeutic repair of bone tissue without the limitation of current clinical grafting and implanted prosthesis like stress-shielding. An ideal bone tissue engineered scaffold should have good mechanical and biological compatibility to native bone tissue and good osteoinductivity and osteoconductivity to guide bone regeneration in addition to basic requirement such as biodegradability and porosity [272,305–308].

Polymer-carbon composite scaffold showed great promise for bone tissue engineering application. Good cell behaviors including attachment and proliferation and osteoblast differentiation after functionalized with oseoinductor protein rhBMP-2 were exhibited on polymer-CNT composite scaffold [306,309]. Abarrategi et al. implanted chitosan/mwCNT scaffolds into mice and observed bone tissue regeneration after 3 weeks [309]. Poly(propylene fumarate)(PPF)/swCNT scaffold prepared by Sitharaman et al. showed three-fold bone ingrowth compared to pure PPF scaffold 12 weeks after implantation [307]. Although the implant was surrounded by a fibrous capsule, the inflammatory cell density was decreased over time [307]. To improve the biocompatibility of polymer-carbon scaffold, electrospun polymer-carbon scaffolds with an ECM-like structure were fabricated later and studied on its application in bone regeneration. Electrospun polymer-carbon scaffold for bone tissue engineering were prepared through composite fibers made of a host polymer like PLGA, PVA and PCL and carbon fillers like CNT, GO and nano-diamond(ND). In order to enhance the bioactivity of scaffold with osteoblast cells, hydroxyapatite (HA), a major component of natural bone, was incorporated into the electrospun polymer-carbon scaffold by co-electrospinning [272,310] or biomimetic mineralization [311].

Compared to other tissues in the body, bone is much harder, with a Young's modulus of around 10–20 GPa [312]. However, traditional electrospun polymeric scaffold showed a low Young's modulus of less than 100 MPa, which impaired their ability to support bone healing. The incorporation of carbon materials significantly increased the mechanical property of electrospun scaffold, with a 2–3-fold increase in elastic modulus and more than 50% increase in

tensile strength [181,264,280,313,314]. A gelatin/HA/mwCNT electrospun fibrous scaffold exhibited a Young's modulus of 820 MPa, which is more compatible with native bone tissue than neat gelatin scaffold [272].

The osteoblast cytotoxicity of carbon materials was studied first. Although there are ongoing debates over the cytotoxicity of CNT, CNT showed no significant inhibition on the viability of osteoblasts [315,316]. The proliferation of osteoblast exposed to ND was not inhibited but showed a slower proliferation rate when the concentration of ND in media is high [237]. As mineral calcium phosphate is one of the most important components of bone, scaffold with good bioactivity to promote mineralization may accelerate the bone regeneration process. A fully covered mineral layer was observed on the surface of electrospun polymer-mwCNT after soaking in the stimulated body fluid at 37 °C for 21 days [311]. Both HA and COOH-functionalized mwCNT displayed accelerating effect on the deposition of apatite owing to their negative charge [272].

In vitro culture of mesenchymal stem cells (MSC) and osteoblasts were conducted to test the biocompatibility of the polymer-carbon composite scaffold for bone tissue engineering. Although there were poorer adhesion and a sign of cell damage at the early stage of culture [237,241], MSCs cultured on polymer-carbon fibrous scaffold showed better proliferation than those on neat polymer one [181,241,264,310,313,317]. Also, MSCs exhibited spread morphology with long filopodia [181,194,313,314,317] and integrated into the structure of the electrospun composite scaffold with a trend of migration inside [176,264,310]. A significant higher expression of vitronectin and tenascin which were related to homeostasis and bone formation was showed on MSCs cultured on PVA-ND fibrous scaffold compared to neat PVA one [237]. Osteogenic differentiation of MSCs on the electrospun scaffold was studied and results showed that the presence of GO markedly enhanced the osteogenesis and mineralization [176,181]. The PLGA-silk-GO fibrous scaffold significantly increased the expression of alkaline phosphatase (ALP) and osteocalcin compared to coverslip after 14-day culture (Fig. 11a–c), which indicated dramatically accelerated new bone formation [181]. The differentiated cell induced formation of minerals with a Ca/P ratio of 1.53, which is quite similar to the theoretical ratio in HA (1.67) [181]. The improved osteogenic differentiation may be attributed to the increased surface roughness and protein absorption after incorporation of GO [181]. In addition to MSCs, osteoblasts were cultured *in vitro* on the electrospun polymer-carbon scaffolds to test its biocompatibility. No difference was showed on the proliferation of osteoblasts between neat polymer and polymer-carbon scaffolds [178,280,308]. Higher ALP activity and mineralized matrix formation were observed on PBAT/CNT scaffold than PBAT scaffold [308]. However, the viability of the osteoblasts was impaired when 23% of ND was incorporated into the scaffold [242]. Potential immune activation of osteoblasts on scaffold was estimated by their secretion of tumor necrosis factor alpha (TNF- α) into the cell culture medium. Electrospun PLGA-ND scaffold did not show considerable inflammatory activity, but its TNF- α level is slightly higher than PLGA scaffold and control polystyrene dishes [242]. With incorporation of carbon materials, the conductivity and charge carry capacity of the polymeric scaffold was notably improved, which could provide a platform for electrically stimulated bone regeneration [194,280]. Application of small electrical current (<100 μ A) did not have any negative effect on the viability of osteoblast and enhanced the proliferation of cells over time while application of high current (>200 μ A) led some cells to death [280]. The electrical stimulation also made a difference on the morphology of osteoblast [280]. Elongated cell morphology and directional orientation along the electrical current direction was observed after electrical stimulation. The change of cell morphology might be attributed to the increased protein absorption induced by electrical stimulation.

Compared to bone, cartilage has much lower regenerative capacity due to low cell density and lack of vascular network. To promote the regeneration of cartilage, electrospun nanofibrous scaffolds made of polymer and carbon were introduced recently. The scaffold showed compatible mechanical property to native cartilage tissue with a Young's modulus of ~0.45–460 MPa [213,271,318], which represented similar range to native tissue (0.5–200 MPa) [319,320]. MSCs cultured on the scaffold exhibited similar proliferation and dramatic increase in chondrogenic differentiation activity compared to neat polymer scaffold (Fig. 11d) [213,318]. The application of poly-L-lysine surface further enhanced the adhesion and differentiation of the MSCs [213,318]. However, more chondrocyte damage was observed on PLA/mwCNT fibrous scaffold compared to PLA scaffold [271].

In addition, electrospun polymer-carbon scaffold hold promise for dental tissue engineering. Promotion of periodontal ligament cell and inhibition of gingival epithelial cell on adhesion and proliferation were observed on PLLA/mwCNT/HA scaffold [321]. The cell selectivity would provide more space for dental regeneration. Dental pulp stem cells also displayed good attachment with elongated and spindle-like morphology on the scaffold [322]. The regenerative ability of the scaffold was evaluated *in vivo*. Results showed that vessels were formed near the scaffold, followed by attachment of osteoblast-like cells, formation of bone-like tissues and deposition of mineral. No significant tissue response was found in the implants area [321,323].

4.1.2. Neural tissue engineering

Nervous system is one of the most important systems in the body as it controls functioning of different parts in the body and react with the external environment. Injury in the nervous system caused by nervous diseases and accidents may lead to a loss of sensation and motor function and even memory and mood [324]. Neurological disorders were found to be the leading cause of disability adjusted life years (10.2%), and the second most deadly group of diseases, representing 16.8% of global deaths in 2015. Already a prime cause of death and disability globally, the burden from these disorders is expected to increase over the next 2 decades with growing populations [325]. Due to the serious consequences and especially hopeless self-recovery from damage to the central nervous system caused by these injuries [326], strategies are needed to assist the functional regeneration and recovery of nerve tissue. Electrospinning of tissue engineering scaffold is one of the promising approaches for neural regeneration.

Due to the intrinsic electric and ionic current flow in native nerve tissue, an ideal nerve tissue engineered scaffold should possess good electrical conductivity and electroactivity. However, traditional electrospun polymeric scaffolds are almost insulating, which limited their ability to promote neural connection and regeneration. With carbon materials, the conductivity of electrospun scaffold could be notably improved by around 9 orders of magnitude [266,327]. In addition, an increase in electroactivity was observed on electrospun polymer-carbon scaffold compared to neat polymer one, which would enable faster charge transfer between electric and ionic signal and thus neural signals transmission [328]. The incorporation of carbon materials slightly increased the strength of the scaffolds [92,263,266], but the higher stiffness of the scaffolds may make it less compatible with native tissue [266,328]. The scaffolds had elastic modulus of more than 20 MPa while the elastic modulus in native nerve tissue is less than 1 MPa [92,263,266,328–331]. Although the biocompatibility and cytotoxicity of carbon materials with neural cells are debatable, the majority of studies showed promising results such as good neural differentiation, preservation of neural physiological activity and nerve regeneration [92,332,333].

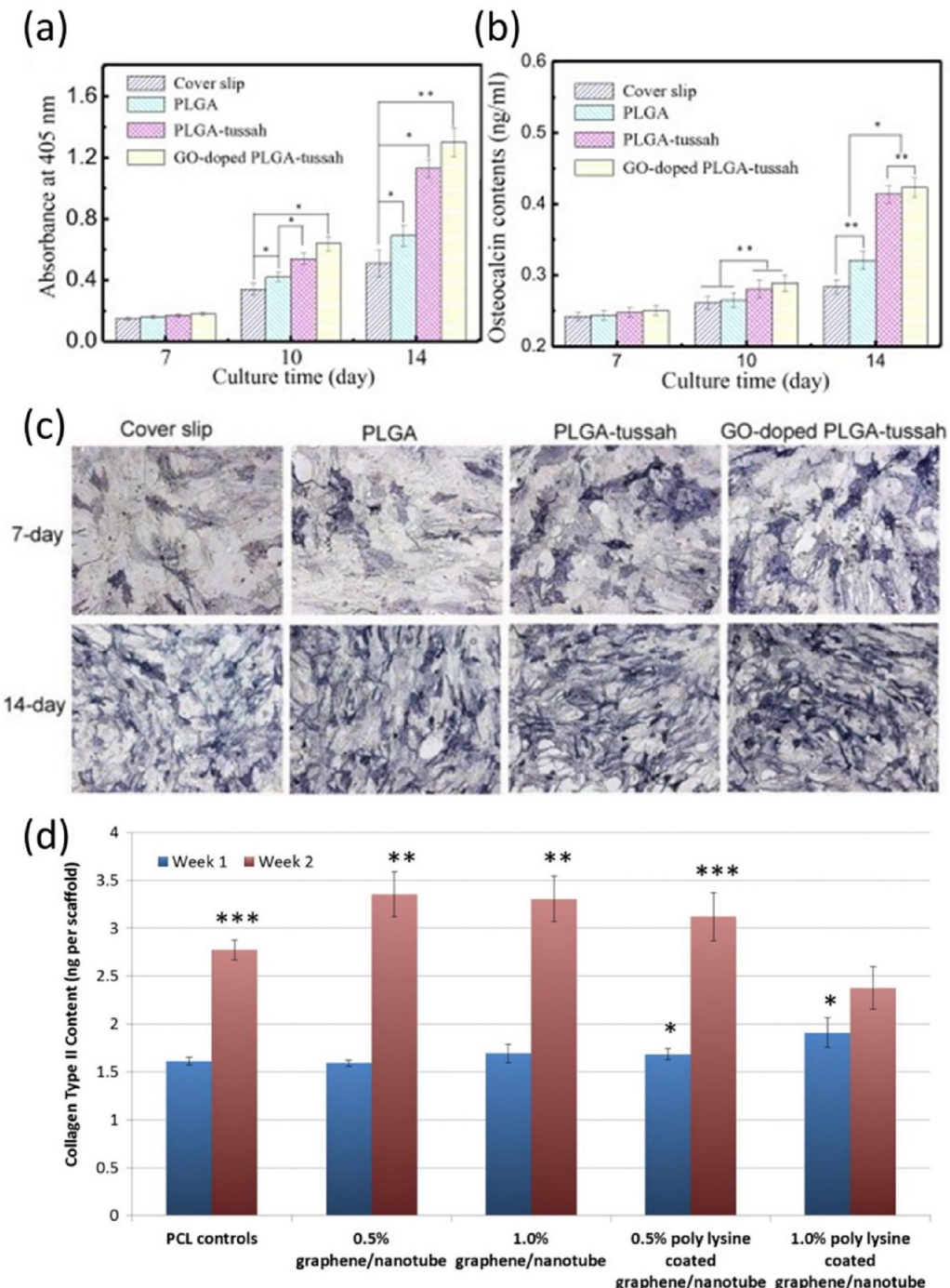


Fig. 11. (a) Alkaline phosphatase enzyme activity of mesenchymal stem cells seeded on different substrates after 7, 10, and 14 days of culture, respectively; (b) Osteocalcin protein produced by mesenchymal stem cells cultured on different substrates after 7, 10, and 14 days of culture, respectively (* $p < 0.05$, ** $p < 0.01$) [181]. Copyright 2016, reproduced with permission from Elsevier Ltd. (d) Greatly enhanced glycosaminoglycan synthesis on electrospun nano scaffolds after 2 weeks when compared to PCL controls. Data are mean \pm standard error of the mean, $N = 3$, * $p < 0.05$ when compared to controls after week 2, ** $p < 0.01$ when compared to controls after week 1 [213]. Copyright 2016, reproduced with permission from Elsevier Ltd.

The *in vitro* biocompatibility of the electrospun polymer-carbon composite scaffold targeting to neural tissue engineering was evaluated through stem cells, neuroblasts, neurons and glial cells. Stem cells and neuroblasts like PC12 and SH-SY5Y cells displayed good adhesion and expansion on electrospun polymer-carbon scaffold [176,328,334], but the incorporation of carbon materials showed a slightly negative effect on the viability and proliferation of cells [176,334]. Good differentiation into neuron-like cell was observed on the scaffolds [176,328,329,334] and the carbons

showed enhancing effect on it with longer neurites and higher expression of neuronal marker [176,334]. During differentiation, newly formed neurites elongated following the direction of fiber orientation [334]. However, a study showed that primary neuron cultured on PLGA/mwCNT fibrous scaffold died with an increase in culture time, resulting in a cell viability of less than 40% after 8 days [92]. Glial cells on electrospun polymer-carbon scaffold exhibited a slightly lower proliferation rate and viability than those on tissue culture plate [92,327,335]. In order to improve the cell activity, elec-

trical stimulation was employed on electrospun polymer-carbon composite scaffold. The use of silk/rGO scaffolds combined with electrical stimulation promoted the differentiation into neural phenotypes reaching comparable or even superior levels to those obtained by means of the traditional treatment with neural growth factor (NGF) [328]. The incorporation of drugs also could promote neural differentiation. Catapol-loaded PLGA/silk/mwCNT scaffold induced higher percentage of cells with neuronal phenotype compared to bare scaffold [329].

The capability of electrospun polymer-carbon fibers as nerve tissue engineering scaffold was assessed *in vivo*. To mimic the structure of nerve and guide the nerve growth directionally, the electrospun polymer-carbon fibrous film was wrapped into a conduit [199,263,335]. Results showed that the implantation of the scaffolds did not evoke a significant inflammation reaction and the addition of graphene benefit the reduction of microglial activation [199]. Neuroblasts' migration along the scaffold surface was observed 3 weeks after implantation [199]. The scaffold degraded gradually and a regenerated nerve was formed through the degrading scaffold [263,335] (Fig. 12a and b). Numerous bundles of regenerated nerves surrounded by fibrous connective tissue and capillaries were observed, although the regenerated nerve is slightly thinner and less mature than the autograft [263,335]. The performance of the regenerated nerve was evaluated through electrophysiological test. A nerve conduction velocity of 39.4 m/s and 8 mV muscle action potential were recorded after stimulation on regenerated nerve, which indicated the normal function of the regenerated nerve [263,335].

4.1.3. Skeletal muscular tissue engineering

Skeletal muscle is an important part of the human body, which accounts for 40% of the muscle. Once a muscle is injured, the satellite cells gather around the injured part to help healing. However, the regeneration capacity of skeletal muscle is limited and scar tissue formation always occurs [148]. Skeletal muscle tissue engineering scaffolds are targeted to bridge the gap formed by the injured muscle and promote regeneration. Ideal skeletal muscle tissue engineering scaffold should have high elasticity as the muscle and ability to contact by stimulus. Electrospun polymer-carbon fibers possess similar aligned and fibrous morphology as muscle fibers, tunable mechanical property and good electrical property, which hold promise as the skeletal muscle tissue engineering scaffold.

The incorporation of the carbon materials increased the strength of the scaffold, which would provide a stronger substrate for regeneration and contraction of muscle fiber. The elastic modulus of the current electrospun polymer-carbon scaffold ranged from hundreds of KPa to tens of MPa, which is larger than that of native skeletal muscle tissue (from tens to hundreds of KPa) [148,267,269,278,336]. The scaffolds showed an improved electrical property compared to neat polymer scaffold, with a conductivity of around 10^{-2} S/cm and electrical stimulation caused actuation [148,269,278].

The capability of the electrospun scaffold to support muscle fiber formation was tested *in vitro* through culture of C2C12 myoblast and primary skeletal muscle cell. C2C12 showed comparable cell viability on polymer-carbon scaffold with those on polymer scaffold [267,278,336]. Alignment of the fibers provided effective topographical guidance, where cell alignment was observed 1 h after seeding [336]. Cellular bundles were formed almost all the surface area of the polymer-carbon scaffold after 3-day culture [278]. The incorporation of carbon materials increased the length of the formed myotubes by ~30–50% [278,336], where myotubes with a length of 630 μm were obtained on gelatin-mwCNT fibrous scaffold after 4 days in differentiation medium [336]. The application of electrical stimulation on the conductive polymer-carbon

scaffold further increased the length of myotubes [336]. Also, carbons promoted the maturation and contraction of myotubes with higher proportion of contractile myotubes, higher contraction amplitude and longer contraction time (Fig. 13a–c) [336]. Additionally, expression of myogenin was higher on polymer-carbon scaffold, indicating an increased activation of myoblast differentiation [175,336]. Free-standing myotube-loaded scaffold could be fabricated by pre-culture of C2C12 on the gelatin-mwCNT scaffold and then release of the myotube-loaded scaffold from the substrate [336]. PCL-mwCNT scaffold displayed significant inhibition on the viability and proliferation of primary skeletal muscle cells, but the issue was addressed by addition of PAA/PVA hydrogel [148]. Increased cell activity over time and large multinucleated cellular constructs with many actin filaments interacting after 3 weeks was observed on PCL-mwCNT-PAA/PVA hydrogel scaffold [148].

4.1.4. Cardiac and vascular tissue engineering

Due to the little repair capability of the heart, strategies to engineer cardiac construct and assist tissue regeneration are needed. In the past few years, electrospun fibrous scaffold have attracted attention for cardiac tissue engineering and studies on electrospun scaffold made of polymer-carbon composite were conducted recently. The incorporation of CNT into poly(glycerol sebacate)/gelatin (PG) scaffold improved the mechanical property of the scaffold including toughness, and tensile strength [273]. Impedance was also reduced with CNT, which indicated increased electroactivity of the scaffold [273]. MSCs exposed to medium containing CNTs showed no toxic effect and increased the differentiation towards cardioprogenitor cells [337]. The biocompatibility and potential of the electrospun polymer-carbon scaffold for cardiac tissue engineering was studied through *in vitro* culture of MSC and cardiomyocytes [273,337]. MSCs on PLA/CNT scaffold displayed similar expression of early markers but significant increase in cardiac marker gene expression (5.6 fold) compared PLA scaffold [337]. The improvement of electrical property in the presence of CNT enabled an effective promotion of differentiation of MSCs towards cardioprogenitor phenotype through electrical stimulation [337]. Electrospun PG-CNT scaffold exhibited positive effect on the retention, viability and proliferation of cardiomyocytes [273]. Alignment of cardiomyocytes and sarcomeres inside the cells was observed on aligned fibrous scaffold and the presence of CNT significantly enhanced it [273]. Compared to random fibers, aligned fibers improved the maturation of cardiomyocytes with enhanced cell-cell coupling and contractile property [273]. Cardiac tissue cultured on PG-CNT scaffold showed superior beating behavior (Fig. 13d and e). Beating rate of 98.5 beats per min at day 5, minimum excitation threshold voltage of 2 V and maximum capture rate of 2.2 Hz were obtained on PG-CNT scaffold, which were dramatically improved compared to PG one [273].

Electrospun polymer-carbon scaffold also finds a good opportunity for vascular tissue engineering due to its ECM-like structure and potential of lining endothelial cells with aligned structure. Human umbilical vein endothelial cell (HUVEC) cultured on polymer-carbon fibers like cellulose acetate/swCNT and PU/mwCNT showed high viability and better proliferation than those on neat polymer fibers and smooth casting polymer films [338–340]. Cell orientation along the direction of fibers and extending morphology as in natural vascular medial layer were observed on aligned composite scaffold, which would be a benefit for regeneration of inner layer of the vessel [339,340]. Collagen and laminin were secreted by cells on the scaffold and the incorporation of carbon and aligned structure showed an enhancing effect on it [340]. Less tissue factor and plasminogen activator inhibitor were released on the fibrous scaffold compared to smooth scaffold, which indicated a good anticoagulant function [339,340].

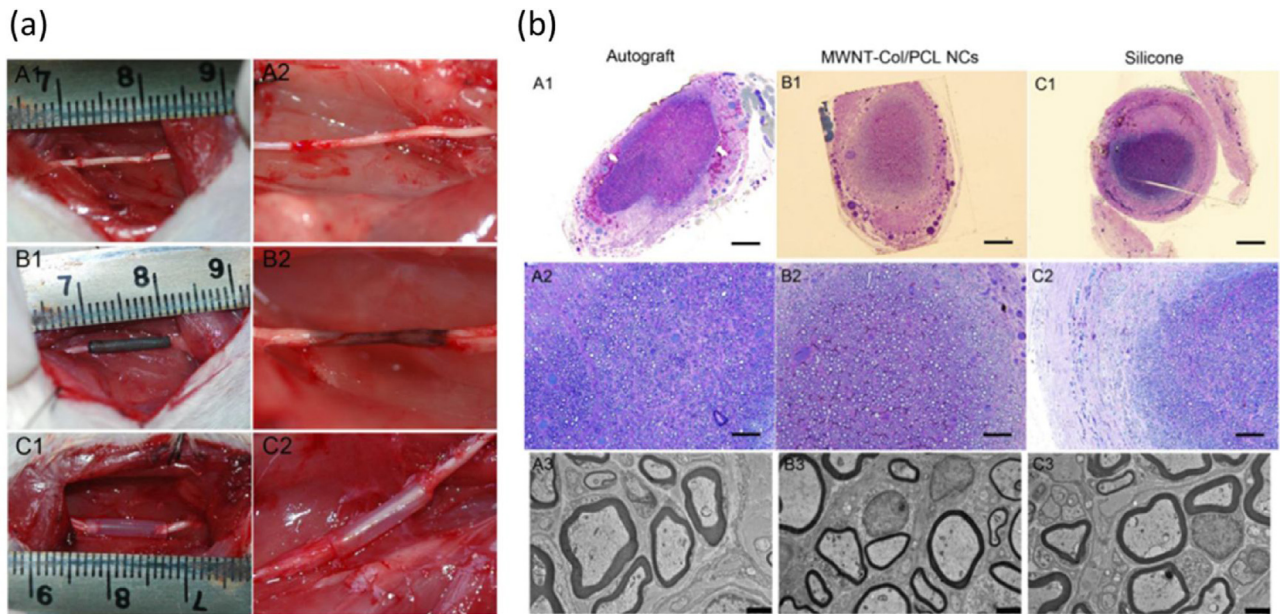


Fig. 12. (a) Surgical implantation of ((A1), (A2)) autograft, ((B1), (B2)) mwCNT-Collagen/PCL nerve conduit and ((C1), (C2)) silicone tube group bridging an 8 mm sciatic nerve defect in rats (1) and the view of the regenerated nerves four months postoperatively (2); (b) Histological observations of regenerated nerves on transverse sections. Light microscopy observation of toluidine blue staining of transverse semithin nerve sections ((A1)–(C1), (A2)–(C2)) and transmission electron microscopy of ultrathin nerve sections ((A3)–(C3)). The bars in (A1), (B1), (C1)=200 μm ; the bars in (A2), (B2), (C2)=50 μm ; the bars in (A3), (B3), (C3)=2 μm . (263). Copyright 2016, reproduced with permission from IOP Publishing (For interpretation of the references to colour in this figure legend, the reader is referred to the web version of this article).

4.2. Chemical and biosensors

4.2.1. Healthcare sensors

Chemical and biosensors play an important role in healthcare due to their potentials on disease diagnosis and physiological monitoring. Diabetes is an increasingly important worldwide public health problem. The diagnosis and management of diabetes requires the careful monitoring of blood glucose levels. The glucose bio - sensor has thus become one of the most important physiological monitoring devices, accounting for about 85% of the entire biosensor market [342]. Due to the high effective surface area of micro- and nanofibrous structures, electrospun polymeric materials show potentials on application of glucose sensors. The large surface area of the electrospun fibers not only provide numbers of sensing sites but also decrease the diffusion resistance. Carbon materials like CNT, graphene and graphene quantum dots (GOD) were incorporated into the electrospun materials to improve the electrical property of the sensors due to their fast electron transfer, good electrical conductivity and electrochemical stability. Also, the incorporation of carbon materials like functionalized CNT are able to anchor the catalyst on the sensor by covalent bonding.

Glucose oxidase (GOX)-loaded sensor is a major kind of glucose sensor made of electrospun polymer-carbon composite. Carbons were incorporated through co-electrospinning [113,184,212,343], electrophoretic deposition [163] or in-solution dipping [344] and GOX were attached through covalent bonding [163,343,344], drop casting [212] and co-electrospinning [113,184] on the composite (Fig. 14a). The electrophoretic deposition of CNT on electrospun PAN fibers showed 3 folds increase of surface area due to their high surface to volume ratio [163]. During the electrochemical characterization, the polymer-carbon fibers exhibited better electrochemical property including larger electroactive area [113,163] and lower charge transfer resistance [113] compared of neat polymer fibers. Well-defined peaks corresponding to the redox reaction of FAD at the GOX active site were observed on GOX-loaded composite [163]. The common detection of glucose with GOX is to electrochemically measure the H_2O_2 generated by glucose. The electrospun

polymer-carbon sensor showed rapid detection of glucose with stable current within 10–20 s [163,184]. A linear response of current to glucose concentration was observed and the range varied with different composites [113,163,184,343,344]. Electrospun PAN/Au NP/mwCNT exhibited a wide linear range of 0–30 mM [163] and low limit of detection (LOD) of 4 μM while PVA/graphene and nylon/mwCNT showed relatively narrow linear range of 0–10 mM and high LOD of more than 9 μM [184,343,344]. The incorporation of carbon materials increased the enzyme activity and sensitivity [184]. A good sensitivity of 38 $\mu\text{A}/\text{mM}$ were observed on PAN/Au NP/mwCNT and PVA/graphene [163,184]. In addition to electrochemical detection of H_2O_2 , fluorescent detection was studied recently through employment of GOD (Fig. 14b) [212]. The feasibility of the fluorescent detection platform was proved by gradual reduction of fluorescent intensity with increasing H_2O_2 concentration and good stability of fluorescent intensity after storage at low temperature [212]. A linear range of 0.25–24 mM and LOD of 10 μM were obtained, which was comparable to the performance of electrochemical detection [212]. The activity of the GOX-loaded PAN/Au NP/mwCNT showed a preservation of 70% after storage of 14 day at 4 ° [163]. No obvious response was observed when adding interfering substances like dopamine and ascorbic, which indicated a good selectivity [212]. To test the reliability of the GOX-loaded electrospun polymer-carbon composite, the glucose level in several beverages was measured. Quite similar results were obtained between electrospun polymer-carbon composite and standard test using spectroscopy and dinitrosalicylic acid [343,344].

Although enzymatic sensor showed superior performance on glucose monitoring, it exhibited limitations such as unstable immobilization of enzyme, low stability and short service life. Hence, nonenzymatic sensor was prepared through employment of catalyst like metal nanoparticle instead of enzyme (Fig. 14c) [186,345]. The electrospun PVDF/mwCNT/Pt NP and PVA/graphene/Ag NP showed high sensitivity of H_2O_2 and good stability of more than 90% activity after 20 day- storage at low temperature [186,345]. The graphene showed an important role on promotion of the sensitivity of PVA/graphene/Ag NP [186]. However, the glucose sensing

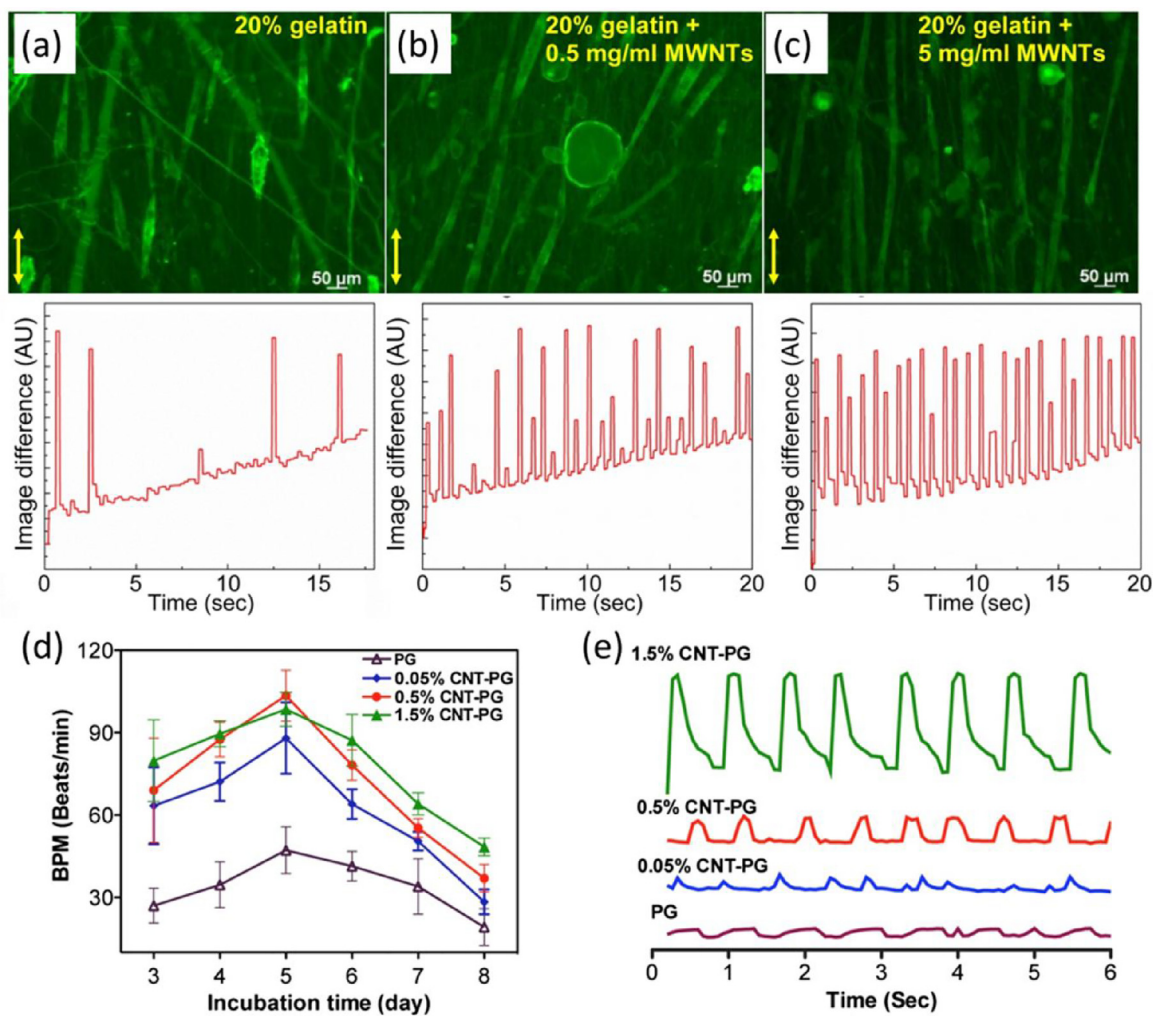


Fig. 13. (a, b and c) Fluorescence microscopy images of myotubes cultured on electrospun aligned nanofibers (top) and myotube contraction analysis after 4 days in differentiation medium followed by 2 additional days with electrical stimulation (5 V, 1 Hz, 1 ms duration) (bottom) [336]. Copyright 2014, reproduced with permission from Elsevier Ltd; (d) Beating frequency (BPM) of constructs as a function of CNT concentration and incubation time. (e) Representative spontaneous contraction patterns of cardiomyocytes cultured on PG scaffolds and CNT incorporated scaffolds recorded after 7 days of cultivation [273]. Copyright 2014, reproduced with permission from Elsevier Ltd.

performance of electrospun PVDF/mwCNT/Pt NP was not satisfied and further improvement is needed [345].

In addition to glucose detection, electrospun polymer-carbon composite showed potentials on detection of other substances for healthcare. The binding of IgE antibody generated in body immune response on an electrospun polymer/mwCNT composite exhibited altered current response to voltage, which indicated a potential *in vivo* monitoring [346].

4.2.2. Environmental sensors

Environmental applications of chemical and biosensors focus on monitoring of hazardous substances in air and water such as flammable gas, heavy metal ions and toxic chemicals. Recently, micro- and nanostructured electrospun polymer-carbon materials attracted attention on environmental detector due to their large effective surface area. Electrospun nylon/mwCNT and PMMA/swCNT fibers were prepared to detect organic vapor like low molecular weight alcohol vapor (Fig. 14d) [72,279]. The absorption of the alcohol vapor changed the conductivity of the fibrous film, resulting in a relation between film resistance and concentration of vapor [72,279]. A flow-through design using porous membrane instead of solid film as substrate of the fibrous film displayed significant amplification of the signals [72]. The elec-

trospun sensor showed good reversibility upon the cyclic test [279]. Also, electrospun polymer-carbon composite was able to detect organic chemical in liquid form. Nylon/polyethylene/carbon black showed capability to detect different solvents like xylene and cyclohexane and the immersion pretreatment and increase of temperature would improve the reproducibility and sensitivity, respectively [347]. Formaldehyde was successfully monitored through poly-methacryloylhydrazide/CNT fibers with a linear range of 0.001–10 mM, a LOD of 0.8 μM and good reproducibility [348]. Carbon quantum dot-loaded electrospun PAN/mesoporous silica was studied as a fluorescent sensor for Fe(III) ions in water (Fig. 14e). The nanofibrous membrane showed improved pH adaptability and photostability compared to free-state carbon quantum dot. On the nanofibrous composite, a linear range of 0–99.1 μM and LOD of 3.95 μM were obtained. The detection of Fe(III) ions in tap water with and without addition of ions exhibited satisfying recoveries of ~100% [256]. Acetylcholinesterase was successfully immobilized on electrospun polyacrylamide/mwCNT with good enzymatic activity, which held potential of detecting agricultural pesticides [152]. In addition to chemical sensor, electrospun polymer-carbon showed potentials on physical sensor. A temperature sensing behaviour was observed on electrospun nylon/mwCNT with a linear dependence of 30–150 degree [349].

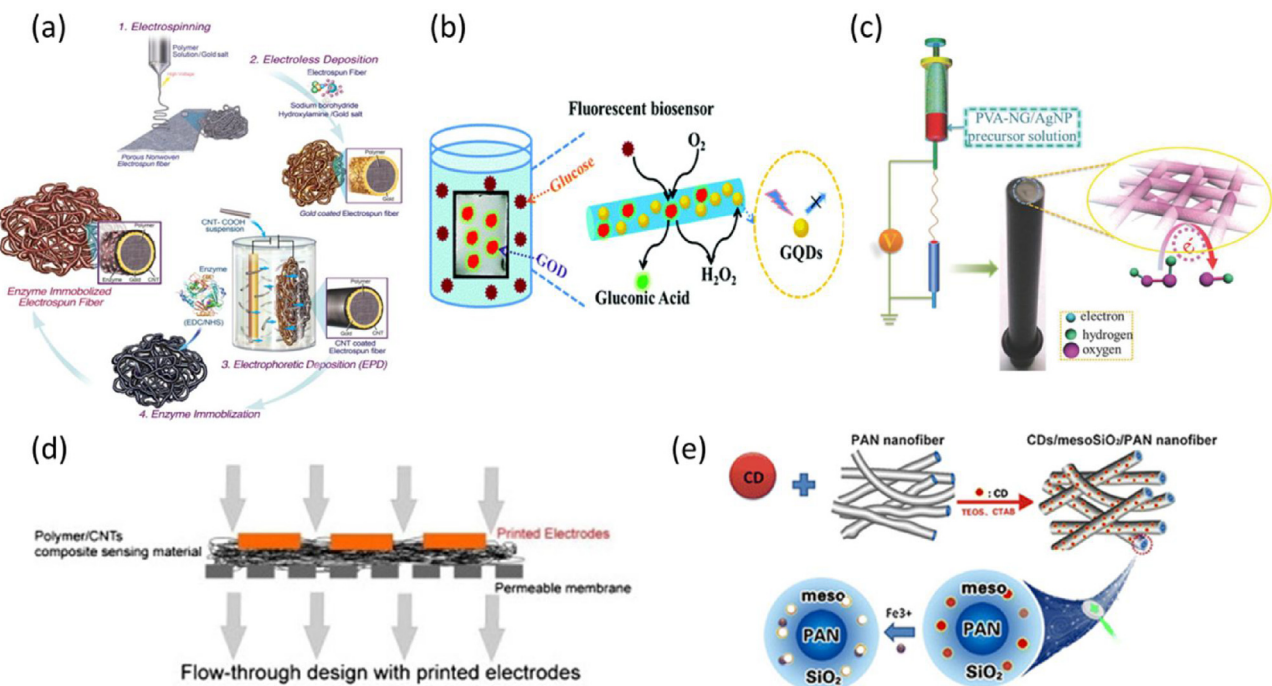


Fig. 14. (a) Schematic of the GOX-loaded PAN/mwCNT sensor fabrication process [163]. Copyright 2012, reproduced with permission from Elsevier Ltd; (b) The possible detection mechanism of PVA/GOD fluorescent sensor [212]. Copyright 2015, reproduced with permission from the Royal Society of Chemistry; (c) Schematic fabrication of PVA/graphene/Ag NPs nonenzymatic sensor and the possible detection mechanism of H₂O₂ [186]. Copyright 2015, reproduced with permission from John Wiley & Sons Inc; (d) Schematic of the PMMA/CNT sensor for detecting volatile organic vapor [72]. Copyright 2013, reproduced with permission from Elsevier Ltd; (e) Schematic of the Carbon quantum dots/mesoSiO₂/PAN nanofibrous membrane to the detection of Fe(III) [256]. Copyright 2016, reproduced with permission from Springer.

4.3. Environmental remediation

With the rapid development of population and industry, extensive environmental pollution is becoming a serious problem in the world [350]. Water contaminants from industrial and domestic wastes such as dye molecules, organic compounds and heavy metal ions show toxicity to human body and may cause diseases and even death [350]. Air pollutants like microparticles can bring about cardiovascular and respiratory illnesses [350]. Moreover, some contaminants are highly persistent [349]. Hence, removal of contaminants in water and air, as an urgent and serious issue, should be paid great attention to. Due to the large surface area, high porosity and good interconnectivity, electrospun nanofibrous membranes emerge as promising materials for filtration and adsorption of contaminants in water and air [350]. The large surface area of the fibrous structure provide huge amount of site for interaction with contaminant molecules. The high porosity and good interconnectivity of the fibrous membrane ensure high permeability to fluid streams. Also, the electrospun nanofibrous membrane can be easily separated from the reaction solution after sorption, which indicates ease of usage and potentials of recyclability [351]. Owning to the superior mechanical, thermal and electrical property, nanocarbon materials like CNT and graphene exhibit ability to reinforce the electrospun nanofibrous membrane for water and air treatment [352,353]. With the strong and stable nanocarbon materials, the stability and service life of the electrospun nanofibrous composite membrane may be improved [354,355]. The high specific surface area of the nanocarbons may provide more reaction site during treatment [351]. Despite the debatable toxicity, nanocarbon materials remain potentials for application of water and air treatment as its incorporation into or immobilization on the electrospun nanofibrous would significantly reduce their possibility of releasing [351,356].

The incorporation of nanocarbon materials significantly improved the performance of electrospun nanofibers on the adsorption and filtration of dye molecules and organic compounds in liquid [187,349,351,355,357,358]. The addition of 2% oxidized CNT into electrospun PAN nanofibers increased the adsorption of pyrene from 20% to 90% (Fig. 15a) [358]. The electrospun PLA/mwCNT composite showed approximately 18 times sorption capacity for perfluorooctane sulfonate in the water and a much faster sorption rate when compared to the electrospun pure PLA [351]. Although the electrospun polymer-nanocarbon composite exhibited high rejection to contaminant, they did not compromise the anti-fouling property [349]. Also, the mwCNT-functionalized electrospun membrane showed higher resistance to mechanical failure during high pressure filtration as compared to non-functionalized membrane, which may be attributed to the superior mechanical property of mwCNT [349]. The electrospun polymer-nanocarbon composite was a good substrate for immobilization of active substance such as enzymes which are able to react with or catalyze the degradation of contaminants [352,355]. The immobilization of laccase on the electrospun polymer-nanocarbon composite greatly improved the storage and operational stability of free laccase while maintaining 85% of the catalytic activity [355]. The incorporation of highly conductive nanocarbons like CNT promoted electron transfer between the active substance and the substrate, leading to a higher removal efficiency of contaminants such as red X-3B and bisphenol A in the water [354,355]. Only 3% of TiO₂/GO in the electrospun fibrous composite yields excellent photocatalytic performance by degrading 100% methylene blue in the solution after 90 min of visible light exposure, owing to the rapid electron transfer and improved ionic interaction between TiO₂ and GO [187]. The electrospun polymer-nanocarbon composite also showed good recyclability with few mass and adsorption capacity loss after five to six times' use [354,355,358]. The type

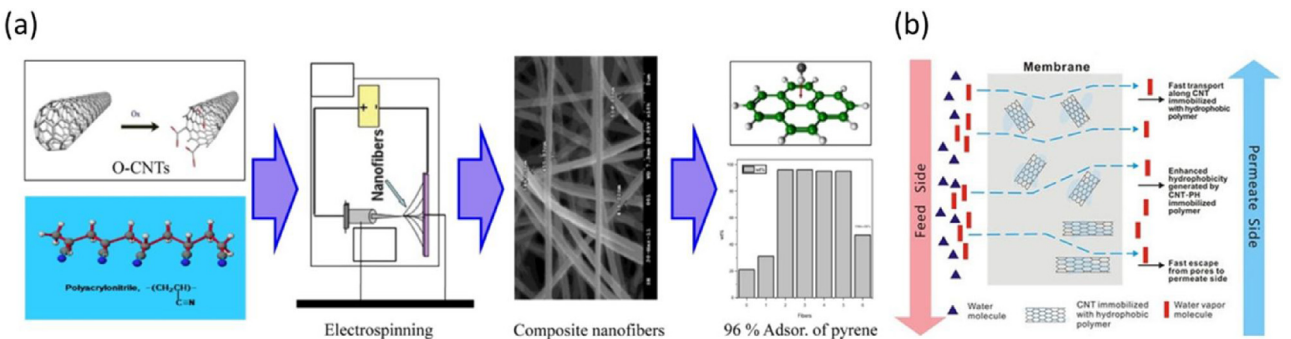


Fig. 15. (a) Application of CNT-polymer nanofibers for efficient removal of pyrene [358]. Copyright 2015, reproduced with permission from Elsevier Ltd; (b) Application of CNT-polymer nanofibers for membrane distillation [142]. Copyright 2017, reproduced with permission from Springer Nature.

of nanocarbon materials and preparation of the electrospun composite also made a difference on the adsorption performance. Oxidized open tips CNT showed more benefit to the improvement of adsorption capacity of the electrospun PAN/CNT composite compared to un-oxidized CNT [358]. A multilevel structure formed by simultaneous electrospinning of polymer fibers and electrospraying of CNT nanoparticle possess higher dye rejection percentage than blended electrospun polymer/CNT composite [357]. In addition to dye molecules and organic compounds, the electrospun polymer-nanocarbon composite showed ability to remove heavy metal ions like hexavalent chromium from aqueous solution [353]. The electrospun polymer-nanocarbon membrane also found potential application on membrane distillation (Fig. 15b). The superhydrophobic composite membrane allowed fast vapor transport and high salt rejection (~99%) [78,142].

In addition to water treatment, the electrospun nanofibrous composite showed potential on air treatment. Ultralow 0.3- μm particle penetration rate (<0.01%) and low pressure drop were achieved with a CNT-polymer nanofibers hybrid fabrics. The performance of the consolidated hybrid fabrics with a thickness of 20 microns and areal density of only 8 g m⁻² was able to reach ultra low particulate filter standard [164].

5. Challenge

Over the course of this review paper, we have demonstrated how electrospun polymer composites reinforced with nanocarbons has enabled the development of high surface area, high porosity, highly functional nanofiber mats and assemblies with novel hierarchical architectures, outstanding performance, and tuneable physical, chemical, mechanical, electrical, thermal, and optical properties, offering engineers unparalleled processing control over the performance of these advanced materials to address many challenges in an expansive spectrum of applications. This technique presents tremendous potential to expand the scientific frontiers in tissue engineering, energy generation and storage, water purification, and chemical sensors to mention just a few domains in which electrospun materials have been introduced.

While electrospinning has been touted as a cost efficient and scaleable technique with some variants such as needleless and multi-needle electrospinning able to have relatively high throughputs, the transition from the laboratory scale to industrial scale production is hampered by some practical production limitations which remain significant challenges to overcome. In addition, electrospun nanofibers of complex architectures can so far only be fabricated by customized multi-fluidic needles with multi-stage post treatment processing, making these highly functional nanofibers difficult to produce on an industrial scale [359]. The typical electrospinning setup itself, being an open system, can also be adversely affected by atmospheric conditions like humidity and

temperature which in turn affect the solvent evaporation behaviour and nanofiber morphology [359]. The limitation of this open system is the loss of control over the experimental parameters which reduces the reproducibility of the spun nanofibers over time and in different locations. In addition, there remain a whole host of parameters to be carefully controlled such as solution concentration, rheology, conductivity, spinneret configuration, electric field intensity and distribution, flow rate, collector geometry and distance, etc [360]. There have been efforts to develop closed electrospinning envelopes to minimize the environmental perturbation, which is a positive step in the right direction.

An interesting development looming in the future of electrospinning is in expanding the technique to the preparation of macroscopic, 3D structures through precision electrospinning, self-assembly, multi-layer spinning, liquid/3D collectors, and processing into bulk aerogels and sponges. In particular, precision electrospinning combines additive manufacturing techniques such as mounting the spinneret on an X-Y movable stage to precisely deposit the nanofibers in pre-ordained patterns. These 3D assemblies retain the outstanding porosity and surface area of the 2D nanofiber mats while being fabricated into useful macroscopic geometries, particularly important in tissue-engineering applications. However, there remain complexities yet to be fully addressed such as retaining the mechanical integrity and control over the fabrication process [360]. 3-dimensional macrostructures having novel sponge-like architectures have also been assembled from electrospun nanofibers. Yang et al. combined electrospinning with a fibrous "freeze-shaping" technique to assemble isotropically bonded 3-dimensional aerogels with outstanding elasticity from 2-dimensional electrospun nanofiber mats. Their technique involved blending a crosslinking agent together with the precursor, dispersing the electrospun nanofibers in a solvent, before freeze-drying to rapidly fix the nanofibers into position in a bulk 3-dimensional network for subsequent cross-linking. Control over the freeze-drying protocol, structural stability and composition of the nanofibers, and cross-linking parameters afforded a high level of control over the eventual structure of the aerogel and consequent physical properties [361]. These soft electrospun hierarchical porous, low specific surface area, high elasticity, biomimetic 3-dimensional structures could have potential applications in bioengineering, separation filters, catalysts, offering the potential for biological and chemical functionalization for a wide spectrum of practical uses [362,363].

Electrospinning represents an interesting approach to produce nanocarbon filled polymer composites because of the relatively simple processing, solvent dispersion, and potential alignment and sequestration of the functional filler in a nanoscale fiber. However, specifically with regard to electrospinning hybrid polymeric nanofibers containing nanocarbons, there remains the primary challenge of dispersing the nanofiller in the electrospinning solution and eventual nanofiber. With nanofillers such as CNT and

graphene, van der waal's forces and tube entanglements lead to aggregation making it difficult to disperse the nanofiller within the polymer matrix, compromising the mechanical, electrical, and thermal performance of the hybrid composite nanofiber. The presently adopted techniques to achieve dispersion such as chemical functionalization, non-covalent wrapping, surfactants, mechanical agitation etc, each come with their associated drawbacks such as damaging the nanofiller or reducing the conductivity [364]. The conflicting objectives must therefore be reconciled through optimizing the trade-offs between improving dispersion and maintaining the performance of the composite - an important consideration in fabricating these materials.

Besides dispersion of the nanofiller, strong interfacial bonding with the host would provide effective stress transfer from the soft matrix phase to the mechanically robust nanofiller. This can be achieved by maximizing the load transfer mechanisms, i.e. van der waals, mechanical interlocking, and chemical bonding through controlling the orientation, dispersion, morphology, shape, size, and surface composition of the nanofillers, and compatibility of the polymer and solvent system. Having a network of well interconnected, well aligned, high aspect ratio nanofillers such as CNT not only improves the mechanical stress transfer, but also allows for better electrical conductivity at lower CNT loadings.

While much research effort has gone into improving the dispersion and interfacial adhesion of the nanofiller, another research imperative should be the preparation of high quality nanofillers themselves. The current state of the art in producing CNTs for example is still not sufficiently mature to produce defect-free, structurally controllable, pure, uniform nanotubes [364], which makes it difficult to achieve the outstanding theoretical properties of individual nanotubes, and consequently in the polymeric composites containing them. The difficulty in separating CNTs of different chiralities, to eliminate surface defects, to remove impurities such as amorphous carbon, metallic catalyst particles, and fullerenes, and to produce dispersible CNTs of consistent morphology in industrially significant quantities are also challenges that need to be addressed urgently.

The electrospun polymer-carbon composite showed promising application on tissue engineering, chemical and biosensors and environmental remediation. Generally, the composite inspired favourable cell response and exhibited potentials on regeneration of different parts of the body including bone, nerve, skeletal muscle, cardiac tissue and vas. Substances such as glucose, organic vapor and heavy metal ions were able to be detected using the composite. However, challenges are remained regarding to the performance of the composite. Although the incorporation of carbon materials improved the mechanical and electrical property of the electrospun polymeric fibers, the improvement was quite limited compared to the intrinsic property of carbons [270]. One of the most important reasons for it should be the inefficient organization of two components in the composite. Nonuniform dispersion of carbon materials in the polymer matrix usually occur, leading to inconsistency and reduced properties. Some approaches such as surface treatment of carbon materials, employment of surfactant and bonding between polymer and carbon may be considered to address this issue. In addition, the toxicity of carbon materials like CNTs and bioactivity of the electrospun polymer-carbon composite remain conflicting. Reduced cell viability was showed *in vitro* study when the percentage of carbon in the composite was high [94,121,165,193,281]. The carbon materials may need to be further treated or functionalized with cell-favorable molecules or drugs to improve their biocompatibility. The majority of studies focuses on the *in vitro* assay of the electrospun polymer-carbon composite, but fails to move forward to *in vivo* study. The *in vivo* bioactivity and ability of regeneration should be assessed in the future. There is still a long way to go before the composite can be approved by Food and Drug

Administration for clinical applications. According to the available results on *in vivo* regeneration, the regenerative performance of the composite was limited with small and immature tissue [263]. Strategies such as incorporation of highly biomimetic 3D structure and external stimulation could be employed. The preparation of 3D electrospun carbon-polymer composite with the help of techniques like 3D printing may resemble the native tissue more effectively compared to 2D film. The application of electrical stimulation with implantable device may be a promising way to promote *in vivo* regeneration. As for application on sensor, the sensitivity and detection range of the materials should be improved and the preparation of device made of the materials could be studied. The application of the composite nanofibers on air treatment could be explored more, such as on removal of toxic gas and ultrasmall particles.

6. Conclusion

The outstanding nanoscale properties of nanocarbons like CNTs have received much acclaim and attention since their discovery over 20 years ago in 1991, but there has been little success in terms of translating those properties into applications on an industrially significant scale – therein lies the challenge with nanotechnology, how can we deploy these materials and make use of their wonderful properties? The answer may lie in the fabrication technique. Electrospun 1-dimensional nanofibers, 2-dimensional nanofiber mats, and eventually 3-dimensional electrospun nanofiber geometries have outstanding characteristics such as large surface areas and porosity, are relatively easy to produce, and have already been used for practical applications such as the production of membranes and filters, but we have barely begun to scratch the surface with regard to achieving highly functional materials. Therefore, combining these concepts, the potential for electrospun hybrid polymer nanofibers enriched with nanocarbons is immense, and presents an exciting prospect for scientists and engineers across a spectrum of research interests.

The mechanical, electrical, and thermal property enhancements reported by numerous research groups using a variety of different materials and methodologies covered in this review further demonstrates the versatility and usefulness of this approach, offering the option to achieve highly tuneable properties specific to different applications. The works presented in this review put forward several innovative strategies in controlling the morphology, composition, and performance of the composite material, from modifications to the processing parameters to altering the composition of the compounds used, and post processing treatments to deliver unique combinations of properties. This provides a blueprint for designing and tailoring the next generation of advanced nanocarbon enriched polymer composite nanofibrous materials.

However, much work still needs to be done, particularly on improving the consistency of the fabricated materials, increasing the scale of production, dispersing the nanofillers, and consistently synthesizing high quality functional nanocarbon fillers in significant quantities. Many hands make light work, and as detailed in the outlook and challenges section, the many and varied approaches adopted by research groups worldwide to address the challenges faced, give the authors confidence that it will only be a matter of time before we see these hybrid nanocarbon incorporated polymer nanofibers be deployed in applications of critical importance to solve the greatest challenges facing the world.

Acknowledgements

This work was financially supported by the Singapore National Research Foundation (NRF-CRP10-2012-06), China Jiangsu Spe-

cially Appointed Professor, the Fundamental Research Funds for the Central Universities (NE2017004, NS2018040), Jiangsu Provincial Founds for Natural Science Foundation (BK20170793), Provincial Natural Science Foundation of Hunan (Grant no. 2016TP1009), Nankai 111 project, No. B12015.

References

- [1] Kroto HW, Heath JR, Obrien SC, Curl RF, Smalley RE. C-60 – buckminsterfullerene. *Nature* 1985;318:162–3.
- [2] Hirsch A. The era of carbon allotropes. *Nat Mater* 2010;9:868–71.
- [3] Iijima S. Helical microtubules of graphitic carbon. *Nature* 1991;354:56–8.
- [4] Novoselov KS, Geim AK, Morozov SV, Jiang D, Zhang Y, Dubonos SV, et al. Electric field effect in atomically thin carbon films. *Science* 2004;306:666–9.
- [5] Greil P. Perspectives of nano-carbon based engineering materials. *Adv Eng Mater* 2015;17:124–37.
- [6] Abergel DSL, Apalkov V, Berashevich J, Ziegler K, Chakraborty T. Properties of graphene: a theoretical perspective. *Adv Phys* 2010;59:261–482.
- [7] Mochalin VN, Shenderova O, Ho D, Gogotsi Y. The properties and applications of nanodiamonds. *Nat Nanotechnol* 2012;7:11–23.
- [8] Behabtu N, Young CC, Tsentalovich DE, Kleinerman O, Wang X, Ma AWK, et al. Strong, light, multifunctional fibers of carbon nanotubes with ultrahigh conductivity. *Science* 2013;339:182–6.
- [9] Stankovich S, Dikin DA, Domke GHB, Kohlhaas KM, Zimney Ej, Stach EA, et al. Graphene-based composite materials. *Nature* 2006;442:282–6.
- [10] Aryal S, Kim CK, Kim KW, Khil MS, Kim HY. Multi-walled carbon nanotubes/TiO₂ composite nanofiber by electrospinning. *Mater Sci Eng C Mater Biol Appl* 2008;28:75–9.
- [11] Bauhofer W, Kovacs JZ. A review and analysis of electrical percolation in carbon nanotube polymer composites. *Compos Sci Technol* 2009;69:1486–98.
- [12] Agarwal S, Wendorff JH, Greiner A. Progress in the field of electrospinning for tissue engineering applications. *Adv Mater* 2009;21:3343–51.
- [13] Bognitzki M, Czado W, Frese T, Schaper A, Hellwig M, Steinhart M, et al. Nanostructured fibers via electrospinning. *Adv Mater* 2001;13:70–2.
- [14] Greiner A, Wendorff JH. Electrospinning: a fascinating method for the preparation of ultrathin fibres. *Angew Chem Int Ed* 2007;46:5670–703.
- [15] Peng S, Jin G, Li L, Li K, Srinivasan M, Ramakrishna S, et al. Multi-functional electrospun nanofibres for advances in tissue regeneration, energy conversion & storage, and water treatment. *Chem Soc Rev* 2016;45:1225–41.
- [16] Hu Y, Ye D, Luo B, Hu H, Zhu X, Wang S, et al. A binder-free and free-standing cobalt sulfide@carbon nanotube cathode material for aluminum-ion batteries. *Adv Mater* 2018;30(1703824):1–6.
- [17] Ji D, Peng S, Safanama D, Yu H, Li L, Yang G, et al. Design of 3-dimensional hierarchical architectures of carbon and highly active transition metals (Fe, Co, Ni) As bifunctional oxygen catalysts for hybrid lithium-air batteries. *Chem Mater* 2017;29:1665–75.
- [18] Peng S, Li L, Hu Y, Srinivasan M, Cheng F, Chen J, et al. Fabrication of spinel one-dimensional architectures by single-spinneret electrospinning for energy storage applications. *ACS Nano* 2015;9:1945–54.
- [19] Heimann RB, Esvyukov SE, Koga Y. Carbon allotropes: a suggested classification scheme based on valence orbital hybridization. *Carbon* 1997;35:1654–8.
- [20] Geim AK. Graphene: status and prospects. *Science* 2009;324:1530–4.
- [21] Hernandez Y, Nicolosi V, Lotya M, Blighe FM, Sun Z, De S, et al. High-yield production of graphene by liquid-phase exfoliation of graphite. *Nat Nanotechnol* 2008;3:563–8.
- [22] Novoselov KS, Fal'ko VI, Colombo L, Gellert PR, Schwab MG, Kim K. A roadmap for graphene. *Nature* 2012;490:192–200.
- [23] Bolotin Ki, Sikes KJ, Jiang Z, Klima M, Fudenberg G, Hone J, et al. Ultrahigh electron mobility in suspended graphene. *Solid State Commun* 2008;146:351–5.
- [24] Morozov SV, Novoselov KS, Katsnelson MI, Schedin F, Elias DC, Jaszczak JA, et al. Giant intrinsic carrier mobilities in graphene and its bilayer. *Phys Rev Lett* 2008;100:1–4, 016602.
- [25] Balandin AA, Ghosh S, Bao W, Calizo I, Teweldebrhan D, Miao F, et al. Superior thermal conductivity of single-layer graphene. *Nano Lett* 2008;8:902–7.
- [26] Loh KP, Bao Q, Ang PK, Yang J. The chemistry of graphene. *J Mater Chem* 2010;20:2277–89.
- [27] De Volder MFL, Tawfick SH, Baughman RH, Hart AJ. Carbon nanotubes: present and future commercial applications. *Science* 2013;339:535–9.
- [28] Koziol K, Vilatela J, Moisala A, Motta M, Cunniff P, Sennett M, et al. High-performance carbon nanotube fiber. *Science* 2007;318:1892–5.
- [29] Prasek J, Drbohlavova J, Chomoucka J, Hubalek J, Jasek O, Adam V, et al. Methods for carbon nanotubes synthesis-review. *J Mater Chem* 2011;21:15872–84.
- [30] Lieber CM, Chen CC. Preparation of fullerenes and fullerene-based materials. *Solid State Phys Adv Res Appl* 1994;48:109–48.
- [31] Yadav J. Fullerene: properties, synthesis and application. *Res Rev J Phys* 2018;6:1–6.
- [32] Mojica M, Alonso JA, Méndez F. Synthesis of fullerenes. *J Phys Org Chem* 2013;26:526–39.
- [33] Hou H, Banks C, Jing M, Zhang Y, Ji X. Carbon Quantum Dots and Their Derivative 3D Porous Carbon Frameworks for Sodium-Ion Batteries with Ultralong Cycle Life. *Adv Mater* 2015;27:7861–6.
- [34] Xu XY, Ray R, Gu YL, Ploehn HJ, Gearheart L, Raker K, et al. Electrophoretic analysis and purification of fluorescent single-walled carbon nanotube fragments. *J Am Chem Soc* 2004;126:12736–7.
- [35] Wang R, Lu KQ, Tang ZR, Xu YJ. Recent progress in carbon quantum dots: synthesis, properties and applications in photocatalysis. *J Mater Chem A Mater Energy Sustain* 2017;5:3717–34.
- [36] Baker SN, Baker GA. Luminescent carbon nanodots: emergent nanolights. *Angew Chem Int Ed* 2010;49:6726–44.
- [37] Fayette L, Marcus B, Mermoux M, Tourillon G, Laffon K, Parent P, et al. Local order in CVD diamond films: comparative Raman, x-ray-diffraction, and x-ray-absorption near-edge studies. *Phys Rev B* 1998;57:14123–32.
- [38] Ramakrishna S, Fujihara K, Teo WE, Yong T, Ma Z, Ramaseshan R. Electrospun nanofibers: solving global issues. *Mater Today* 2006;9:40–50.
- [39] Sahay R, Kumar PS, Sridhar R, Sundaramurthy J, Venugopal J, Mhaisalkar SG, et al. Electrospun composite nanofibers and their multifaceted applications. *J Mater Chem* 2012;22:12953–71.
- [40] Góra A, Sahay R, Thavasi V, Ramakrishna S. Melt-electrospun fibers for advances in biomedical engineering, clean energy, filtration, and separation. *Polym Rev* 2011;51:265–87.
- [41] Kumar PS, Sundaramurthy J, Sundarrajan S, Babu VJ, Singh G, Allakhverdiev SI, et al. Hierarchical electrospun nanofibers for energy harvesting, production and environmental remediation. *Energy Environ Sci* 2014;7:3192–222.
- [42] Li L, Peng S, Lee JKY, Ji D, Srinivasan M, Ramakrishna S. Electrospun hollow nanofibers for advanced secondary batteries. *Nano Energy* 2017;39:111–39.
- [43] Huang ZM, Zhang YZ, Kotaki M, Ramakrishna S. A review on polymer nanofibers by electrospinning and their applications in nanocomposites. *Compos Sci Technol* 2003;63:2223–53.
- [44] A. Formhals. Process and apparatus for preparing artificial threads. US Patent, 1975504 A; 1934.
- [45] Mathews N, Varghese B, Sun C, Thavasi V, Andreasson BP, Sow CH, et al. Oxide nanowire networks and their electronic and optoelectronic characteristics. *Nanoscale* 2010;2:1984–98.
- [46] Jose R, Archana P, Le A, Reddy M, Yusoff M, Ramakrishna S. Electrospun metal oxides nanostructures for energy related devices. In: Proc IEEE First Conference On: Clean Energy And Technology; 2011. p. 161–5.
- [47] Peng S, Li L, Lee JKY, Tian L, Srinivasan M, Adams S, et al. Electrospun carbon nanofibers and their hybrid composites as advanced materials for energy conversion and storage. *Nano Energy* 2016;22:361–95.
- [48] Wu H, Hu L, Rowell MW, Kong D, Cha JJ, McDonough JR, et al. Electrospun metal nanofiber webs as high-performance transparent electrode. *Nano Lett* 2010;10:4242–8.
- [49] Barakat NA, Kim B, Kim HY. Production of smooth and pure nickel metal nanofibers by the electrospinning technique: nanofibers possess splendid magnetic properties. *J Phys Chem C Nanomater Interfaces* 2009;113:531–6.
- [50] Thavasi V, Singh G, Ramakrishna S. Electrospun nanofibers in energy and environmental applications. *Energy Environ Sci* 2008;1:205–21.
- [51] Ramakrishna S, Jose R, Archana P, Nair A, Balamurugan R, Venugopal J, et al. Science and engineering of electrospun nanofibers for advances in clean energy, water filtration, and regenerative medicine. *J Mater Sci* 2010;45:6283–312.
- [52] Kaur S, Sundarrajan S, Rana D, Sridhar R, Gopal R, Matsuura T, et al. The characterization of electrospun nanofibrous liquid filtration membranes. *J Mater Sci* 2014;49:6143–59.
- [53] Nguyen LT, Chen S, Elumalai NK, Prabhakaran MP, Zong Y, Vijila C, et al. Biological, chemical, and electronic applications of nanofibers. *Macromol Mater Eng* 2013;298:822–67.
- [54] Khin MM, Nair AS, Babu VJ, Murugan R, Ramakrishna S. A review on nanomaterials for environmental remediation. *Energy Environ Sci* 2012;5:8075–109.
- [55] Wang G, Yu D, Kelkar AD, Zhang L. Electrospun nanofiber: emerging reinforcing filler in polymer matrix composite materials. *Prog Polym Sci* 2017;75:73–107.
- [56] Sridhar R, Lakshminarayanan R, Madhaiyan K, Barathi VA, Lim KHC, Ramakrishna S. Electrosprayed nanoparticles and electrospun nanofibers based on natural materials: applications in tissue regeneration, drug delivery and pharmaceuticals. *Chem Soc Rev* 2015;44:790–814.
- [57] Garg K, Bowlin GL. Electrospinning jets and nanofibrous structures. *Biomicrofluidics* 2011;5:1–19, 013403.
- [58] Reneker DH, Yarin AL. Electrospinning jets and polymer nanofibers. *Polymer* 2008;49:2387–425.
- [59] Palangetic L, Reddy NK, Srinivasan S, Cohen RE, McKinley GH, Clasen C. Dispersity and spinnability: why highly polydisperse polymer solutions are desirable for electrospinning. *Polymer* 2014;55:4920–31.
- [60] Almuhamadi K, Alfano M, Yang Y, Lubineau G. Analysis of interlaminar fracture toughness and damage mechanisms in composite laminates reinforced with sprayed multi-walled carbon nanotubes. *Mater Des* 2014;53:921–7.
- [61] Zheng N, Huang Y, Liu HY, Gao J, Mai YW. Improvement of interlaminar fracture toughness in carbon fiber/epoxy composites with carbon nanotubes/polysulfone interleaves. *Compos Sci Technol* 2017;140:8–15.
- [62] Coleman JN, Khan U, Gun'ko YK. Mechanical reinforcement of polymers using carbon nanotubes. *Adv Mater* 2006;18:689–706.

- [63] Haberreutinger SN, Leijtens T, Eperon GE, Stranks SD, Nicholas RJ, Snaith HJ. Carbon nanotube/polymer composites as a highly stable hole collection layer in perovskite solar cells. *Nano Lett* 2014;14:5561–8.
- [64] Cai Y, Xu X, Gao C, Wang L, Wei Q, Song L, et al. Effects of carbon nanotubes on morphological structure, thermal and flammability properties of electrospun composite fibers consisting of lauric acid and polyamide 6 as thermal energy storage materials. *Fiber Polym* 2012;13:837–45.
- [65] Simotwo SK, DelRe C, Kalra V. Supercapacitor electrodes based on high-purity electrospun polyaniline and polyaniline–carbon nanotube nanofibers. *ACS Appl Mater Interfaces* 2016;8:21261–9.
- [66] Tebyetekerwa M, Yang S, Peng S, Xu Z, Shao W, Pan D, et al. Unveiling polyindole: freestanding as-electrospun polyindole nanofibers and polyindole/carbon nanotubes composites as enhanced electrodes for flexible all-solid-state supercapacitors. *Electrochim Acta* 2017;247:400–9.
- [67] Xu W, Ding Y, Jiang S, Zhu J, Ye W, Shen Y, et al. Mechanical flexible PI/MWCNTs nanocomposites with high dielectric permittivity by electrospinning. *Eur Polym J* 2014;59:129–35.
- [68] Pan L, Pei X, He R, Wan Q, Wang J. Multiwall carbon nanotubes/polycaprolactone composites for bone tissue engineering application. *Colloids Surf B Biointerfaces* 2012;93:226–34.
- [69] Venkatesan J, Ryu B, Sudha P, Kim SK. Preparation and characterization of chitosan–carbon nanotube scaffolds for bone tissue engineering. *Int J Biol Macromol* 2012;50:393–402.
- [70] Wang ZG, Ke BB, Xu ZK. Covalent immobilization of redox enzyme on electrospun nonwoven poly (acrylonitrile-co-acrylic acid) nanofiber mesh filled with carbon nanotubes: a comprehensive study. *Biotechnol Bioeng* 2007;97:708–20.
- [71] Saetia K, Schnorr JM, Mannarino MM, Kim SY, Rutledge GC, Swager TM, et al. Spray-layer-by-layer carbon nanotube/electrospun fiber electrodes for flexible chemiresistive sensor applications. *Adv Funct Mater* 2014;24:492–502.
- [72] Han L, Andrade AL, Ensor DS. Chemical sensing using electrospun polymer/carbon nanotube composite nanofibers with printed-on electrodes. *Sens Actuators B Chem* 2013;186:52–5.
- [73] Baji A, Mai YW, Abtahi M, Wong SC, Liu Y, Li Q. Microstructure development in electrospun carbon nanotube reinforced polyvinylidene fluoride fibers and its influence on tensile strength and dielectric permittivity. *Compos Sci Technol* 2013;88:1–8.
- [74] Zainab G, Iqbal N, Babar AA, Huang C, Wang X, Yu J, et al. Free-standing, spider-web-like polyamide/carbon nanotube composite nanofibrous membrane impregnated with polyethyleneimine for CO₂ capture. *Compos Commun* 2017;6:41–7.
- [75] Lee JG, Lee Ej, Jeong S, Guo J, An AK, Guo H, et al. Theoretical modeling and experimental validation of transport and separation properties of carbon nanotube electrospun membrane distillation. *J Membr Sci* 2017;526:395–408.
- [76] Wang X, Chen X, Yoon K, Fang D, Hsiao BS, Chu B. High flux filtration medium based on nanofibrous substrate with hydrophilic nanocomposite coating. *Environ Sci Technol* 2005;39:7684–91.
- [77] Dai Y, Yao J, Song Y, Wang S, Yuan Y. Enhanced adsorption and degradation of phenolic pollutants in water by carbon nanotube modified laccase-carrying electrospun fibrous membranes. *Environ Sci Nano* 2016;3:857–68.
- [78] Tijing LD, Woo YC, Shim WG, He T, Choi JS, Kim SH, et al. Superhydrophobic nanofiber membrane containing carbon nanotubes for high-performance direct contact membrane distillation. *J Membr Sci* 2016;502:158–70.
- [79] Ye H, Lam H, Titchenal N, Gogotsi Y, Ko F. Reinforcement and rupture behavior of carbon nanotubes–polymer nanofibers. *Appl Phys Lett* 2004;85:1775–7.
- [80] Imaizumi S, Matsumoto H, Konosu Y, Tsuoboi K, Minagawa M, Tanioka A, et al. Top-down process based on electrospinning, twisting, and heating for producing one-dimensional carbon nanotube assembly. *ACS Appl Mater Interfaces* 2011;3:469–75.
- [81] Liu F, Guo R, Shen M, Wang S, Shi X. Effect of processing variables on the morphology of electrospun poly [(lactic acid)-co-(glycolic acid)] nanofibers. *Macromol Mater Eng* 2009;294:666–72.
- [82] Pankonian A, Ounaies Z, Yang C. Electrospinning of cellulose and SWNT-cellulose nano fibers for smart applications. *J Mech Sci Technol* 2011;25:2631–9.
- [83] McCullen SD, Stano KL, Stevens DR, Roberts WA, Monteiro-Riviere NA, Clarke LI, et al. Development, optimization, and characterization of electrospun poly (lactic acid) nanofibers containing multi-walled carbon nanotubes. *J Appl Polym Sci* 2007;105:1668–78.
- [84] Mazinan S, Ajji A, Dubois C. Fundamental study of crystallization, orientation, and electrical conductivity of electrospun PET/carbon nanotube nanofibers. *J Polym Sci B Polym Phys* 2010;48:2052–64.
- [85] Wong KKH, ZinckAllmang M, Hutter JL, Hrapovic S, Luong JHT, Wan W. The effect of carbon nanotube aspect ratio and loading on the elastic modulus of electrospun poly(vinyl alcohol)-carbon nanotube hybrid fibers. *Carbon* 2009;47:2571–8.
- [86] Ahn Y, Lim JY, Hong SM, Lee J, Ha J, Choi HJ, et al. Enhanced piezoelectric properties of electrospun poly (vinylidene fluoride)/multiwalled carbon nanotube composites due to high β-phase formation in poly (vinylidene fluoride). *J Phys Chem C Nanomater Interfaces* 2013;117:11791–9.
- [87] Salighem O, Forouharshad M, Arasteh R, Eslami-Farsani R, Khajavi R, Roudbari BY. The effect of multi-walled carbon nanotubes on morphology, crystallinity and mechanical properties of PBT/MWCNT composite nanofibers. *J Polym Res* 2013;20(65):1–6.
- [88] Ayutsede J, Gandhi M, Sukigara S, Ye H, Hsu CM, Gogotsi Y, et al. Carbon nanotube reinforced Bombyx mori silk nanofibers by the electrospinning process. *Biomacromolecules* 2006;7:208–14.
- [89] Nirmala R, Jeon KS, Navamathavan R, Park M, Kim HY, Park SJ. Enhanced electrical properties of electrospun nylon66 nanofibers containing carbon nanotube fillers and Ag nanoparticles. *Fiber Polym* 2014;15:918–23.
- [90] Kannan P, Young RJ, Eichhorn SJ. Debundling, isolation, and identification of carbon nanotubes in electrospun nanofibers. *Small* 2008;4:930–3.
- [91] Mathew G, Hong J, Rhee J, Lee H, Nah C. Preparation and characterization of properties of electrospun poly (butylene terephthalate) nanofibers filled with carbon nanotubes. *Polym Test* 2005;24:712–7.
- [92] Marchesan S, Ballerini L, Prato M. Nanomaterials for stimulating nerve growth. *Science* 2017;356:1010–1.
- [93] Li Y, Zhu Z, Yu J, Ding B. Carbon nanotubes enhanced fluorinated polyurethane macroporous membranes for waterproof and breathable application. *ACS Appl Mater Interfaces* 2015;7:13538–46.
- [94] Macossay J, Sheikh FA, Cantu T, Eubanks TM, Salinas ME, Farhangi CS, et al. Imaging, spectroscopic, mechanical and biocompatibility studies of electrospun Tecoflex (R) EG 80A nanofibers and composites thereof containing multiwalled carbon nanotubes. *Appl Surf Sci* 2014;321:205–13.
- [95] Wu CM, Chou MH. Polymorphism, piezoelectricity and sound absorption of electrospun PVDF membranes with and without carbon nanotubes. *Compos Sci Technol* 2016;127:127–33.
- [96] Wan YQ, He JH, Yu JY. Carbon nanotube-reinforced polyacrylonitrile nanofibers by vibration-electrospinning. *Polym Int* 2007;56:1367–70.
- [97] Lee ER, Cho JW. Near infrared laser-heated electrospinning and mechanical properties of poly (ethylene terephthalate)/multi-walled carbon nanotube nanofibers. *RSC Adv* 2015;5:78476–82.
- [98] Vaisman L, Wachtel E, Wagner HD, Marom G. Polymer-nanoinclusion interactions in carbon nanotube based polyacrylonitrile extruded and electrospun fibers. *Polymer* 2007;48:6843–54.
- [99] Dror Y, Salalha W, Khalpin RL, Cohen Y, Yarin AL, Zussman E. Carbon nanotubes embedded in oriented polymer nanofibers by electrospinning. *Langmuir* 2003;19:7012–20.
- [100] Kim JH, Kataoka M, Jung YC, Ko YI, Fujisawa K, Hayashi T, et al. Mechanically tough, electrically conductive poly(ethylene oxide) nanofiber web incorporating DNA-wrapped double-walled carbon nanotubes. *ACS Appl Mater Interfaces* 2013;5:4150–4.
- [101] Fahim N, Rachel P, Sokunthearith S, Lauren N, Mokhtar I, Alex A, et al. Fabrication of conductive polymer nanofibers through SWNT supramolecular functionalization and aqueous solution processing. *Nanotechnology* 2015;26, 395301/1–13.
- [102] Diouri N, Baitoul M, Maaza M. Effect of wrapped carbon nanotubes on optical properties, morphology, and thermal stability of electrospun poly (vinyl alcohol) composite nanofibers. *J Nanomater* 2013;2013, 949108/1–6.
- [103] Diouri N, Baitoul M. Effect of carbon nanotubes dispersion on morphology, internal structure and thermal stability of electrospun poly (vinyl alcohol)/carbon nanotubes nanofibers. *Opt Quantum Electron* 2014;46:259–69.
- [104] Zhou W, Wu Y, Wei F, Luo G, Qian W. Elastic deformation of multiwalled carbon nanotubes in electrospun MWCNTs–PEO and MWCNTs–PVA nanofibers. *Polymer* 2005;46:12689–95.
- [105] Salimbeygi G, Nasouri K, Shoushtari AM, Malek R, Mazaheri F. Fabrication of polyvinyl alcohol/multi-walled carbon nanotubes composite electrospun nanofibres and their application as microwave absorbing material. *Micro Nano Lett* 2013;8:455–9.
- [106] Bao J, Clarke LI, Gorga RE. Effect of constrained annealing on the mechanical properties of electrospun poly (ethylene oxide) webs containing multiwalled carbon nanotubes. *J Polym Sci B Polym Phys* 2016;54:787–96.
- [107] Salalha W, Dror Y, Khalpin RL, Cohen Y, Yarin AL, Zussman E. Single-walled carbon nanotubes embedded in oriented polymeric nanofibers by electrospinning. *Langmuir* 2004;20:9852–5.
- [108] Fang X, Olesik SV. Carbon nanotube and carbon nanorod-filled polyacrylonitrile electrospun stationary phase for ultrathin layer chromatography. *Analy Chim Acta* 2014;830:1–10.
- [109] Kaur N, Kumar V, Dhakate SR. Synthesis and characterization of multiwalled CNT–PAN based composite carbon nanofibers via electrospinning. *Springerplus* 2016;5(483), /1–7.
- [110] Hou H, Ge JJ, Zeng J, Li Q, Reneker DH, Greiner A, et al. Electrospun polyacrylonitrile nanofibers containing a high concentration of well-aligned multiwall carbon nanotubes. *Chem Mater* 2005;17:967–73.
- [111] Ge JJ, Hou H, Li Q, Graham MJ, Greiner A, Reneker DH, et al. Assembly of well-aligned multiwalled carbon nanotubes in confined polyacrylonitrile environments: electrospun composite nanofiber sheets. *J Am Chem Soc* 2004;126:15754–61.
- [112] Lu P, Hsieh YL. Multiwalled carbon nanotube (MWCNT) reinforced cellulose fibers by electrospinning. *ACS Appl Mater Interfaces* 2010;2:2413–20.
- [113] Sapountzi E, Braiek M, Farre C, Arab M, Chateaux JF, Jaffrezic-Renault N, et al. One-step fabrication of electrospun photo-cross-linkable polymer nanofibers incorporating multiwall carbon nanotubes and enzyme for biosensing. *J Electrochem Soc* 2015;162:B275–81.
- [114] Zhang K, Choi H, Kim J. Preparation and characteristics of electrospun multiwalled carbon nanotube/Polyvinylpyrrolidone nanocomposite nanofiber. *J Nanosci Nanotechnol* 2011;11:5446–9.

- [115] Gao J, Yu A, Itkis ME, Belyarova E, Zhao B, Niyogi S, et al. Large-scale fabrication of aligned single-walled carbon nanotube array and hierarchical single-walled carbon nanotube assembly. *J Am Chem Soc* 2004;126:16698–9.
- [116] Tijing LD, Park CH, Choi WL, Ruelo MTG, Amarjargal A, Pant HR, et al. Characterization and mechanical performance comparison of multiwalled carbon nanotube/polyurethane composites fabricated by electrospinning and solution casting. *Compos B Eng* 2013;44:613–9.
- [117] Kimmer D, Slobodian P, Petráš D, Zatloukal M, Olejník R, Sáha P. Polyurethane/multiwalled carbon nanotube nanowebs prepared by an electrospinning process. *J Appl Polym Sci* 2009;111:2711–4.
- [118] Zha JW, Sun F, Wang SJ, Wang D, Lin X, Chen G, et al. Improved mechanical and electrical properties in electrospun polyimide/multiwalled carbon nanotubes nanofibrous composites. *J Appl Phys* 2014;116(134104), 1–5.
- [119] Chen D, Liu T, Zhou X, Tjiu WC, Hou H. Electrospinning fabrication of high strength and toughness polyimide nanofiber membranes containing multiwalled carbon nanotubes. *J Phys Chem B* 2009;113:9741–8.
- [120] Wei K, Jh Xia, Kim BS, Kim IS. Multiwalled carbon nanotubes incorporated bombyx mori silk nanofibers by electrospinning. *J Polym Res* 2011;18:579–85.
- [121] Zhu Y, Li C, Cebe P. Poly(lactides) co-electrospun with carbon nanotubes: thermal and cell culture properties. *Eur Polym J* 2016;75:565–76.
- [122] Liao H, Qi R, Shen M, Cao X, Guo R, Zhang Y, et al. Improved cellular response on multiwalled carbon nanotube-incorporated electrospun polyvinyl alcohol/chitosan nanofibrous scaffolds. *Colloids Surf B Biointerfaces* 2011;84:528–35.
- [123] Liao GY, Zhou XP, Chen L, Zeng XY, Xie XL, Mai YW. Electrospun aligned PLLA/PCL/functionalised multiwalled carbon nanotube composite fibrous membranes and their bio/mechanical properties. *Compos Sci Technol* 2012;72:248–55.
- [124] Zhao X, Luo J, Fang C, Xiong J. Investigation of polylactide/poly(γ -caprolactone)/multi-walled carbon nanotubes electrospun nanofibers with surface texture. *RSC Adv* 2015;5:99179–87.
- [125] Aqeel SM, Wang Z, Than L, Sreenivasulu G, Zeng X. Poly(vinylidene fluoride)/poly(acrylonitrile)-based superior hydrophobic piezoelectric solid derived by aligned carbon nanotubes in electrospinning: fabrication, phase conversion and surface energy. *RSC Adv* 2015;5:76383–91.
- [126] Sundaray B, Choi A, Park YW. Highly conducting electrospun polyaniline-polyethylene oxide nanofibrous membranes filled with single-walled carbon nanotubes. *Synth Met* 2010;160:984–8.
- [127] Zhang Z, Zhang F, Jiang X, Liu Y, Guo Z, Leng J. Electrospinning and microwave absorption of polyaniline/polyacrylonitrile/multiwalled carbon nanotubes nanocomposite fibers. *Fiber Polym* 2014;15:2290–6.
- [128] Baji A, Mai YW, Wong SC, Abtahi M, Du X. Mechanical behavior of self-assembled carbon nanotube reinforced nylon 6, 6 fibers. *Compos Sci Technol* 2010;70:1401–9.
- [129] Cao L, Su D, Su Z, Chen X. Fabrication of multiwalled carbon nanotube/polypropylene conductive fibrous membranes by melt electrospinning. *Ind Eng Chem Res* 2014;53:2308–17.
- [130] Wu D, Yang T, Sun Y, Shi T, Zhou W, Zhang M. Banded spherulites of electrospun poly(trimethylene terephthalate)/carbon nanotube composite mats. *Polym Int* 2011;60:1497–503.
- [131] Navarro-Pardo F, Martinez-Hernandez AL, Velasco-Santos C. Carbon nanotube and graphene based polyamide electrospun nanocomposites: a review. *J Nanomat* 2016;2016:1–16, 3182761.
- [132] Wickham AM, Islam MM, Mondal D, Phopase J, Sadhu V, Tamás É, et al. Polycaprolactone-thiophene-conjugated carbon nanotube meshes as scaffolds for cardiac progenitor cells. *J Biomed Mater Res B Appl Biomater* 2014;102:1553–61.
- [133] Sen R, Zhao B, Perea D, Itkis ME, Hu H, Love J, et al. Preparation of single-walled carbon nanotube reinforced polystyrene and polyurethane nanofibers and membranes by electrospinning. *Nano Lett* 2004;4:459–64.
- [134] Mangeon C, Mahouche-Chergui S, Versace DL, Guerrouache M, Carbone B, Langlois V, et al. Poly(3-hydroxyalkanoate)-grafted carbon nanotube nanofillers as reinforcing agent for PHAs-based electrospun mats. *React Funct Polym* 2015;89:18–23.
- [135] Saeed K, Park SY, Haider S, Baek JB. In situ polymerization of multi-walled carbon nanotube/nylon-6 nanocomposites and their electrospun nanofibers. *Nanoscale Res Lett* 2009;4:39–46.
- [136] Kausar A. Polyamide-grafted-multi-walled carbon nanotube electrospun nanofibers/epoxy composites. *Fiber Polym* 2014;15:2564–71.
- [137] Saeed K, Park S, Lee HJ, Baek JB, Huh WS. Preparation of electrospun nanofibers of carbon nanotube/polycaprolactone nanocomposite. *Polymer* 2006;47:8019–25.
- [138] Kong Y, Yuan J, Qiu J. Preparation and characterization of aligned carbon nanotubes/polylactic acid composite fibers. *Physica B Condens Matter* 2012;407:2451–7.
- [139] Ji J, Sui G, Yu Y, Liu Y, Lin Y, Du Z, et al. Significant improvement of mechanical properties observed in highly aligned carbon-nanotube-reinforced nanofibers. *J Phys Chem C Nanomater Interfaces* 2009;113:4779–85.
- [140] Chen IH, Wang CC, Chen CY. Fabrication and structural characterization of polyacrylonitrile and carbon nanofibers containing plasma-modified carbon nanotubes by electrospinning. *J Phys Chem C Nanomater Interfaces* 2010;114:13532–9.
- [141] Wang K, Gu M, Wang J, Qin C, Dai L. Functionalized carbon nanotube/polyacrylonitrile composite nanofibers: fabrication and properties. *Polym Adv Technol* 2012;23:262–71.
- [142] An AK, Lee EJ, Guo JX, Jeong S, Lee JG, Ghaffour N. Enhanced vapor transport in membrane distillation via functionalized carbon nanotubes anchored into electrospun nanofibres. *Sci Rep* 2017;7(41562):1–11.
- [143] Ko F, Fogotsi Y, Ali A, Naguib N, Ye H, Yang G, et al. Electrospinning of continuous carbon nanotube-filled nanofiber yarns. *Adv Mater* 2003;15:1161–5.
- [144] Bazbouz MB, Stylios GK. Novel mechanism for spinning continuous twisted composite nanofiber yarns. *Eur Polym J* 2008;44:1–12.
- [145] Rakesh G, Ranjit G, Karthikeyan K, Radhakrishnan P, Biji P. A facile route for controlled alignment of carbon nanotube-reinforced, electrospun nanofibers using slotted collector plates. *Express Polym Lett* 2015;9:105–18.
- [146] Miyauchi M, Miao J, Simmons TJ, Lee JW, Doherty TV, Dordick JS, et al. Conductive cable fibers with insulating surface prepared by coaxial electrospinning of multiwalled nanotubes and cellulose. *Biomacromolecules* 2010;11:2440–5.
- [147] Longson TJ, Bhowmick R, Gu C, Cruden BA. Core-shell interactions in coaxial electrospinning and impact on electrospun multiwall carbon nanotube core, poly(methyl methacrylate) shell fibers. *J Phys Chem C Nanomater Interfaces* 2011;115:12742–50.
- [148] McKeon-Fischer K, Flagg D, Freeman J. Coaxial electrospun poly(ϵ -caprolactone), multiwalled carbon nanotubes, and polyacrylic acid/polyvinyl alcohol scaffold for skeletal muscle tissue engineering. *J Biomed Mater Res A* 2011;99:493–9.
- [149] Ojha SS, Stevens DR, Stano K, Hoffman T, Clarke LI, Gorga RE. Characterization of electrical and mechanical properties for coaxial nanofibers with poly(ethylene oxide)(PEO) core and multiwalled carbon nanotube/PEO sheath. *Macromolecules* 2008;41:2509–13.
- [150] Sarvi A, Chimello V, Silva A, Bretas R, Sundararaj U. Coaxial electrospun nanofibers of poly(vinylidene fluoride)/polyaniline filled with multi-walled carbon nanotubes. *Polym Compos* 2014;35:1198–203.
- [151] Yang T, Wu D, Lu L, Zhou W, Zhang M. Electrospinning of polylactide and its composites with carbon nanotubes. *Polym Compos* 2011;32:1280–8.
- [152] Amini N, Mazinani S, Ranaei-Siadat SO, Kalaei MR, Hormozi S, Niknam K, et al. Acetylcholinesterase immobilization on polyacrylamide/functionalized multi-walled carbon nanotube nanocomposite nanofibrous membrane. *Appl Biochem Biotechnol* 2013;170:91–104.
- [153] Ebadi SV, Fakhrali A, Ranaei-Siadat SO, Gharehaghaji AA, Mazinani S, Dinari M, et al. Immobilization of acetylcholinesterase on electrospun poly(acrylic acid)/multi-walled carbon nanotube nanofibrous membranes. *RSC Adv* 2015;5:42572–9.
- [154] Kim GM, Michler GH, Pötschke P. Deformation processes of ultrahigh porous multiwalled carbon nanotubes/polycarbonate composite fibers prepared by electrospinning. *Polymer* 2005;46:7346–51.
- [155] Bayle GM, Mallon PE. Porous microfibers by the electrospinning of amphiphilic graft copolymer solutions with multi-walled carbon nanotubes. *Polymer* 2012;53:5523–39.
- [156] Bounioux C, Avrahami R, Vasilyev G, Patil N, Zussman E, Yerushalmi-Rosen R. Single-step electrospinning of multi walled carbon nanotubes – poly(3-octylthiophene) hybrid nano-fibers. *Polymer* 2016;86:15–21.
- [157] Kim HS, Jin HJ, Myung SJ, Kang M, Chin JJ. Carbon nanotube-adsorbed electrospun nanofibrous membranes of nylon 6. *Macromol Rapid Commun* 2006;27:146–51.
- [158] Havel M, Behler K, Korneva G, Gogotsi Y. Transparent thin films of multiwalled carbon nanotubes self-assembled on polyamide 11 nanofibers. *Adv Funct Mater* 2008;18:2322–7.
- [159] Mercante LA, Pavinatto A, Iwaki LEO, Scagion VP, Zucolotto V, Oliveira ON, et al. Electrospun polyamide 6/Poly(allylamine hydrochloride) nanofibers functionalized with carbon nanotubes for electrochemical detection of dopamine. *ACS Appl Mater Interfaces* 2015;7:4784–90.
- [160] Li F, Scampicchio M, Mannino S. Carbon nanotube-adsorbed electrospun nanofibrous membranes as coating for electrochemical sensors for sulphydryl compounds. *Electroanalysis* 2011;23:1773–5.
- [161] Kang M, Jin HJ. Electrically conducting electrospun silk membranes fabricated by adsorption of carbon nanotubes. *Colloid Polym Sci* 2007;285:1163–7.
- [162] Gao J, Li W, Shi H, Hu M, Li RKY. Preparation, morphology, and mechanical properties of carbon nanotube anchored polymer nanofiber composite. *Compos Sci Technol* 2014;92:95–102.
- [163] Jose MV, Marx S, Murata H, Koepsell RR, Russell AJ. Direct electron transfer in a mediator-free glucose oxidase-based carbon nanotube-coated biosensor. *Carbon* 2012;50:4010–20.
- [164] Yildiz O, Stano K, Faraji S, Stone C, Willis C, Zhang X, et al. High performance carbon nanotube-polymer nanofiber hybrid fabrics. *Nanoscale* 2015;7:16744–54.
- [165] Luo Y, Wang SG, Shen MW, Qi RL, Fang Y, Guo R, et al. Carbon nanotube-incorporated multilayered cellulose acetate nanofibers for tissue engineering applications. *Carbohyd Polym* 2013;91:419–27.
- [166] Tan Y, Song Y, Zheng Q. Hydrogen bonding-driven rheological modulation of chemically reduced graphene oxide/poly(vinyl alcohol) suspensions and its application in electrospinning. *Nanoscale* 2012;4:6997–7005.
- [167] Das S, Wajid AS, Bhattacharya SK, Wilting MD, Rivero IV, Green MJ. Electrospinning of polymer nanofibers loaded with noncovalently functionalized graphene. *J Appl Polym Sci* 2013;128:4040–6.

- [168] Ghobadi S, Sadighikia S, Papila M, Cebeci FC, Gursel SA. Graphene-reinforced poly(vinyl alcohol) electrospun fibers as building blocks for high performance nanocomposites. *RSC Adv* 2015;5:85009–18.
- [169] Ramakrishnan S, Dhakshnamoorthy M, Jelmy E, Vasanthakumari R, Kothurkar NK. Synthesis and characterization of graphene oxide–polyimide nanofiber composites. *RSC Adv* 2014;4:9743–9.
- [170] Shin YC, Lee JH, Jin LH, Kim MJ, Kim YJ, Hyun JK, et al. Stimulated myoblast differentiation on graphene oxide-impregnated PLGA-collagen hybrid fibre matrices. *J Nanobiotechnol* 2015;13(21):1–11.
- [171] Ma HB, Su WX, Tai ZX, Sun DF, Yan XB, Liu B, et al. Preparation and cytocompatibility of polylactic acid/hydroxyapatite/graphene oxide nanocomposite fibrous membrane. *Chin Sci Bull* 2012;57:3051–8.
- [172] Wang C, Li Y, Ding G, Xie X, Jiang M. Preparation and characterization of graphene oxide/poly (vinyl alcohol) composite nanofibers via electrospinning. *J Appl Polym Sci* 2013;127:3026–32.
- [173] Rose A, Raghavan N, Thangavel S, Uma Maheswari B, Nair DP, Venugopal G. Investigation of cyclic voltammetry of graphene oxide/polyaniline/polypyrrolidene fluoride nanofibers prepared via electrospinning. *Mater Sci Semicond Process* 2015;31:281–6.
- [174] Thampi S, Muthuvijayan V, Parameswaran R. Mechanical characterization of high-performance graphene oxide incorporated aligned fibroporous poly(carbonate urethane) membrane for potential biomedical applications. *J Appl Polym Sci* 2015;132(41809):1–8.
- [175] Chaudhuri B, Mondal B, Kumar S, Sarkar S. Myoblast differentiation and protein expression in electrospun graphene oxide (GO)-poly (ε-caprolactone, PCL) composite meshes. *Mater Lett* 2016;182:194–7.
- [176] Song J, Gao H, Zhu G, Cao X, Shi X, Wang Y. The preparation and characterization of polycaprolactone/graphene oxide biocomposite nanofiber scaffolds and their application for directing cell behaviors. *Carbon* 2015;95:1039–50.
- [177] Azarniya A, Eslahi N, Mahmoudi N, Simchi A. Effect of graphene oxide nanosheets on the physico-mechanical properties of chitosan/bacterial cellulose nanofibrous composites. *Compos Part A Appl Sci Manuf* 2016;85:113–22.
- [178] Qi Y, Tai Z, Sun D, Chen J, Ma H, Yan X, et al. Fabrication and characterization of poly (vinyl alcohol)/graphene oxide nanofibrous biocomposite scaffolds. *J Appl Polym Sci* 2013;127:1885–94.
- [179] Huang CL, Peng SY, Wang YJ, Chen WC, Lin JH. Microstructure and characterization of electrospun poly(vinyl alcohol) nanofiber scaffolds filled with graphene nanosheets. *J Appl Polym Sci* 2015;132, 41891/1–11.
- [180] Wang B, Chen Z, Zhang J, Cao J, Wang S, Tian Q, et al. Fabrication of PVA/graphene oxide/TiO₂ composite nanofibers through electrospinning and interface sol-gel reaction: effect of graphene oxide on PVA nanofibers and growth of TiO₂. *Colloids Surf A Physicochem Eng Asp* 2014;457:318–25.
- [181] Shao W, He J, Sang F, Wang Q, Chen L, Cui S, et al. Enhanced bone formation in electrospun poly (l-lactic-co-glycolic acid)-tussah silk fibroin ultrafine nanofiber scaffolds incorporated with graphene oxide. *Mater Sci Eng C Mater Biol Appl* 2016;62:823–34.
- [182] Nirmala R, Navamathan R, Kim HY, Park SJ. Electrical properties of conductive nylon66/graphene oxide composite nanofibers. *J Nanosci Nanotechnol* 2015;15:5718–22.
- [183] Albañil-Sánchez L, Romo-Uribe A, Flores A, Cruz-Silva R. Electrospun nylon-graphene nanocomposites synthesis and microstructure. *Mater Res Soc Symp Proc* 2012;1453, gg05-02/1-8.
- [184] Wu C, Yu S, Lin S. Graphene modified electrospun poly(vinyl alcohol) nanofibrous membranes for glucose oxidase immobilization. *Express Polym Lett* 2014;8:565–73.
- [185] Leyva-Porras C, Ornelas-Gutierrez C, Miki-Yoshida M, Avila-Vega YI, Macossay J, Bonilla-Cruz J. EELS analysis of Nylon 6 nanofibers reinforced with nitroxide-functionalized graphene oxide. *Carbon* 2014;70:164–72.
- [186] Li Y, Zhang P, Ouyang Z, Zhang M, Lin Z, Li J, et al. Nanoscale graphene doped with highly dispersed silver nanoparticles: quick synthesis, facile fabrication of 3D membrane-modified electrode, and super performance for electrochemical sensing. *Adv Funct Mater* 2016;26:2122–34.
- [187] Almeida NA, Martins PM, Teixeira S, da Silva JAL, Sencadas V, Kuhn K, et al. TiO₂/graphene oxide immobilized in P(VDF-TrFE) electrospun membranes with enhanced visible-light-induced photocatalytic performance. *J Mater Sci* 2016;51:6974–86.
- [188] Sarvari R, Sattari S, Massoumi B, Agbolaghi S, Beygi-Khosrowshahi Y, Kahaie-Khosrowshahi A. Composite electrospun nanofibers of reduced graphene oxide grafted with poly(3-dodecylthiophene) and poly(3-thiophene ethanol) and blended with polycaprolactone. *J Biomater Sci Polym Ed* 2017;28:1740–61.
- [189] Zhang C, Wang L, Zhai T, Wang X, Dan Y, Turng LS. The surface grafting of graphene oxide with poly (ethylene glycol) as a reinforcement for poly (lactic acid) nanocomposite scaffolds for potential tissue engineering applications. *J Mech Behav Biomed Mater* 2016;53:403–13.
- [190] Bao Q, Zhang H, Jx Yang, Wang S, Tang DY, Jose R, et al. Graphene–polymer nanofiber membrane for ultrafast photonics. *Adv Funct Mater* 2010;20:782–91.
- [191] Moayeri A, Ajji A. Fabrication of polyaniline/poly (ethylene oxide)/non-covalently functionalized graphene nanofibers via electrospinning. *Synth Met* 2015;200:7–15.
- [192] Lin CJ, Liu CL, Chen WC. Poly(3-hexylthiophene)-graphene composite-based aligned nanofibers for high-performance field effect transistors. *J Mater Chem C Mater Opt Electron Devices* 2015;3:4290–6.
- [193] Aznar-Cervantes S, Martinez JG, Bernabeu-Escalope A, Lozano-Perez AA, Meseguer-Olmo L, Otero TF, et al. Fabrication of electrospun silk fibroin scaffolds coated with graphene oxide and reduced graphene for applications in biomedicine. *Bioelectrochemistry* 2016;108:36–45.
- [194] Jin L, Wu D, Kuddannaya S, Zhang Y, Wang Z. Fabrication, characterization, and biocompatibility of polymer cored reduced graphene oxide nanofibers. *ACS Appl Mater Interfaces* 2016;8:5170–7.
- [195] Huang YL, Baji A, Tien HW, Yang YK, Yang SY, Ma CCM, et al. Self-assembly of graphene onto electrospun polyamide 66 nanofibers as transparent conductive thin films. *Nanotechnology* 2011;22, 475603/1–7.
- [196] Yuan W, Huang L, Zhou Q, Shi G. Ultrasensitive and selective nitrogen dioxide sensor based on self-assembled graphene/polymer composite nanofibers. *ACS Appl Mater Interfaces* 2014;6:17003–8.
- [197] Hsiao ST, Ma CCM, Tien HW, Liao WH, Wang YS, Li SM, et al. Preparation and characterization of silver nanoparticle-reduced graphene oxide decorated electrospun polyurethane fiber composites with an improved electrical property. *Copolym Sci Technol* 2015;118:171–7.
- [198] Hsiao ST, Ma CCM, Liao WH, Wang YS, Li SM, Huang YC, et al. Lightweight and flexible reduced graphene Oxide/Water-Borne polyurethane composites with high electrical conductivity and excellent electromagnetic interference shielding performance. *ACS Appl Mater Interfaces* 2014;6:10667–78.
- [199] Zhou K, Motamed S, Thousa GA, Bernard CC, Li D, Parkington HC, et al. Graphene functionalized scaffolds reduce the inflammatory response and supports endogenous neuroblast migration when implanted in the adult brain. *PLoS One* 2016;11:e0151589, /1–15.
- [200] Gan JK, Lim YS, Pandikumar A, Huang NM, Lim HN. Graphene/polypyrrole-coated carbon nanofiber core–shell architecture electrode for electrochemical capacitors. *RSC Adv* 2015;5:12692–9.
- [201] Cheng C, Shen L, Yu X, Yang Y, Li X, Wang X. Robust construction of a graphene oxide barrier layer on a nanofibrous substrate assisted by the flexible poly(vinylalcohol) for efficient pervaporation desalination. *J Mater Chem A Mater Energy Sustain* 2017;5:3558–68.
- [202] Heidari M, Bahrami H, Ranjbar-Mohammadi M. Fabrication, optimization and characterization of electrospun poly(caprolactone)/gelatin/graphene nanofibrous mats. *Mater Sci Eng C Mater Biol Appl* 2017;78:218–29.
- [203] Sisti L, Belcaro J, Mazzocchetti L, Totaro G, Vannini M, Giorgini L, et al. Multicomponent reinforcing system for poly(butylene succinate): composites containing poly(L-lactide) electrospun mats loaded with graphene. *Polym Test* 2016;50:283–91.
- [204] Goodarzi M, Bahrami SH, Sadighi M, Saber-Samandari S. The influence of graphene reinforced electrospun nano-interlayers on quasi-static indentation behavior of fiber-reinforced epoxy composites. *Fiber Polym* 2017;18:322–33.
- [205] Dias ML, Dip RMM, Souza DHS, Nascimento JP, Santos AP, Furtado CA. Electrospun nanofibers of poly(lactic acid)/Graphene nanocomposites. *J Nanosci Nanotechnol* 2017;17:2531–40.
- [206] Issa AA, Al-Maadeed MAS, Mrlik M, Luyt AS. Electrospun PVDF graphene oxide composite fibre mats with tunable physical properties. *J Polym Res* 2016;23(232):1–13.
- [207] Huang T, Lu MX, Yu H, Zhang QH, Wang HZ, Zhu MF. Enhanced power output of a triboelectric nanogenerator composed of electrospun nanofiber mats doped with graphene oxide. *Sci Rep* 2015;5(13942), /1–8.
- [208] Liu C, Wong HM, Yeung KWK, Tjong SC. Novel electrospun polylactic acid nanocomposite Fiber mats with hybrid graphene oxide and nanohydroxyapatite reinforcements having enhanced biocompatibility. *Polymers* 2016;8(287), /1–19.
- [209] DiezPascual AM, DiezVicente AL. Multifunctional poly(glycolic acid-co-propylene fumarate) electrospun fibers reinforced with graphene oxide and hydroxyapatite nanorods. *J Mater Chem B Mater Biol Med* 2017;5:4084–96.
- [210] Barzegar F, Bello A, Fabiane M, Khamlich S, Momodu D, Taghizadeh F, et al. Preparation and characterization of poly (vinyl alcohol)/graphene nanofibers synthesized by electrospinning. *J Phys Chem Solids* 2015;77:139–45.
- [211] Khan WS, Asmatulu R, Rodriguez V, Ceylan M. Enhancing thermal and ionic conductivities of electrospun PAN and PMMA nanofibers by graphene nanoflake additions for battery-separator applications. *Int J Energy Res* 2014;38:2044–51.
- [212] Zhang P, Zhao X, Ji Y, Ouyang Z, Wen X, Li J, et al. Electrospinning graphene quantum dots into a nanofibrous membrane for dual-purpose fluorescent and electrochemical biosensors. *J Mater Chem B Mater Biol Med* 2015;3:2487–96.
- [213] Holmes B, Fang X, Zarate A, Keidar M, Zhang LG. Enhanced human bone marrow mesenchymal stem cell chondrogenic differentiation in electrospun constructs with carbon nanomaterials. *Carbon* 2016;97:1–13.
- [214] Liu M, Du Y, Miao YE, Ding Q, He S, Tjuu WW, et al. Anisotropic conductive films based on highly aligned polyimide fibers containing hybrid materials of graphene nanoribbons and carbon nanotubes. *Nanoscale* 2015;7:1037–46.
- [215] Yao S, Li Y, Zhou Z, Yan H. Graphene oxide-assisted preparation of poly (vinyl alcohol)/carbon nanotube/reduced graphene oxide nanofibers with high carbon content by electrospinning technology. *RSC Adv* 2015;5:91878–87.
- [216] Matsumoto H, Imaizumi S, Konosu Y, Ashizawa M, Minagawa M, Tanioka A, et al. Electrospun composite nanofiber yarns containing oriented graphene nanoribbons. *ACS Appl Mater Interfaces* 2013;5:6225–31.
- [217] Taylor R, Walton DR. The chemistry of fullerenes. *Nature* 1993;363:685–93.

- [218] Scaffaro R, Maio A, Lopresti F, Botta L. Nanocarbons in electrospun polymeric nanomats for tissue engineering: a review. *Polymers* 2017;9(76):1–35.
- [219] Yan W, Seifermann SM, Pierrat P, Bräse S. Synthesis of highly functionalized C₆₀ fullerene derivatives and their applications in material and life sciences. *Org Biomol Chem* 2015;13:25–54.
- [220] Gatti T, Menna E, Meneghetti M, Maggini M, Petrozza A, Lamberti F. The Renaissance of fullerenes with perovskite solar cells. *Nano Energy* 2017;41:84–100.
- [221] Lai YY, Cheng YJ, Hsu CS. Applications of functional fullerene materials in polymer solar cells. *Energy Environ Sci* 2014;7:1866–83.
- [222] Gaboardi M, Sarzi Amadé N, Aramini M, Milanese C, Magnani G, Sanna S, et al. Extending the hydrogen storage limit in fullerene. *Carbon* 2017;120:77–82.
- [223] Papavasileiou KD, Avramopoulos A, Leonis G, Papadopoulos MG. Computational investigation of fullerene-DNA interactions: Implications of fullerene's size and functionalization on DNA structure and binding energetics. *J Mol Graph Model* 2017;74:177–92.
- [224] Shi J, Wang L, Gao J, Liu Y, Zhang J, Ma R, et al. A fullerene-based multi-functional nanoplateform for cancer theranostic applications. *Biomaterials* 2014;35:5771–84.
- [225] Li J, Vadhanambli S, Kee CD, Oh IK. Electrospun fullerene-cellulose biocompatible actuators. *Biomacromolecules* 2011;12:2048–54.
- [226] Qiao L, Sun X, Yang Z, Wang X, Wang Q, He D. Network structures of fullerene-like carbon core/nano-crystalline silicon shell nanofibers as anode material for lithium-ion batteries. *Carbon* 2013;54:29–35.
- [227] Bounioux C, Itzhak R, Avrahami R, Zussman E, Frey J, Katz EA, et al. Electrospun fibers of functional nanocomposites composed of single-walled carbon nanotubes, fullerene derivatives, and poly (3-hexylthiophene). *J Polym Sci B Polym Phys* 2011;49:1263–8.
- [228] Suk Şeker A, Arslan YE, Elçin Ya M. Electrospun nanofibrous PLGA/fullerene-C₆₀ coated quartz crystal microbalance for real-time gluconic acid monitoring. *IEEE Sens J* 2010;10:1342–8.
- [229] Liu W, Wei J, Chen Y, Huo P, Wei Y. Electrospinning of poly (L-lactide) nanofibers encapsulated with water-soluble fullerenes for bioimaging application. *ACS Appl Mater Interfaces* 2013;5:680–5.
- [230] Liu W, Wei J, Chen Y. Electrospun poly (l-lactide) nanofibers loaded with paclitaxel and water-soluble fullerenes for drug delivery and bioimaging. *Nouv J Chim* 2014;38:6223–9.
- [231] Pierini F, Lanzi M, Nakielski P, Pawłowska S, Urbanek O, Zembrzycki K, et al. Single-material organic solar cells based on electrospun fullerene-grafted polythiophene nanofibers. *Macromolecules* 2017;50:4972–81.
- [232] Stoilova O, Jérôme C, Detrembleur C, Mouithys-Mickalad A, Manolova N, Rashkov I, et al. New nanostructured materials based on fullerene and biodegradable polyesters. *Chem Mater* 2006;18:4917–23.
- [233] Kincer MR, Choudhury R, Srinivasarao M, Beckham HW, Briggs GAD, Porfyrikis K, et al. Shear alignment of fullerenes in nanotubular supramolecular complexes. *Polymer* 2015;56:516–22.
- [234] Chen M, Pierstorff ED, Lam R, Li SY, Huang H, Osawa E, et al. Nanodiamond-mediated delivery of water-insoluble therapeutics. *ACS Nano* 2009;3:2016–22.
- [235] Shimkunas RA, Robinson E, Lam R, Lu S, Xu X, Zhang XQ, et al. Nanodiamond-insulin complexes as pH-dependent protein delivery vehicles. *Biomaterials* 2009;30:5720–8.
- [236] Cai N, Dai Q, Wang Z, Luo X, Xue Y, Yu F. Preparation and properties of nanodiamond/poly (lactic acid) composite nanofiber scaffolds. *Fiber Polym* 2014;15:2544–52.
- [237] Salaam AD, Mishra M, Nyairo E, Dean D. Electrospun polyvinyl alcohol/nanodiamond composite scaffolds: morphological, structural, and biological analysis. *J Biomater Tissue Eng* 2014;4:173–80.
- [238] Man HB, Ho D. Diamond as a nanomedical agent for versatile applications in drug delivery, imaging, and sensing. *Physica Status Solidi A Appl Res* 2012;209:1609–18.
- [239] Schrand AM, Hens SAC, Shenderova OA. Nanodiamond particles: properties and perspectives for bioapplications. *Crit Rev Solid State* 2009;34:18–74.
- [240] Khabasheshku V, Margrave J, Barrera E. Functionalized carbon nanotubes and nanodiamonds for engineering and biomedical applications. *Diam Relat Mater* 2005;14:859–66.
- [241] Brady MA, Renzing A, Douglas TE, Liu Q, Wille S, Parizek M, et al. Development of composite poly (lactide-co-glycolide)-nanodiamond scaffolds for bone cell growth. *J Nanosci Nanotechnol* 2015;15:1060–9.
- [242] Parizek M, Douglas TE, Novotna K, Kromka A, Brady MA, Renzing A, et al. Nanofibrous poly (lactide-co-glycolide) membranes loaded with diamond nanoparticles as promising substrates for bone tissue engineering. *Int J Nanomed* 2012;7:1931–51.
- [243] Cao L, Hou Y, Lafdi K, Urmey K. Fluorescent composite scaffolds made of nanodiamonds/polycaprolactone. *Chem Phys Lett* 2015;641:123–8.
- [244] Ullah M, Seyyed Monfared Zanjani J, Haghghi Poudeh L, Siddiq M, Saner Okan B, Yıldız M, et al. Manufacturing functionalized mono-crystalline diamond containing electrospun fibers reinforced epoxy composites with improved mechanical characteristics. *Diam Relat Mater* 2017;76:90–6.
- [245] Wang Z, Cai N, Zhao D, Xu J, Dai Q, Xue Y, et al. Mechanical reinforcement of electrospun water-soluble polymer nanofibers using nanodiamonds. *Polym Compos* 2013;34:1735–44.
- [246] Behler KD, Stravato A, Mochalin V, Korneva G, Yushin G, Gogotsi Y. Nanodiamond-polymer composite fibers and coatings. *ACS Nano* 2009;3:363–9.
- [247] Kausar A, Ashraf R. Electrospun, non-woven, nanofibrous membranes prepared from nano-diamond and multi-walled carbon nanotube-filled poly(azo-pyridine) and epoxy composites reinforced with these membranes. *J Plast Film Sheet* 2014;30:369–87.
- [248] Mahdavi M, Mahmoudi N, Rezaie Anaran F, Simchi A. Electrospinning of nanodiamond-modified polysaccharide nanofibers with physico-mechanical properties close to natural skins. *Mar Drugs* 2016;14(128), 1–12.
- [249] Tarasova E, Byzova A, Savest N, Viirsalu M, Gudkova V, Märtson T, et al. Influence of preparation process on morphology and conductivity of carbon black-based electrospun nanofibers. *Fuller Nanotub Car N* 2015;23: 695–700.
- [250] Apul OG, von Reitzenstein NH, Schoepf J, Ladner D, Hristovski KD, Westerhoff P. Superfine powdered activated carbon incorporated into electrospun polystyrene fibers preserve adsorption capacity. *Sci Total Environ* 2017;592:458–64.
- [251] Schiffman JD, Blackford AC, Wegst UG, Schauer CL. Carbon black immobilized in electrospun chitosan membranes. *Carbohydr Polym* 2011;84:1252–7.
- [252] Hwang J, Muth J, Ghosh T. Electrical and mechanical properties of carbon-black-filled, electrospun nanocomposite fiber webs. *J Appl Polym Sci* 2007;104:2410–7.
- [253] Chuangchote S, Sirivat A, Supaphol P. Mechanical and electro-rheological properties of electrospun poly (vinyl alcohol) nanofibre mats filled with carbon black nanoparticles. *Nanotechnology* 2007;18(145705), 1/8.
- [254] Alam AM, Liu Y, Park M, Park SJ, Kim HY. Preparation and characterization of optically transparent and photoluminescent electrospun nanofiber composed of carbon quantum dots and polyacrylonitrile blend with polyacrylic acid. *Polymer* 2015;59:35–41.
- [255] Xie R, Zhang L, Liu H, Xu H, Zhong Y, Sui X, et al. Construction of CQDs-Bi2TiO3/ZnO electrospun fiber membranes and their photocatalytic activity for isoproturon degradation under visible light. *Mater Res Bull* 2017;94:7–14.
- [256] Li S, Zhou S, Xu H, Xiao L, Wang Y, Shen H, et al. Luminescent properties and sensing performance of a carbon quantum dot encapsulated mesoporous silica/polyacrylonitrile electrospun nanofibrous membrane. *J Mater Sci* 2016;51:6801–11.
- [257] Mosconi D, Mazzier D, Silvestrini S, Privitera A, Marega C, Franco L, et al. Synthesis and photochemical applications of processable polymers enclosing photoluminescent carbon quantum dots. *ACS Nano* 2015;9:4156–64.
- [258] Feng C, Xu L, Liu Y, Mo LF, Liu FJ, Han L. Electrospun PET/graphite nanofibers. *Adv Sci Lett* 2012;10:618–20.
- [259] Mack JJ, Viculis LM, Ali A, Luoh R, Yang G, Hahn HT, et al. Graphite nanoplatelet reinforcement of electrospun polyacrylonitrile nanofibers. *Adv Mater* 2005;17:77–80.
- [260] Huang ZX, Liu X, Wong SC, Qu JP. Electrospinning polyvinylidene fluoride/expanded graphite composite membranes as high efficiency and reusable water harvester. *Mater Lett* 2017;202:78–81.
- [261] Gao J, Hu M, Dong Y, Li RK. Graphite-nanoplatelet-decorated polymer nanofiber with improved thermal, electrical, and mechanical properties. *ACS Appl Mater Interfaces* 2013;5:7758–64.
- [262] Cai J, Chawla S, Naraghi M. Microstructural evolution and mechanics of hot-drawn CNT-reinforced polymeric nanofibers. *Carbon* 2016;109: 813–22.
- [263] Yu W, Jiang X, Cai M, Zhao W, Ye D, Zhou Y, et al. A novel electrospun nerve conduit enhanced by carbon nanotubes for peripheral nerve regeneration. *Nanotechnology* 2014;25:165102, 1/12.
- [264] McCullen SD, Stevens DR, Roberts WA, Clarke LI, Bernacki SH, Gorga RE, et al. Characterization of electrospun nanocomposite scaffolds and biocompatibility with adipose-derived human mesenchymal stem cells. *Int J Nanomed* 2007;2:253–63.
- [265] Karbasi S, Zarei M, Foroughi MR. Effects of Multi-Wall carbon Nano-Tubes (MWNTs) on structural and mechanical properties of electrospun poly(3-hydroxybutyrate) scaffold for tissue engineering applications. *Sci Iran* 2016;23:3145–52.
- [266] Zuo L, Zhang F, Gao B, Zuo B. Fabrication of electrical conductivity and reinforced electrospun silk nanofibers with MWNTs. *Fibres Text East Eur* 2017;25:40–4.
- [267] Ribeiro S, Costa P, Ribeiro C, Sencadas V, Botelho G, Lanceros-Méndez S. Electrospun styrene-butadiene-styrene elastomer copolymers for tissue engineering applications: effect of butadiene/styrene ratio, block structure, hydrogenation and carbon nanotube loading on physical properties and cytotoxicity. *Compos B Eng* 2014;67:30–8.
- [268] Wang K, Tang RY, Zhao XB, Li JJ, Lang YR, Jiang XX, et al. Covalent bonding of YIGSR and RGD to PEDOT/PSS/MWCNT-COOH composite material to improve the neural interface. *Nanoscale* 2015;7:18677–85.
- [269] McKeon-Fischer KD, Browne DP, Olabisi RM, Freeman JW. Poly(3,4-ethylenedioxythiophene) nanoparticle and poly(ϵ -caprolactone) electrospun scaffold characterization for skeletal muscle regeneration. *J Biomed Mater Res A* 2015;103:3633–41.
- [270] Gandhi M, Yang H, Shor L, Ko F. Post-spinning modification of electrospun nanofiber nanocomposite from *Bombyx mori* silk and carbon nanotubes. *Polymer* 2009;50:1918–24.
- [271] Markowski J, Magiera A, Lesiak M, Sieron AL, Pilch J, Blazewicz S. Preparation and characterization of nanofibrous polymer scaffolds for cartilage tissue engineering. *J Nanomater* 2015;2015:564087, 1/9.

- [272] Wang H, Chu C, Cai R, Jiang S, Zhai L, Lu J, et al. Synthesis and bioactivity of gelatin/multiwalled carbon nanotubes/hydroxyapatite nanofibrous scaffolds towards bone tissue engineering. *RSC Adv* 2015;5:53550–8.
- [273] Kharazia M, Shin SR, Nikkhah M, Topkaya SN, Masoumi N, Annabi N, et al. Tough and flexible CNT-polymeric hybrid scaffolds for engineering cardiac constructs. *Biomaterials* 2014;35:7346–54.
- [274] Tijing LD, Choi W, Jiang Z, Amarjargal A, Park CH, Pant HR, et al. Two-nozzle electrospinning of (MWNT/PU)/PU nanofibrous composite mat with improved mechanical and thermal properties. *Curr Appl Phys* 2013;13:1247–55.
- [275] Moradi R, KarimiSabet J, Shariaty-Niassar M, Koochaki MA. Preparation and characterization of polyvinylidene fluoride/graphene superhydrophobic fibrous films. *Polymers* 2015;7:1444–63.
- [276] Mandieh ZM, Mottaghitalab V, Piri N, Hagh AK. Conductive chitosan/multi walled carbon nanotubes electrospun nanofiber feasibility. *Korean J Chem Eng* 2012;29:111–9.
- [277] Kabiri M, Soleimani M, Shabani I, Futrega K, Ghaemi N, Ahvaz HH, et al. Neural differentiation of mouse embryonic stem cells on conductive nanofiber scaffolds. *Biotechnol Lett* 2012;34:1357–65.
- [278] Xu J, Xie Y, Zhang H, Ye Z, Zhang W. Fabrication of PLGA/MWNTs composite electrospun fibrous scaffolds for improved myogenic differentiation of C2C12 cells. *Colloids Surf B Biointerfaces* 2014;123:907–15.
- [279] Choi J, Park EJ, Park DW, Shim SE. MWNT-OH adsorbed electrospun nylon 6, 6 nanofibers chemiresistor and their application in low molecular weight alcohol vapours sensing. *Synth Met* 2010;160:2664–9.
- [280] Shao S, Zhou S, Li L, Li J, Luo C, Wang J, et al. Osteoblast function on electrically conductive electrospun PLA/MWCNTs nanofibers. *Biomaterials* 2011;32:2821–33.
- [281] Meng Z, Zheng W, Li L, Zheng Y. Fabrication and characterization of three-dimensional nanofiber membrane of PCL–MWCNTs by electrospinning. *Mater Sci Eng C Mater Biol Appl* 2010;30:1014–21.
- [282] Krafts KP. Tissue repair the hidden drama. *Organogenesis* 2010;6:225–33.
- [283] Langone AJ, Helderman JH. Disparity between solid-organ supply and demand. *N Engl J Med* 2003;349:704–6.
- [284] Specchio F, Saraceno R, Chimenti S, Nisticò S. Management of non-melanoma skin Cancer in solid organ transplant recipients. *Int J Immunopathol Pharmacol* 2014;27:21–4.
- [285] Vacanti CA. The history of tissue engineering. *J Cell Mol Med* 2006;10:569–76.
- [286] Place ES, Evans ND, Stevens MM. Complexity in biomaterials for tissue engineering. *Nature Mater* 2009;8:457–70.
- [287] Hopley EL, Salmasi S, Kalaskar DM, Seifalian AM. Carbon nanotubes leading the way forward in new generation 3D tissue engineering. *Biotechnol Adv* 2014;32:1000–14.
- [288] Ikegami M, Tajima K, Aida T. Template synthesis of polypyrrole nanofibers insulated within one-dimensional silicate channels: hexagonal versus lamellar for recombination of polarons into bipolarons. *Angew Chem Int Ed* 2003;42:2154–7.
- [289] Tiwari A, Terada D, Yoshikawa C, Kobayashi H. An enzyme-free highly glucose-specific assay using self-assembled aminobenzene boronic acid upon polyelectrolytes electrospun nanofibers-mat. *Talanta* 2010;82:1725–32.
- [290] Pan H, Zhang YP, Hang YC, Shao HL, Hu XC, Xu YM, et al. Significantly reinforce composite fibers electrospun from silk fibroin/carbon nanotube aqueous solutions. *Biomacromolecules* 2012;13:2859–67.
- [291] Kobayashi N, Izumi H, Morimoto Y. Review of toxicity studies of carbon nanotubes. *J Occup Health* 2017;59:394–407.
- [292] Gupta A, Liberati TA, Verhulst SJ, Main BJ, Roberts MH, Potty AGR, et al. Biocompatibility of single-walled carbon nanotube composites for bone regeneration. *Bone Joint Res* 2015;4:70–7.
- [293] Chen M, Qin XS, Zeng GM. Biodegradation of carbon nanotubes, graphene, and their derivatives. *Trends Biotechnol* 2017;35:836–46.
- [294] FloresCervantes DX, Maes HM, Schaffer A, Hollender J, Kohler HPE. Slow biotransformation of carbon nanotubes by horseradish peroxidase. *Environ Sci Technol* 2014;48:4826–34.
- [295] Bhattacharya K, Mukherjee SP, Gallud A, Burkert SC, Bistarelli S, Bellucci S, et al. Biological interactions of carbon-based nanomaterials: from coronation to degradation. *Nanomedicine* 2016;12:333–51.
- [296] Kotchey GP, Zhao Y, Kagan VE, Star A. Peroxidase-mediated biodegradation of carbon nanotubes in vitro and in vivo. *Adv Drug Deliv Rev* 2013;65:1921–32.
- [297] Aljamal KT, Nunes A, Methven L, Ali-Boucetta H, Li SP, Toma FM, et al. Degree of chemical functionalization of carbon nanotubes determines tissue distribution and excretion profile. *Angew Chem Int Ed* 2012;51:6389–93.
- [298] ObarzanekFojt M, Elbs-Glatz Y, Lizundia E, Diener L, Sarasua JR, Bruinink A. From implantation to degradation - are poly (L-lactide)/multiwall carbon nanotube composite materials really cytocompatible? *Nanomedicine* 2014;10:1041–51.
- [299] Meyyappan M. Carbon nanotubes: science and applications. New York: CRC Press; 2004. p. 304.
- [300] Geim AK, Novoselov KS. The rise of graphene. *Nat Mater* 2007;6:183–91.
- [301] Mi HY, Salick MR, Jing X, Crone WC, Peng XF, Turng LS. Electrospinning of unidirectionally and orthogonally aligned thermoplastic polyurethane nanofibers: fiber orientation and cell migration. *J Biomed Mater Res A* 2015;103:593–603.
- [302] Mackle JN, Blond DJP, Mooney E, McDonnell C, Blau WJ, Shaw G, et al. In vitro characterization of an electroactive carbon-nanotube-Based nanofiber scaffold for tissue engineering. *Macromol Biosci* 2011;11:1272–82.
- [303] Sharma Y, Tiwari A, Hattori S, Terada D, Sharma AK, Ramalingam M, et al. Fabrication of conducting electrospun nanofibers scaffold for three-dimensional cells culture. *Int J Biol Macromol* 2012;51:627–31.
- [304] Tiwari A, Sharma Y, Hattori S, Terada D, Sharma AK, Turner APF, et al. Influence of poly(n-isopropylacrylamide)-CNT-polyaniline three-dimensional electrospun microfibric scaffolds on cell growth and viability. *Biopolymers* 2013;99:334–41.
- [305] Dimitriou R, Jones E, McGonagle D, Giannoudis PV. Bone regeneration: current concepts and future directions. *BMC Med* 2011;9(1):1–66.
- [306] Shi X, Sitharaman B, Pham QP, Liang F, Wu K, Billups WE, et al. Fabrication of porous ultra-short single-walled carbon nanotube nanocomposite scaffolds for bone tissue engineering. *Biomaterials* 2007;28:4078–90.
- [307] Sitharaman B, Shi X, Walboomers XF, Liao H, Cuijpers V, Wilson LJ, et al. In vivo biocompatibility of ultra-short single-walled carbon nanotube/biodegradable polymer nanocomposites for bone tissue engineering. *Bone* 2008;43:362–70.
- [308] Rodrigues BV, Silva AS, Melo GF, Vasconcellos LM, Mariano FR, Lobo AO. Influence of low contents of superhydrophilic MWCNT on the properties and cell viability of electrospun poly (butylene adipate-co-terephthalate) fibers. *Mater Sci Eng C Mater Biol Appl* 2016;59:782–91.
- [309] Abarrategi A, Gutiérrez MC, Moreno-Vicente C, Hortigüela MJ, Ramos V, López-Lacomba JL, et al. Multiwall carbon nanotube scaffolds for tissue engineering purposes. *Biomaterials* 2008;29:94–102.
- [310] Zhang H, Chen Z. Fabrication and characterization of electrospun PLGA/MWNTs/hydroxyapatite biocomposite scaffolds for bone tissue engineering. *J Bioact Compat Polym* 2010;25:241–59.
- [311] Zhang H, Liu J, Yao Z, Yang J, Pan L, Chen Z. Biomimetic mineralization of electrospun poly (lactic-co-glycolic acid)/multi-walled carbon nanotubes composite scaffolds in vitro. *Mater Lett* 2009;63:2313–6.
- [312] Pal S. Mechanical properties of biological materials. In: Pal S, editor. Design of artificial human joints & organs. New York: Springer Science; 2014. p. 23–40.
- [313] Zhang H. Electrospun poly (lactic-co-glycolic acid)/multiwalled carbon nanotubes composite scaffolds for guided bone tissue regeneration. *J Bioact Compat Polym* 2011;26:347–62.
- [314] Deshpande HD, Dean DR, Thomas V, Clem WC, Jose MV, Nyairo E, et al. Carbon nanofiber reinforced polycaprolactone fibrous meshes by electrostatic Co-spinning. *Curr Nanosci* 2012;8:753–61.
- [315] Chłopek J, Czajkowska B, Szaraniec B, Frackowiak E, Szostak K, Beguin F. In vitro studies of carbon nanotubes biocompatibility. *Carbon* 2006;44:1106–11.
- [316] Balani K, Anderson R, Laha T, Andara M, Tercero J, Crumpler E, et al. Plasma-sprayed carbon nanotube reinforced hydroxyapatite coatings and their interaction with human osteoblasts in vitro. *Biomaterials* 2007;28:618–24.
- [317] Zhang H. Effects of electrospinning parameters on morphology and diameter of electrospun PLGA/MWNTs fibers and cytocompatibility in vitro. *J Bioact Compat Polym* 2011;26:590–606.
- [318] Holmes B, Castro NJ, Li J, Keidar M, Zhang LG. Enhanced human bone marrow mesenchymal stem cell functions in novel 3D cartilage scaffolds with hydrogen treated multi-walled carbon nanotubes. *Nanotechnology* 2013;24(365102):1–10.
- [319] Higginson G, Snaith J. The mechanical stiffness of articular cartilage in confined oscillating compression. *Eng Med* 1979;8:11–4.
- [320] Rains J, Bert J, Roberts C, Pare P. Mechanical properties of human tracheal cartilage. *J Appl Physiol* 1992;72:219–25.
- [321] Mei F, Zhong J, Yang X, Ouyang X, Zhang S, et al. Improved biological characteristics of poly (L-lactic acid) electrospun membrane by incorporation of multiwalled carbon nanotubes/hydroxyapatite nanoparticles. *Biomacromolecules* 2007;8:3729–35.
- [322] Deng XL, Xu M, Li D, Sui G, Hu X, Yang XP. Electrospun PLLA/MWNTs/HA hybrid nanofiber scaffolds and their potential in dental tissue engineering. *Key Eng Mater* 2007;330–332:393–6.
- [323] Khan AS, Hussain AN, Sidra I, Sarfraz Z, Khalid H, Khan M, et al. Fabrication and in vivo evaluation of hydroxyapatite/carbon nanotube electrospun fibers for biomedical/dental application. *Mater Sci Eng C Mater Biol Appl* 2017;80:387–96.
- [324] Kandel ER, Schwartz JH, Jessell TM, Siegelbaum SA, Hudspeth AJ. Principles of neural science. New York: McGraw-Hill Education; 2000, 1414 pp.
- [325] Feigin VL, Abajobir AA, Abate KH, Abd-Allah F, Abdulle AM, Abera SF, et al. Global, regional, and national burden of neurological disorders during 1990–2015: a systematic analysis for the Global Burden of Disease Study 2015. *Lancet Neurol* 2017;16:877–97.
- [326] Braughler JM, Hall ED. Current application of high-dose steroid-therapy for cns injury - A pharmacological perspective. *J Neurosurg* 1985;62:806–10.
- [327] Kabiri M, Oraee-Yazdani S, Dodel M, Hanaee-Ahvaz H, Soudi S, Seyedjafari E, et al. Cytocompatibility of a conductive nanofibrous carbon nanotube/poly (L-Lactic acid) composite scaffold intended for nerve tissue engineering. *EXCLI J* 2015;14:851–60.
- [328] Aznar-Cervantes S, Pagán A, Martínez JG, Bernabeu-Escalapez A, Otero TF, Meseguer-Olmo L, et al. Electrospun silk fibroin scaffolds coated with reduced graphene promote neurite outgrowth of PC-12 cells under electrical stimulation. *Mater Sci Eng C Mater Biol Appl* 2017;79:315–25.

- [329] Guo JH, Liu Y, Lv ZJ, Wei WJ, Guan X, Guan QL, et al. Potential neurogenesis of human adipose-derived stem cells on electrospun catalpol-loaded composite nanofibrous scaffolds. *Ann Biomed Eng* 2015;43:2597–608.
- [330] Pettikiriarachchi JT, Parish CL, Shoichet MS, Forsythe JS, Nisbet DR. Biomaterials for brain tissue engineering. *Aust J Chem* 2010;63:1143–54.
- [331] Jabbari E, Kim DH, Lee LP. Handbook of biomimetics and bioinspiration: biologically-driven engineering of materials, processes, devices, and systems. Singapore: World Scientific Publishing Company; 2014, 1462 pp.
- [332] Huang YJ, Wu HC, Tai NH, Wang TW. Carbon nanotube rope with electrical stimulation promotes the differentiation and maturity of neural stem cells. *Small* 2012;8:2869–77.
- [333] Fabbro A, Scaini D, Leon V, Vazquez E, Cellot G, Privitera G, et al. Graphene-based interfaces do not alter target nerve cells. *ACS Nano* 2016;10:615–23.
- [334] Vicentini N, Gatti T, Salice P, Scapin G, Marega C, Filippini F, et al. Covalent functionalization enables good dispersion and anisotropic orientation of multi-walled carbon nanotubes in a poly (L-lactic acid) electrospun nanofibrous matrix boosting neuronal differentiation. *Carbon* 2015;95:725–30.
- [335] Mottaghitalab F, Farokhi M, Zaminy A, Kokabi M, Soleimani M, Mirahmadi F, et al. A biosynthetic nerve guide conduit based on silk/SWNT/fibronectin nanocomposite for peripheral nerve regeneration. *PLoS One* 2013;8:1–12, e74417.
- [336] Ostrovodov S, Shi X, Zhang L, Liang X, Kim SB, Fujie T, et al. Myotube formation on gelatin nanofibers–multi-walled carbon nanotubes hybrid scaffolds. *Biomaterials* 2014;35:6268–77.
- [337] Mooney E, Mackle JN, Blond DJP, O’Cearbhail E, Shaw G, Blau WJ, et al. The electrical stimulation of carbon nanotubes to provide a cardiomimetic cue to MSCs. *Biomaterials* 2012;33:6132–9.
- [338] Han D, Goldgraben S, Frame MD, Gouma PI. A novel nanofiber scaffold by electrospinning and its utility in microvascular tissue engineering. *Mater Res Soc Symp Proc* 2004;845:363–8.
- [339] Han Z, Kong H, Meng J, Wang C, Xie S, Xu H. Electrospun aligned nanofibrous scaffold of carbon nanotubes-polyurethane composite for endothelial cells. *J Nanosci Nanotechnol* 2009;9:1400–2.
- [340] Meng J, Han Z, Kong H, Qi X, Wang C, Xie S, et al. Electrospun aligned nanofibrous composite of MWCNT/polyurethane to enhance vascular endothelium cells proliferation and function. *J Biomed Mater Res A* 2010;95:312–20.
- [341] Edwards SL, Church JS, Werkmeister JA, Ramshaw JA. Tubular micro-scale multiwalled carbon nanotube-based scaffolds for tissue engineering. *Biomaterials* 2009;30:1725–31.
- [342] Wang J. Electrochemical glucose biosensors. *Chem Rev* 2008;108:814–25.
- [343] Demirci Uzun S, Kayaci F, Uyar T, Timur S, Toppore L. Bioactive surface design based on functional composite electrospun nanofibers for biomolecule immobilization and biosensor applications. *ACS Appl Mater Interfaces* 2014;6:5235–43.
- [344] Mason M, Longo E, Scampicchio M. Monitoring of glucose in beer brewing by a carbon nanotubes based nylon nanofibrous biosensor. *J Nanometer* 2016;2016:1–11, 5217023.
- [345] Zhang P, Zhao X, Zhang X, Lai Y, Wang X, Li J, et al. Electrospun doping of carbon nanotubes and platinum nanoparticles into the β -phase polyvinylidene difluoride nanofibrous membrane for biosensor and catalysis applications. *ACS Appl Mater Interfaces* 2014;6:7563–71.
- [346] Olubi O, Gadi D, Sannigrahi B, Williams M, Baird B, Khan I. Fabrication of electroactive composite nanofibers of functionalized polymer and CNT capable of specifically binding with the IgE (Immunoglobulin E) antibody. *Surf Interface Anal* 2014;46:237–42.
- [347] Wang N, Xu Z, Qu Y, Zheng G, Dai K, Liu C, et al. Liquid-sensing behaviors of carbon black/polyamide 6/high-density polyethylene composite containing ultrafine conductive electrospun fibrous network. *Colloid Polym Sci* 2016;294:1343–50.
- [348] Dai H, Gong L, Xu G, Li X, Zhang S, Lin Y, et al. An electrochemical impedimetric sensor based on biomimetic electrospun nanofibers for formaldehyde. *Analyst* 2015;140:582–9.
- [349] Guan X, Zheng G, Dai K, Liu C, Yan X, Shen C, et al. Carbon nanotubes-adsorbed electrospun PA66 nanofiber bundles with improved conductivity and robust flexibility. *ACS Appl Mater Interfaces* 2016;8:14150–9.
- [350] Azemi E, Stauffer WR, Gostock MS, Lagenaar CF, Cui XT. Surface immobilization of neural adhesion molecule L1 for improving the biocompatibility of chronic neural probes: in vitro characterization. *Acta Biomater* 2008;4:1208–17.
- [351] Dai YR, Niu JF, Yin LF, Xu JJ, Sun K. Enhanced sorption of perfluorooctane sulfonate (PFOS) on carbon nanotube-filled electrospun nanofibrous membranes. *Chemosphere* 2013;93:1593–9.
- [352] Xiao SL, Shen MW, Guo R, Huang QG, Wang SY, Shi XY. Fabrication of multiwalled carbon nanotube-reinforced electrospun polymer nanofibers containing zero-valent iron nanoparticles for environmental applications. *J Mater Chem* 2010;20:5700–8.
- [353] Beheshti H, Irani M, Hosseini L, Rahimi A, Aliabadi M. Removal of Cr (VI) from aqueous solutions using chitosan/MWCNT/Fe3O4 composite nanofibers-batch and column studies. *Chem Eng J* 2016;284:557–64.
- [354] Chen SL, Huang XJ, Xu ZK. Decoration of phthalocyanine on multiwalled carbon nanotubes/cellulose nanofibers nanocomposite for decoloration of dye wastewater. *Compos Sci Technol* 2014;101:11–6.
- [355] Dai YR, Yao J, Song YH, Liu XL, Wang SY, Yuan Y. Enhanced performance of immobilized laccase in electrospun fibrous membranes by carbon nanotubes modification and its application for bisphenol A removal from water. *J Hazard Mater* 2016;317:485–93.
- [356] Li P, Wang CY, Zhang YY, Wei F. Air filtration in the free molecular flow regime: a review of high-efficiency particulate air filters based on carbon nanotubes. *Small* 2014;10:4543–61.
- [357] Shi J, Wu TF, Teng KY, Wang W, Shan MJ, Xu ZW, et al. Simultaneous electrospinning and spraying toward branch-like nanofibrous membranes functionalised with carboxylated MWCNTs for dye removal. *Mater Lett* 2016;166:26–9.
- [358] Jadhav AH, Mai XT, Ofori FA, Kim H. Preparation, characterization, and kinetic study of end opened carbon nanotubes incorporated polyacrylonitrile electrospun nanofibers for the adsorption of pyrene from aqueous solution. *Chem Eng J* 2015;259:348–56.
- [359] Wu J, Wang N, Zhao Y, Jiang L. Electrospinning of multilevel structured functional micro-/nanofibers and their applications. *J Mater Chem A Mater Energy Sustain* 2013;1:7290–305.
- [360] Sun B, Long Y, Zhang H, Li M, Duvail J, Jiang X, et al. Advances in three-dimensional nanofibrous macrostructures via electrospinning. *Prog Polym Sci* 2014;39:862–90.
- [361] Si Y, Yu J, Tang X, Ge J, Ding B. Ultralight nanofibre-assembled cellular aerogels with superelasticity and multifunctionality. *Nat Commun* 2014;5(5802):1–9.
- [362] Duan G, Jiang S, Jérôme V, Wendorff JH, Fathi A, Uhm J, et al. Ultralight, Soft polymer sponges by self-assembly of short electrospun fibers in colloidal dispersions. *Adv Funct Mater* 2015;25:2850–6.
- [363] Xu T, Miszuk JM, Zhao Y, Sun H, Fong H. Electrospun polycaprolactone 3D nanofibrous scaffold with interconnected and hierarchically structured pores for bone tissue engineering. *Adv Healthc Mater* 2015;4:2238–46.
- [364] Du J, Bai J, Cheng H. The present status and key problems of carbon nanotube based polymer composites. *Express Polym Lett* 2007;1:253–73.
- [365] Yu YH, Chan CC, Lai YC, Lin YY, Huang YC, Chi WF, et al. Biocompatible electrospinning poly(vinyl alcohol) nanofibres embedded with graphene-based derivatives with enhanced conductivity, mechanical strength and thermal stability. *RSC Adv* 2014;4:56373–84.